Universitetet i Stavanger

FACULTY OF SCIENCE AND TECHNOLOGY

MASTER'S THESIS

Study programme/specialisation:	Spring semester, 2019
Petroleum Engineering/Reservoir Engineering	

Author:
ABM Hedayatul Islam

Programme coordinator:

Supervisor(s):

Dmitry Shogin

Title of master's thesis:

Experimental Investigation of Material Functions of EOR Polymer Solutions

Credits: 30

Keywords: Polymer
Material function
Shear stress start-up
Shear stress relaxation
FENE-P
C-FENE-P

Number of pages:
……

+ supplemental material/other: ……

Abstract

The material functions of multiple EOR polymers were measured and analyzed. Investigating the start-up and relaxation behaviour of multiple polymeric solutions were the main focus of this thesis work. The experimented data were analyzed and compared with Charged-FENE-P Dumbbell model qualitatively. And it has been discovered that Finitely Extensible Nonlinear Elastic-Peterlin (FENE-P) cannot predict the sudden decay of shear stress at sudden relaxation while Charged-FENE-P is able to predict and explain the behavior. The shear thinning viscosity of polymer was analyzed against FENE-P dumbbell model and exponential Phan-Thien-Tanner model (PTT) for different concentrations. The storage and loss moduli data were compared with C-FENE-P Dumbbell model. It has been concluded that both shear stress growth rate at the beginning of a shear flow and shear stress decay rate after sudden cessation of the flow not only depends on the concentration and shear rate but also on the molecular weight of the polymer. This outcome can be implemented to reduce the shear thinning behavior of the polymer at a sudden stage. But further investigations are needed. With further investigation, this outcome can be implemented in both technical and experimental fields.

Acknowledgment

Firstly, I would like to express my appreciation and gratitude to my supervisor Associate Professor Dr. Dmitry Shogin for giving me the opportunity to work under his supervision. I am thankful for his valuable suggestions and discussion seasons without which it would be impossible to complete this thesis.

Dmitry guided me from the beginning of the thesis with both theoretical and experimental fields. He also guided me during writing the thesis. He was the mentor whom a student wants to be a supervisor.

My great gratitude also goes to Kim Andre Vorland, who taught me how to use rheometers, mixers and magnet devices.

Special thanks to The National IOR Centre of Norway.

Finally, but not least, I would like to thank my parents, my wife, and friends for supporting me in every endeavor during my stay in Stavanger.

Table of contents

List of Figures

List of Tables

Nomenclature

- normal Latin fonts for Scalar
- boldface Latin fonts for Vector
- boldface Greek letters for Tensor notation

α cone angle

γ strain amplitude (%) for SAOS flow

$\dot{\gamma}$ shear rate

$\dot{\gamma}$ amplitude of shear rate oscillation (SAOS flow)

$\dot{\boldsymbol{\gamma}}$ rate of stress tensor

$\dot{\gamma}_0$ shear rate at time t < 0 for start-up and relaxation

$\boldsymbol{\delta}$ identical tensor; Kronecker Delta

δ phase shiht angle between present and resulting curve

ε permitivity of solvent

ε_0 permitivity of vacuum

$\eta(\dot{\gamma})$ shear stress dependence viscosity

$\Psi_1(\dot{\gamma})$ first normal stress coefficient

$\Psi_2(\dot{\gamma})$ second normal stress coefficient

η^* complex viscosity

η', η'' complex viscosity coefficients

λ time constant

μ Newtonian fluid viscosity

$\boldsymbol{\pi}$ total stress tensor

ρ fluid density

$\boldsymbol{\tau}$ anisotropic stress tensor

τ_{xx} normal stress to X direction

τ_{xy} shear stress

τ_{yy} normal stress to Y direction

τ_{zz} normal stress to Z direction

$\Psi_1(\dot{\gamma})$ first normal stress coefficient

$\Psi_2(\dot{\gamma})$ second normal stress coefficient

ω frequency

c desired concentration of the diluted solution

c_0 true concentration of the mother solution

c_{ss} conversion factor between M and τ

c_{sr} conversion factor between n and $\dot{\gamma}$

$\boldsymbol{F}$ spring force

H spring stiffness

$\boldsymbol{g}$ gravitational force

G' storage modulus

G'' loss modulus

k Boltzmann's constant

m consistency index (section 2)

m desired mass of the diluted solution (section 3)

M_c theoretical mass of concentrated polymer

M_p required polymer

M_s measured mass of polymer solvent

$\boldsymbol{n}$ normal unit vector

n Power-law index (section 2)

n rotation per minute (section 3)

P thermodynamic pressure

$\boldsymbol{Q}$ vector between beads

Q extension of the spring

Q_0 maximum extension of the spring

q effective charge

S surface area

T temperature

t time

$\boldsymbol{v}$ fluid velocity

V volume item[Z] Z-factor

$\boldsymbol{\nabla}$ vector differential operator

1. Introduction

The demand for energy has increased over the past years with a rising population. As per the projections, both fossil fuel and renewables will remain as the major energy sources (678 quadrillions BTU) till 2030 with fossil fuel contributing 78% of total energy consumption [Rellegadla et al., 2017]. Oil plays a vital rule both as a global energy source and in a country's economy. According to Norwegian Petroleum Directorate, the current recovery factor in the Norwegian continental shelf is just under 50% [NPD, 2017]. 1% increase in the oil recovery will lead to adding billions of dollar in the Norwegian economy. According to Norwegian Petroleum Directorate, the most promising method of improved oil recovery (IOR) on the Norwegian Continental Shelf (NCS) is polymer combined with low salinity flooding for enhanced IOR [NPD, 2018]. But due to lack of the understanding of how polymer solution behaves, it has not yet an implemented EOR method in Norway. Therefore, it is very important to understand the rheological properties i.e. properties which the deformation and flow behavior of the polymer and how the material function (the functions of kinematic parameters that characterize the behavior of fluids in medium) are affecting each other. It is also necessary to develop advanced mathematical models of polymeric liquids based on microscopic physics is a cornerstone of this understanding.

This research work is a part of a research project which focuses on developing extended polymer fluid models and solving the realistic equations of non-Newtonian fluid dynamics for idealized geometries and calibrating the results to rheological experiments.

1.1. Structure of this Master thesis

The structure of this work has been divided mainly into three sections.

•Background:

In this section, the main goal is to give an overview of polymer and the physical properties of the polymers that are used in this investigation, the rheology of the polymer as a non-Newtonian fluid, the models which describe these properties.

•Experiment:

In the experimental section, the experimental preparation, experimental setup, as well as explaining the processing of the experimental data and presenting the final experimental results in plots.

•**Analysis:**

In this section, the data obtained from the experiment are calibrated with the physical models and are observed to what extent the data do agree with the models and not.

In the final chapter, the discussion of everything of this thesis work, the conclusion of the research and the future works are presented.

1.2. Objective

The main objectives of this work are to measure the following material functions of EOR polymer solutions and investigate the relations between them:

- Steady shear flow material function: non-Newtonian viscosity;
- Small-amplitude oscillatory flow material functions: storage and loss moduli;
- Start-up and cessation of steady shear flow material functions shear stress growth and relaxation functions.

The results are compared to those predicted by tensor polymer fluid models: FENE-P dumb-bell and C-FENE-P, linear and exponential Phan-Thien-Tanner models, and Rigid dumbbell model in order to find out which models suit best for a detailed description of various kinds of polymers.

2. Literature Review

2.1. Polymer in Oil recovery

Waterflooding is the most commonly used secondary recovery method worldwide. But due to its higher mobility, it shows viscous fingering effect, which to cause less sweep efficiency and leads to an early breakthrough of injected fluid. This was first recognized by Muskat in 1949 that fluids mobility would affect waterflooding performance [Thomas, 2016]. This research leads to further studies and it was suggested to increase water viscosity to improve reservoir sweep efficiency. It was established a couple of years later by Pye and Sandiford that the mobility of the injected brine could be effectively reduced by the addition of small quantities of hydrolyzed polyacrylarmide, a water-soluble polymers [Thomas, 2016]. A schematic different between water flooding and polymer flooding can be observed in figure 1.

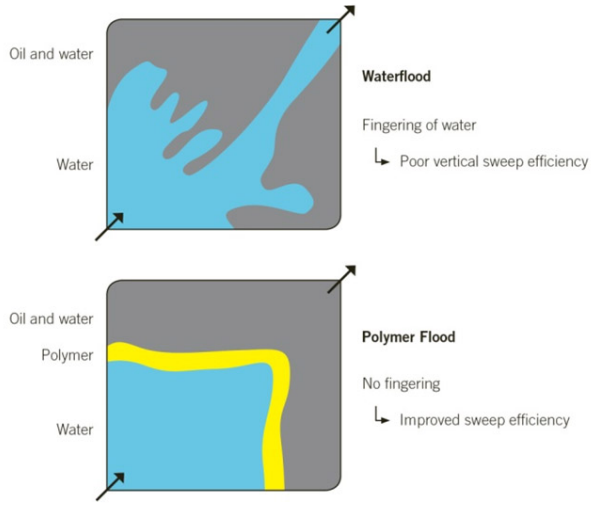

Figure 1: Typical difference between polymer and water flooding [typhonix.com, 2019].

Polymer flooding is often implemented in two cases [Thomas, 2016]:

- When the mobility ratio during a waterflood is not favorable, continuous polymer injection can improve the sweep efficiency in the reservoir.
- Even with a favorable mobility ratio, if the reservoir has some degree of heterogeneity, polymer injection can help to reduce the water mobility in the high permeability layers supporting the displacement of oil from the low-permeability layers.

It is very important to choose the right recovery method since the properties of reservoir fluid, rock, the interaction between them and how they will behave with the flooded fluid or method, because wrong method might even ruin the well or, at the very least leads to loss of resources and time [Jahn et al., 2008]. And the understanding of the rheology and material functions of the flooded fluid are essentially important since we need to know how the fluid will behave at the reservoir.

2.2. Basic Fluid Mechanics

The two physical laws governing the isothermal deformation of matter are the law of conservation of mass and the law of conservation of linear momentum. These two equations are sometimes called the equations of change [Morrison, 2001]. The Navier-Stokes equations represent both conservation of mass and conservation of momentum, while the continuity equation represents the conservation of mass. To find the velocity field of a fluid which is needed to calculate as example: forces, someone will be needed to solve these two equations.

Mathematical description

To distinguish between a scalar, a vector and a tensor quantity following notations have been used in this paper:

- normal Latin fonts for scalar
- boldface Latin fonts for vector
- boldface Greek letters for Tensor notation.

2.2.1. Conservation of Mass

In an isolated system mass is neither can be created nor destroyed and thus mass is conserved . This conservation principle is applied in continuum mechanics by the statement that the mass of any body of a continuous medium changes because of a net influx of fluid across the boundary surface S [Bird et al., 1987a].

Let assume that at an infinitesimal surface element dS the fluid is crossing the surface of volume (V) with a velocity $\boldsymbol{v}$ (figure 2). Thus,

$$\text{Local volume flow rate out} : (\boldsymbol{n} \cdot \boldsymbol{v})\mathrm{d}S$$

and

$$\text{Local mass flow rate out} : \quad \rho(\boldsymbol{n} \cdot \boldsymbol{v})\mathrm{d}S$$

where, $\boldsymbol{n}$ is the *normal unit vector*.

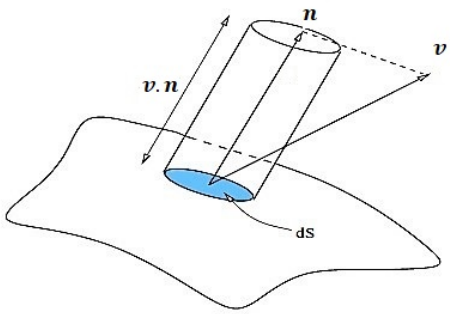

Figure 2: Arbitrary "control volume", fixed in space.

And by applying conservation of mass, the rate of change in mass inside V is caused by the net mass flow across the surface S into V. Which can be expressed as:

$$\frac{\mathrm{d}}{\mathrm{d}t}\int_V \rho \mathrm{d}V = -\int_S \rho(\boldsymbol{n} \cdot \boldsymbol{v})\mathrm{d}S. \tag{1}$$

The surface integral can be transformed into a volume integral by using Gauss divergence theorem:

$$\frac{\mathrm{d}}{\mathrm{d}t}\int_V \rho \mathrm{d}V = -\int_V (\boldsymbol{\nabla} \cdot (\rho \boldsymbol{v}))\mathrm{d}V \tag{2}$$

which leads to:

$$\int_V [\frac{\partial \rho}{\partial t} + (\boldsymbol{\nabla} \cdot \rho \boldsymbol{v})]dV = 0, \tag{3}$$

and which is true for any volume V. And by integrating over an arbitrary volume, equation 3 can be rewritten as:

$$\frac{\partial \rho}{\partial t} + (\boldsymbol{\nabla} \cdot \rho \boldsymbol{v}) = 0. \tag{4}$$

Equation 4 is valid for any general fluid and known as *equation of continuity*. Since the density (ρ) of liquids is often assumed to be constant, this equation reduces to:

$$\boldsymbol{\nabla} \cdot \boldsymbol{v} = 0. \tag{5}$$

2.2.2. Conservation of Momentum

The momentum equation governs the motion of fluids and can be seen as Newton's second law of motion for fluids. The law of momentum conservation states: "The total momentum of the fluid within volume V will increase because of a net influx of momentum across the bounding surface and because of the external force of gravity acting on the fluid". Here net influx is presented by bulk flow and by molecular motions. In other words, there is a contribution from macroscopic (bulk flow) and microscopic (molecular) motion to momentum transfer [Bird et al., 1987a]. This is known as macroscopic phenomena.

If the local volume flow rate (as mentioned in 2.2.1) is multiplied by the momentum per unit volume of the fluid, one can obtain the local momentum flow rate out due to fluid motions:

$$\begin{aligned} & (\boldsymbol{n} \cdot \boldsymbol{v}) \rho \boldsymbol{v} \mathrm{d}S \\ = \quad & (\boldsymbol{n} \cdot \rho \boldsymbol{v} \boldsymbol{v}) \mathrm{d}S. \end{aligned}$$

The microscopic phenomena which encounters due to the transport of momentum i.e., when the molecules travel must have same form as microscopic one and it can be written as: $(\boldsymbol{n} \cdot \boldsymbol{\pi})\mathrm{d}S$. Where, $\boldsymbol{\pi}$ is the total stress tensor acting on a fluid body. Now, according

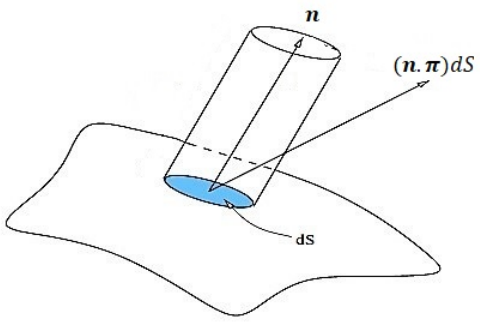

Figure 3: Element of surface dS with a transmitted force $\boldsymbol{\pi}_n dS$.

to the conservation of momentum, the rate of increase of momentum of fluid inside V:

$$\frac{\mathrm{d}}{\mathrm{d}t} \int_V \rho \boldsymbol{v} dV = \; - \int_S [\boldsymbol{n} \cdot \rho \boldsymbol{v} \boldsymbol{v}] \mathrm{d}S - \int_S [\boldsymbol{n} \cdot \boldsymbol{\pi}] dS + \int_V \rho \boldsymbol{g} \mathrm{d}V. \tag{6}$$

Again, applying the Gauss divergence theorem it leads to:

$$\int_V \frac{\partial}{\partial t} \rho \boldsymbol{v} dV = \; - \int_V [\boldsymbol{\nabla} \cdot \rho \boldsymbol{v} \boldsymbol{v}] \mathrm{d}V - \int_V [\boldsymbol{\nabla} \cdot \boldsymbol{\pi}] dV + \int_V \rho \boldsymbol{g} \mathrm{d}V. \tag{7}$$

Since the volume V is arbitrary, this can be written as:

$$\frac{\partial}{\partial t}\rho \boldsymbol{v} = -[\boldsymbol{\nabla} \cdot \rho \boldsymbol{v}\boldsymbol{v}] - [\boldsymbol{\nabla} \cdot \boldsymbol{\pi}] + \rho g. \tag{8}$$

Equation 8 is know as *equation of motion*.

A third conservation law is conservation of energy, and it is essential in solving non-isothermal problems. But it will not be discussed here.

2.2.3. Stress Tensor

In many physical problems it is often needed to work with quantities that require the simultaneous specification of two directions. Since the quantities are sometimes not the same in both directions, specifying the two directions is not sufficient; the order or magnitude in which the directions are given must be agreed upon [Bird et al., 1987a]. A tensor is an ordered pair of coordinate directions. While scalars (rank zero) and vectors (rank zero) are also tensors and express physical entities (magnitude, magnitude and direction), tensors are operators (magnitude and two or more directions)[Morrison, 2001]. A rank two tensor can be expressed as a matrix. It needs to understand that all rank two tensors are two dimensional matrices, but not all matrices are rank two tensors necessarily.

The tensors are discussed in this thesis work are second-order tensors. Second-order tensors are formed by the indeterminate vector product of two vectors. A second order tensor, or a rank two tensor, is nine scalar components that can be expressed as,

$$\text{Tensor} \qquad \boldsymbol{\tau}_{i,j} = \begin{bmatrix} \tau_{xx} & \tau_{xy} & \tau_{xz} \\ \tau_{xy} & \tau_{yy} & \tau_{yz} \\ \tau_{xz} & \tau_{yz} & \tau_{zz} \end{bmatrix} \tag{9}$$

Total Stress Tensor The total stress ($\boldsymbol{\pi}$) acting on a fluid body is a unique property of fluid type. It can be expressed as:

$$\text{Total stress tensor,} \qquad \boldsymbol{\pi} = P\boldsymbol{\delta} + \boldsymbol{\tau} \tag{10}$$

where,

P is known as thermodynamic pressure, a function of ρ and T,

$\boldsymbol{\delta}$ is known as Kronecker Delta, an Identity tensor and

$\boldsymbol{\tau}$ is the anisotropic stress tensor, depends on the nature of fluid. Also know as extra stress tensor which associates with viscosity of the fluid [Bird et al., 1987a]. The stress

distribution of a body can be expressed as figure 4. It can be represented by equation 10. At equilibrium condition the value of $\boldsymbol{\tau}$ is zero. In this thesis it will be referred as *stress tensor*. An equation which specify $\boldsymbol{\tau}$ is known as *constitutive equation*. The

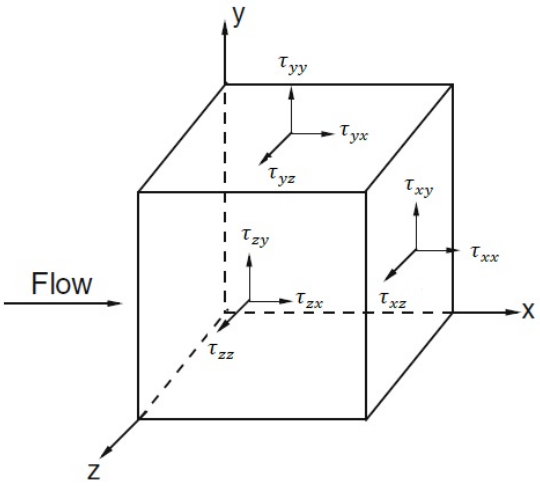

Figure 4: Stress components in three dimensional flow .

diagonal components of the stress tensor are the *normal stresses*. And the Off-diagonal components are *shear stresses*. This stress tensor is symmetric for most fluids.

2.3. Newtonian and Non-Newtonian Fluids

Now it is convenient to spotlight on the definition of Newtonian and Non-Newtonian fluids after defining the technical terms.

Matters may take three forms: solid, liquid or gaseous. Depending on temperature a solid has a definite volume and a definite form. A matter is called liquid when it has a definite volume but not a definite form. It takes the shape of the container. And a gaseous matter known as gas, whose doesn't have a specific volume or shape.

Since liquids and gases macroscopically behave similarly, the equations of motion and the energy equation for these materials have the same form, and the simplest constitutive models applied are in principle the same for liquids and gases. A common name for these models is therefore of practical interest, and the models are called fluids. A fluid is a material that deforms continuously when it is subjected to anisotropic states of stress (fig. 5) [Irgens, 2007].

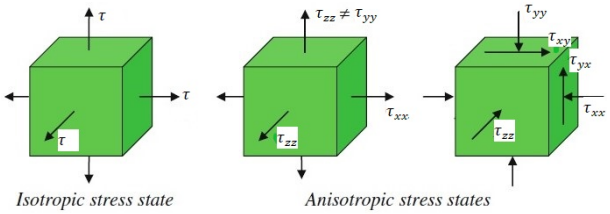

Figure 5: Isotropic state of stress and anisotropic states of stress. [Irgens, 2007]

2.3.1. Newtonian Fluid

Newton stated that the stress tensor $\boldsymbol{\tau}$ can not depend upon directly on the velocity of the fluid $\boldsymbol{v}$. But it is linear to the first derivative of $\boldsymbol{v}$, while assuming that velocity distribution $v_x(y,t)$ is linear function of y (figure 6) [Bird et al., 1987a].

After testing the Newton's assumption experimentally an equation has been established for fluid, which can be expressed as:

$$\boldsymbol{\tau} = -\mu\dot{\boldsymbol{\gamma}}. \tag{11}$$

where,

$\boldsymbol{\tau}$ is anisotropic stress tensor,

$\boldsymbol{v}$ is the velocity of the fluid

$\dot{\boldsymbol{\gamma}}$ is rate of strain tensor which is defined as,

$$\dot{\boldsymbol{\gamma}} = \boldsymbol{\nabla v} + (\boldsymbol{\nabla v})^T \tag{12}$$

Equation 11 is the most general representation of this law when the density, ρ of a fluid is constant.

Fluids that obey Newton's linear law of friction equation (11), are known as a *Newtonian fluid*, named after Newton [Irgens, 2007]. Most low molecular weight substances exhibit Newtonian flow characteristics, i.e., at constant temperature and pressure, in simple shear, the shear stress(τ) is proportional to the rate of shear ($\dot{\gamma}$) and the constant of proportionality is the familiar dynamic viscosity (μ). Such fluids are classically known as the Newtonian fluids [Krishnan et al., 2010]. Oil, water, gas are some examples of Newtonian fluid.

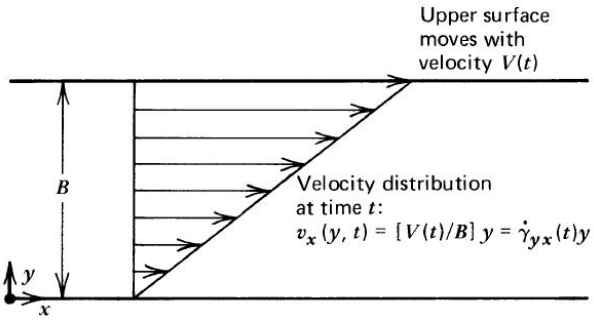

Figure 6: Velocity profile for a unsteady shear flow of a Newtonian fluid [Bird et al., 1987a].

2.3.2. Non-Newtonian Fluid

Fluids that do not follow the Newton's linear law equation (11) are called **non-Newtonian**. Fluids consist of large molecules (example: 10^6 g/mole), polymer solutions, polymer melts, Biological fluids (bloods, lymph, DNA), drilling mud are some examples of Non-Newtonian fluid.

2.3.3. Polymer

Eras of civilization have frequently been named for materials discovered and subsequently used extensively by humans (e.g., the Stone Age, the Bronze Age, etc.). Toward that end, the 20th century might appropriately be labeled as the Plastics Age or, somewhat more broadly, the Polymer Age [Wnek, 2008]. Though biological polymers (eg. DNA, protein) are the reasons to originate life. Figure 7 shows a typical structure of a biological polymer (DNA). Natural polymers like as, cotton, wood, silk, wool, rubber have been used for thousands of years in human history though their chemical composition and structure were unknown.

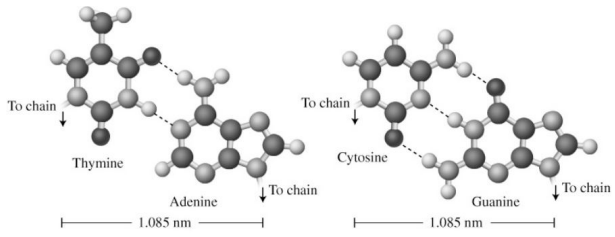

Figure 7: The pairing of bases in the DNA double helix.

Polymers are the giant molecules of chemistry. Chemists also call them macro-molecules. The word polymer derived from Greek words *poly* means many and *meros* which means parts.

The process by which polymers form is known as polymerization; which leads from a small molecule in the molecular weight range between about 30 and 150 to a large molecule in the molecule in the range of 10000 to 10 million [Kaufman and Joseph J. Falcetta, 1978].

Polymerization can happen two distinct ways:

Chain growth (addition polymerization)

Rapid chain reaction

Step growth (condensation polymerization)

Chemical reaction between pairs of reactive monomers Much slower.

2.4. Polymeric Flow Phenomena

As polymer is a non-Newtonian fluid, there are significant amount of qualitative differences between the behavior of traditional Newtonian fluids and polymer. Some examples of the effects that distinguish between Newtonian and non-Newtonian fluids are presented here. There are many more phenomena discussed and illustrated in [Bird et al., 1987a].

2.4.1. Non-Newtonian Viscosity Effect

Viscosity is the most commonly sought after rheological quantity, and viscosity is a qualitatively different property for Newtonian and non-Newtonian fluids [Morrison, 2001]. Polymeric liquids have a "Shear-rate dependent" viscosity. Means the viscosity for Non-Newtonian fluids is not a constant material function like Newtonian fluids.

The most common non-Newtonian effect is shear-thinning. Shear-thinning is the tendency of some materials to decrease in viscosity when they are driven to flow at high rates, such as by higher pressure drops. This can be shown by the following experiment:

Let's take two identical vertical tubes of which the bottoms are covered by a plate. One of them is filled with a Newtonian fluid (N) and the other one with polymeric (nN),Figure: 8. The fluids are chosen that way such that they have approximately same viscosity at lower shear rates i.e., $\eta(\dot{\gamma}) \approx \mu$ for small $\dot{\gamma}$. In addition the density of the spheres should be much larger than the densities of the fluids, so that the difference in density of fluids

may be neglected [Bird et al., 1987a]. If both fluids were Newtonian, the two spheres

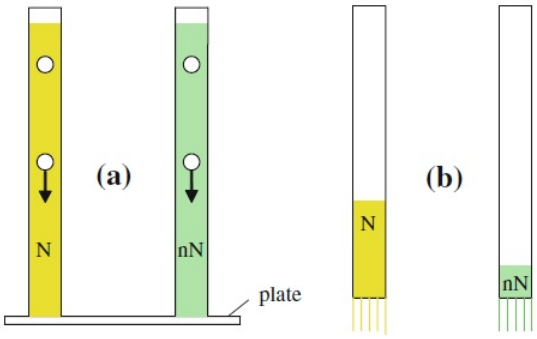

Figure 8: Falling spheres in a Newtonian fluid (N) and a shear-thinning fluid (nN) (**a**). Tube flow of the two fluids (**b**).

drop at the same rate in experiment figure 8(a) would mean that the fluids have same viscosity. Which would allow to drain the both fluids at the same rate [Bird et al., 1987a]. But due to the fact that polymer liquid has a lower viscosity at higher shear rate which is known as shear thinning effect, the polymeric fluid accelerates to higher velocities than the Newtonian fluid and which can be observable in figure 8(b). This effect can be quite shocking, with viscosity decreasing by a factor of as much 10^3 or 10^4.

Though shear thinning is the most common phenomena for non-Newtonian fluids, some of the fluids behaves just the opposite, known as shear thickening effect, viscosity increases with increasing shear rate. But these fluids are not polymers and thus shall not be discussed here.

2.4.2. Normal Stress Effects

Another most important fact that distinguish the behaviour of Newtonian and polymeric fluids is the normal stress. As mentioned earlier, Newtonian fluids don't have any normal stresses while the polymeric hence all non-Newtonian fluids exhibits normal stress in "shear flow".

The existence of non-zero normal stress components in the extra stress tensor of polymer melts differentiates viscoelastic from pure viscous flows, where the normal components are zero. The normal stresses are directly related to flow phenomena that impact polymer melt processing, e.g. die-swelling and polymer melt flow instabilities [13]. [Weissenberg, 1947] showed that polymers have "*extra tension*" along the streamline [Bird et al., 1987a]. The

fluids tend to contract along the streamlines, hence expand perpendicular to the streamlines. Some phenomena that occur due to the normal stress effect:

Rod Climbing

Also known as Weissenberg effect. When a liquid is stirred using a cylindrical rod, a vortex forms near the rod due to the centrifugal force which pushed outward the liquid from the rod in the case of Newtonian fluid (figure 9). But for the case of polymer the contrary happens. The polymer solution moves toward the center of the beaker and climbs up the rod until an equilibrium condition has been established (figure 9).

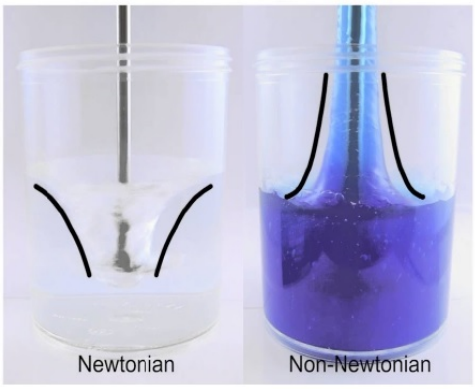

Figure 9: Rod climbing effect.

Extrudate or Die Swell Effect

This behavior is observed when polymeric melts are extruded through a die. The diameter (d_e) of liquid as it exits a circular die can be 300% larger than the diameter of the die, whereas in the case of Newtonian fluids it is just about 10% higher in the low Reynolds number limit. One of the important reasons for this phenomenon is again the normal stress difference induced by the shear flow in the die [Krishnan et al., 2010].The flowing polymeric fluids have an extra tension along the stream line [Bird et al., 1987a]. As the fluid exits the die to form a free surface with the surrounding air, the accumulated stress difference tends to push the fluid in the gradient direction, [Krishnan et al., 2010] as can be seen in figure 10.

Tubeless Siphon

In this type of typical siphoning experiment, a tube filled with liquid drains a container containing the liquid at a lower pressure, even though the tube goes higher than the liquid

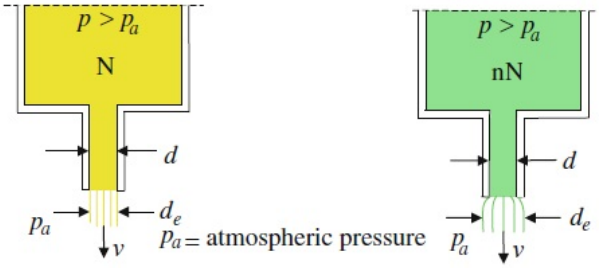

Figure 10: Swelling at extrusion.

surface. In the case of Newtonian fluid the flow through the tube will stop as soon as the siphon has been lifted up. On contrary, for non-Newtonian fluid the flow will continue with a free surface with the air without the tube. For a highly viscoelastic fluid, it is also possible to empty the container without the siphon if the container is tilted to let the fluid to start to flow over the edge. The elasticity of the fluid up to the edge and over it [Irgens, 2007] (figure 11). It is believed that the orientation and elongation of the polymer molecules along the streamlines are responsible for the large axial stresses that make the siphon work [Bird et al., 1987a].

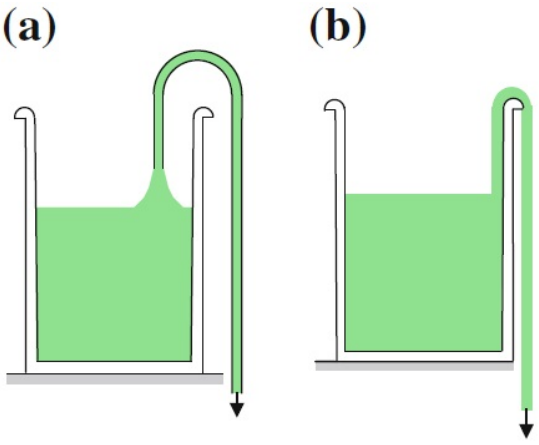

Figure 11: Tubeless siphon, Non-Newtonian fluid.

2.4.3. Time Dependent Phenomena or Memory Effect

Multiple effects caused by the fact that polymer needs time to react to the flow change which doesn't occur in the case of Newtonian fluids.

Elastic Recoil

Polymer has a tendency to turn back to the condition before the stress was applied, like a elastic solid. If a highly viscous polymer solution is poured from a bottle, the fluid will pulled out of the bottle by the weight of the entire fluid column and the tubeless siphon effect. if the fluid column is cut into two parts, the top part of the column will snap back into the bottle by the elastic recoil [Bird et al., 1987a].

Contraction flow

Sudden contraction in the confining geometry leads to very different streamline patterns in polymeric liquids. In Newtonian liquids at low Reynolds number, no secondary flows are observed, whereas in polymeric liquids, including in dilute polymer solutions, different patterns of secondary flow are observed at same Reynolds number. These include large vortices and other instabilities figure 12. These flows are undesirable in many situations in polymer processing as they lead to stagnation and improper mixing of the fluid in the vortices [Krishnan et al., 2010]. Other time dependent phenomena can be observed like

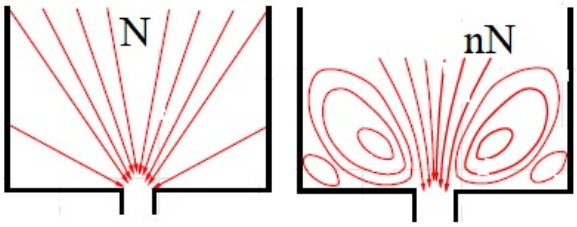

Figure 12: Flow through a contraction; a. Newtonian fluid, b. non-Newtonian fluid.

pressure stress overshoot at flow start up or relaxation effect i.e., when the when the flow is stopped, the stress inside the viscoelastic fluid does not instantly vanish. For these types of fluids the internal molecular configuration of the fluid can sustain stress for some time. This time, called relaxation time [Morrison, 2001]. But for the case of Newtonian fluid when the stress is removed the deformation stops immediately, or when the stress is applied, the deformation is constant from the beginning while in the case of polymer to reach the constant deformation it takes time.

These phenomena all have the same origin, ”hidden” in the microscopic nature of polymeric fluids. Mathematical description of such behavior cannot be done using models based on Newtonian fluid behavior and must be formulated in terms of tensors. These

phenomena can be described by material functions.

2.5. Material Function

The flow properties of incompressible Newtonian fluids are governed by the continuity equation, the equation of motion and the Newtonian constitutive equation 9110. At constant temperature, these type of fluids can be characterized by just two *material constants*: the density, ρ and viscosity, μ. To predict the behavior of incomressible Newtonian fluids the values of these two parameters are needed. The governing equations for the velocity and stress distributions in the fluid are fixed for any flow system.
par On contrary, for incompressible non-Newtonian fluids, the experimental description is much more complicated. The the continuity equation and the equation of motion remain the same, but there's no equation for τ analogous to 11, and thus it's unknown what other property or properties are needed to be measured to predict the behavior of this fluid.

A variety of experiments are performed on a polymeric liquid will yeild a host of material functions that depends on the shear rate, frequency, time and so on [Bird et al., 1987a]. The functions of kinematic parameters that characterize the rheological behavior of fluids are called *rheological material functions* [Morrison, 2001]. These material functions are used to classify fluids, and they can be used to determine constants in specific non-Newtonian constitutive equations.

Different types of material functions rises depending on the flow type of the fluid. This flow can be shear flow i.e. steady and unsteady, shear free flow/elongated flow. In this work only *shear flow* behaviors are examined.

Shear Flow

Before going further, it is important to know that during a shear flow, locally at any point there are three directions perpendicular to each other:

1. Flow direction (X).
2. The direction in which velocity changes (Y).
3. Neutral (Z)

The simplest example of this flow is fluid is flowing between two infinitely long plates (figure 13) Other some examples are, laminer pressure driven pipe flow, axial annular flow, Couette flow etc.

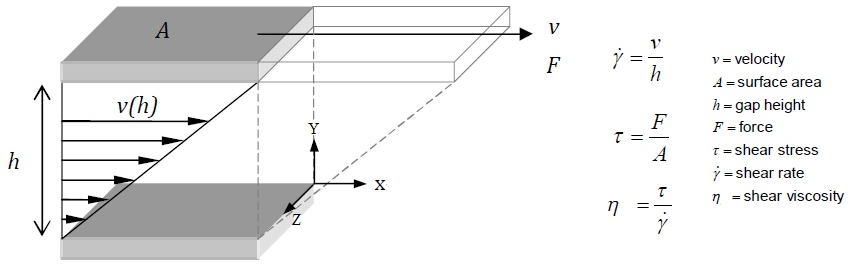

Figure 13: Velocity fields in simple shear flow.

The most common type of flow discussed in rheology is shear flow. Figure 13 shows a schematic diagram of the velocity profile in a simple shear flow. In this flow, layers of fluid slide past each other and do not mix. The flow is rectilinear in this example, and the velocity only varies in one direction, the direction Y in this diagram. Particle path lines in simple shear flow are straight parallel lines. Simple shear flow can be produced by sandwiching material between two parallel plates and then causing one plate to move at a constant velocity in some unchanging direction [Morrison, 2001]. A simple shear flow is easily generated between two parallel plates as shown in figure 13. The fluid is isotropic at equilibrium and incompressible. And the deformation is to be homogeneous [Bird et al., 1987a].

The velocity profile for *simple shear flow* is defined in Cartesian coordinates as:

$$\boldsymbol{v} = \begin{pmatrix} v_x \\ v_z \\ v_z \end{pmatrix} = \begin{pmatrix} \dot{\gamma}_{yx} y \\ 0 \\ 0 \end{pmatrix} \tag{13}$$

where, $\dot{\gamma}_{yx}$ is the velocity gradient or rate of strain, can be a function of time. The absolute value of $\dot{\gamma}_{yx}$ is called the *shear rate* $\dot{\gamma}$.

$$\text{Rate of strain, } \dot{\boldsymbol{\gamma}} = \begin{bmatrix} 0 & \partial_2 v_1 & 0 \\ \partial_2 v_1 & 0 & 0 \\ 0 & 0 & 0 \end{bmatrix} \tag{14}$$

From equation 14, $\dot{\gamma}_{xx} = 0$. Which leads equation 11 for X direction to,

$$\tau_{XX} = -0 \times \mu = 0. \tag{15}$$

The Stress Tensor for Shear Flow

For Newtonian liquids it is known that the normal stresses are equal to zero in equation 9, one example is shown in equation 15. The condition isotropic implies that the state of stress must have the the same symmetry as the state of rate of deformation as expressed in equation 14[Irgens, 2007].Besides, since no momentum has been transported in Z-Direction, $\tau_{iz} = 0$ i.e. $\tau_{zz} = \tau_{yz} = 0$. Which implies that there's only the shear stress τ_{xy} is nonzero.

For non-Newtonian fluids the normal stresses cannot be assumed to be zero. The state of stress is can be expressed as:

$$\boldsymbol{\pi} = P\boldsymbol{\delta} + \boldsymbol{\tau} = \begin{bmatrix} P + \tau_{xx} & \tau_{xy} & 0 \\ \tau_{xy} & P + \tau_{yy} & 0 \\ 0 & 0 & P + \tau_{zz} \end{bmatrix} \tag{16}$$

As polymer melts in normal cases are considered incompressible, and if the the normal stresses are isotropic, and they do not cause any deformation. Therefore, the absolute normal stress values have no rheological significant. However, the difference between the normal stresses acting in different directions causes deformation and significant from the rheological point of views [Aho, 2011].

In a viscometric flow we seek constitutive equations for the following stress and stress differences:

$$\begin{aligned} \text{Shear Stress :} \quad & \tau_{xy} \\ \text{First Normal Stress Difference :} \quad & \tau_{xx} - \tau_{yy} \\ \text{Second Normal Stress Difference :} \quad & \tau_{yy} - \tau_{zz} \end{aligned} \tag{17}$$

in simple shear flow, there are only three independent, experimentally accessible quantities as in equation 17.

2.5.1. Material Functions at Steady Shear Flow

For steady shear flow, the shear rate in equation 14 and all flow variables are time independent. It is presumed that the shear rate has been constant for such a long time that all the stresses in the fluid are *time independent*. Steady shear flow is also know as *viscometric* flow [Bird et al., 1987a].

This type of flow can be produced in a rheometer where the fluid is forced through a capil-

lary at a constant rate, and the steady pressure required to maintain in the flow measured. Another most commonly used method is to use a cone-and-plate or parallel-plate geometry and to rotate the cone or plate at a constant angular velocity while measuring the torque generated by the fluid [Morrison, 2001].

Three material functions know as viscometric functions, can be introduced in a steady shear flow:

$$\eta(\dot{\gamma}): \quad \text{the shear-rate dependent viscosity} \tag{18}$$

$$\Psi_1(\dot{\gamma}): \quad \text{the first normal stress coefficient} \tag{19}$$

$$\Psi_2(\dot{\gamma}): \quad \text{the second normal stress coefficient.} \tag{20}$$

These functions are defined as:

$$\tau_{xy} = -\eta(\dot{\gamma})\dot{\gamma}_{xy} \tag{21}$$

$$\tau_{xx} - \tau_{yy} = -\Psi_1(\dot{\gamma})\dot{\gamma}_{xy}^2 \tag{22}$$

$$\tau_{yy} - \tau_{zz} = -\Psi_2(\dot{\gamma})\dot{\gamma}_{xy}^2. \tag{23}$$

η, Ψ_1, Ψ_2 are introduced in that way so that they do not change sign if $\dot{\gamma}_{xy}$ does so.

As it has been already established that the viscosity (μ) of a Newtonian fluid is constant beyond the changing of the shear rate. And on contrary, polymer has a shear thinning feature. Which means, the viscosity ($\eta(\dot{\gamma})$) of polymer decreases with increasing shear rate. At low shear rate the viscosity $\eta(\dot{\gamma})$ is nearly constant and equal to the *zero-shear-rate viscosity*, $\eta(\dot{\gamma} = 0) = \eta_0$. This zone is also know as *Lower Newtonian Region*.

At higher shear rate, the viscosity of polymers start to decrease with increasing shear rate ($\dot{\gamma}$). At very high shear rate, the viscosity of polymers doesn't decrease anymore and show a constant characteristic and approaches equal to the *infinite-shear-rate viscosity*, $\eta(\dot{\gamma} \approx \infty) = \eta_\infty$. And this zone is also know as *Upper Newtonian Region*. For melts and concentrated solutions, η_∞ may impossible to measure since polymer degradation becomes a serious problem before reaching sufficient high shear rate [Bird et al., 1987a].

The zone where the viscosity changes with shear rate, probably is the most important property in the concept of engineering application. this region is know as "*power-law*" region.

The viscosity changing over time with respect to shear rate is mainly plotted in logarithmic scale as it is difficult to identify the power law region in linear scale while in log-log plot the linear section can be identified as the power-law region (figure 14(a)).

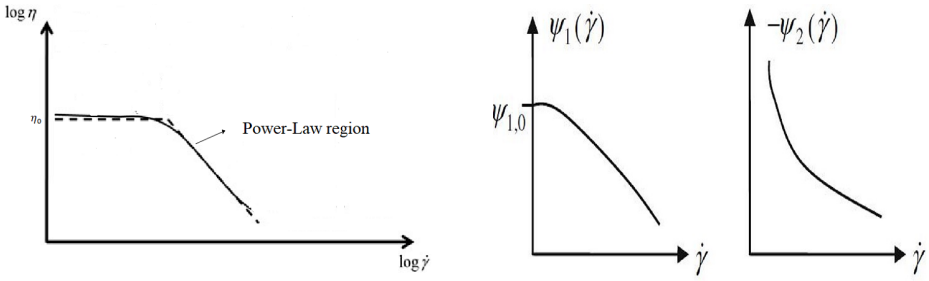

(a) (b)

Figure 14: Characteristic behavior of viscometric functions: a. viscosity function $\eta(\dot{\gamma})$, b. primary normal stress coefficient $\Psi_1(\dot{\gamma})$, and secondary normal stress coefficient $\Psi_2(\dot{\gamma})$

The first (or primary) normal stress coefficient's behavior is analogous to the viscosity behavior (figure 14(b)), i.e., at lower shear rate it is constant and equivalent to $\Psi_{1,0} = \Psi_1(0)$ and with increasing shear rate it shows a decreasing behavior. Though in the power-law region the decline rate of Ψ_1 with $\dot{\gamma}$ is much higher than that of η with $\dot{\gamma}$, and at increasing shear rate, Ψ_1 in it's large power-law region can be dropped by a factor of as much as 10^6 [Bird et al., 1987a]. At very high shear rate the value of Ψ_1 can be reach a leveling-of trend towards zero.

There's a lack of study about the second (or secondary) normal stress coefficient. But the magnitude of Ψ_2 is much smaller than Ψ_1, for polymer it's usually around 10% of Ψ_1 and typically less than zero.

Unsteady Shear Flow Material Function

The shear rate in unsteady shear flow is assumed to be time dependent, i.e., is not constant. The difference between steady state and unsteady state shear flow is that the material functions in unsteady state can depend on time or frequency as well as shear rate. This state measurement can be made in the same geometry as steady-state measurements, that is capillary flow, conr-and-plate flow etc.

Linear viscoelasticity

When very small deformation is applied to the polymer melts, or when the deforma-

tion rate is very slow, the molecules have enough time to relax through the Brownian motion and the polymer structure remains unaltered; the entangled and coiled state of the molecules is not disturbed. The deformation is said to be in the *linear viscoelastic region* [Aho, 2011]. Small-Amplitude Oscillatory Shear (SAOS) experiment is used to characterized the linear viscoelastic properties of polymer.

Non-Linear viscoelasticity

When the deformation amplitude or rate is increased, the entanglements of molecule chains start to reorganized and orientate along the flow. This applies that the deformation exceeds the limit of the linear viscoelasticity and the melt structure is destroyed. The material response becomes dependent on the rate, kinematics and magnitude of deformation, and the load is said to be in the *non-liner* region [Aho, 2011].

2.5.2. Material Functions at Small-Amplitude Oscillatory Shear (SAOS) Flow

Dynamic oscillatory shear tests are performed by subjecting a material to a sinusoidal deformation and measuring the resulting mechanical response as a function of time [Kádár et al., 2016]. Oscillatory shear tests can be divided into two regimes. One regime evokes a linear viscoelastic response (small amplitude oscillatory shear, SAOS) and the other regime is defined by a measurable nonlinear material response (large amplitude oscillatory shear, LAOS). In this work only SAOS flow will be tested.

The SAOS experiment involves measurement of the unsteady response of a sample that is contained between two parallel plates, where the upper one undergoes small-amplitude sinusoidal oscillation in its own with a frequency ω.

For a linear velocity profile, the shear rate a time t in the fluid will be independent of position and represents as:

$$\dot{\gamma}_{xy}(t) = \dot{\gamma}_0 \cos \omega t \tag{24}$$

where, $\dot{\gamma}_0$ is the positive amplitude of shear rate oscillations.
For Newtonian fluid, τ_{xy} oscillates in phase with $\dot{\gamma}$ and with frequency ω. On the other hand in the case of polymeric fluid the shear stress τ_{xy} oscillates with ω, but not in phase with $\dot{\gamma}$ where the normal stresses oscillate with 2ω, around a non-zero mean value but not in phase with $\dot{\gamma}$ or $\dot{\gamma}_{xy}$.

The shear stress is defined with two equivalent sets of linear viscoelastic material functions

and η', η'':

$$\tau_{xy} = -\eta'(\omega)\dot{\gamma}_0 \cos\omega t - \eta''(\omega)\dot{\gamma}_0 \sin\omega t. \tag{25}$$

Where, η', and η'' are known as complex viscosity (η^*) coefficient which can be expressed as:

$$\eta^* = \sqrt{\eta'^2 + \eta''^2}. \tag{26}$$

η' is also known as dynamic viscosity. It can be expressed as a function of *storage modulus*, G', which gives the information about the elastic character of the fluid or the energy storage that takes places during the deformation [Bird et al., 1987a]. Where,

$$G' = \eta''(\omega)\omega \tag{27}$$

η'' can be expressed as a function of *loss modulus*, G'', which describes the viscous character of the fluid, or the energy dissipation that occurs in flow [Bird et al., 1987a]. Where,

$$G'' = \eta'(\omega)\omega \tag{28}$$

The dynamic moduli are determined from the stress vs. strain response of the material. When the loss modulus is higher than the storage modulus, the material acts behaves more like liquid which can be observed at low frequency. While the storage modulus is higher the material acts more like a solid, which can be observed at higher frequency [Aho, 2011].

In the linear regime the strain amplitude is sufficiently small that both viscoelastic moduli are independent of strain amplitude and the oscillatory stress response is sinusoidal. The strain amplitudes used in linear oscillatory shear tests are generally very small, often on the order of $\gamma_0 \approx 10^{-2}$–10^{-1} for homopolymer melts and polymer solutions [Hyun et al., 2011]. In short, η carries a *"fluids viewpoint"* while G gives a *"solids viewpoint"* [Thompson et al., 2015].

the first and second normal stress difference can be introduced by:

$$\begin{aligned} \tau_{xx} - \tau_{yy} &= -\Psi_1^d(\omega)\dot{\gamma}_0^2 - \Psi_1'(\omega)\dot{\gamma}_0^2 \cos 2\omega t - \Psi_1''(\omega)\dot{\gamma}_0^2 \sin 2\omega t \\ \tau_{yy} - \tau_{zz} &= -\Psi_2^d(\omega)\dot{\gamma}_0^2 - \Psi_2'(\omega)\dot{\gamma}_0^2 \cos 2\omega t - \Psi_2''(\omega)\dot{\gamma}_0^2 \sin 2\omega t. \end{aligned} \tag{29}$$

Where,

Ψ_1^d, Ψ_2^d are first and second normal stress displacement coefficients;

Ψ_1', Ψ_1'', Ψ_2', Ψ_2'' are the components of complex first and second normal stress coefficients respectively.

But there is almost a little or no information about the normal stress coefficients (Ψ_s') is available.

2.5.3. Start up of Steady Shear Flow

When a sudden steady shear flow begins from a rest period, for a Newtonian fluid the stress is constant function of shear rate $\dot{\gamma}$ i.e., the viscosity is constant from the beginning of the flow. But in the case of a polymeric fluid, there's a there is a startup portion to the experiment in which the stress grows from its zero at-rest value to the steady shear value.Which means viscosity doesn't reach to it's constant value at the beginning. The condition of this experiment is:

$$\dot{\gamma} = \begin{cases} 0, & t < 0, \\ \dot{\gamma}, & t \geq 0. \end{cases} \tag{30}$$

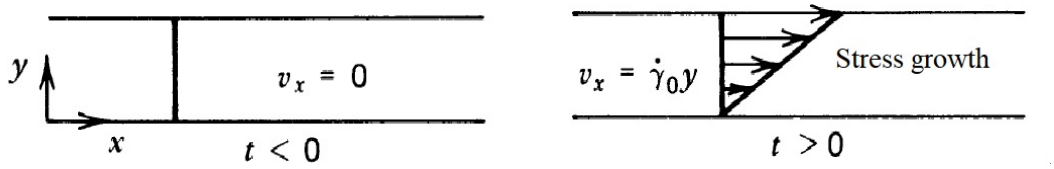

a. Fluid at rest b. Steady shear flow

Figure 15: Stress growth upon beginning steady shear flow [Bird et al., 1987a]

For the polymeric fluids the material functions aren't so simple as they are function of both time t and shear rate.

The material functions are:

$$\tau_{xy} = -\eta^+(\dot{\gamma}_0, t)\dot{\gamma}_0 \tag{31}$$

$$\tau_{xx} - \tau_{yy} = -\Psi_1^+(\dot{\gamma}_0, t)\dot{\gamma}_0^2 \tag{32}$$

$$\tau_{yy} - \tau_{zz} = -\Psi_2^+(\dot{\gamma}_0, t)\dot{\gamma}_0^2 \tag{33}$$

Here the (+) sign indicates that a steady shear rate is applied for positive times.

For polymer at high shear rate there's can be observed oscillations at the beginning of the startup. To reach stable phase it takes time, And the time varies with shear rate.

Experimentally it is found that for small shear rates the shear stress approach to its steady state value monotonically. On the other hand, for large shear rates η^+ shifts away from the linear viscoelastic envelope, goes through a maximum, and approach towards the steady state value with one or few oscillation of $\eta(\dot{\gamma})$ [Bird et al., 1987a]. Figure 16 shows the behavior. It has been observed that the time at which η^+ departs from the linear envelop decreases as $\dot{\gamma}$ is increased in such a way that the shear strain is constant where non-linear effects are first detected [Bird et al., 1987a].

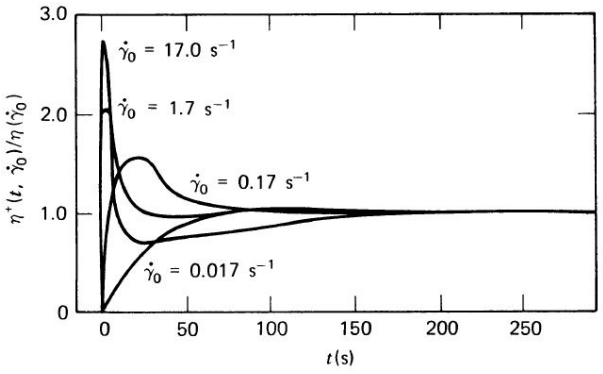

Figure 16: Shear Stress growth function $\eta^+(t, \dot{\gamma}_0)/\eta(\dot{\gamma}_0)$ for 2.0% polyisobutylene in primol [Bird et al., 1987a].

The material function will be observed in this experiment is the η^+. And it will be observed as a ratio of $\eta^+(t, \dot{\gamma}_0)/\eta(\dot{\gamma}_0)$ as it is very convenient to represent these fractions graphically, where $\eta(\dot{\gamma}_0)$ is the value at constant shear stress. And This property can be measured in cone and plate instrument. The material functions for Newtonian fluid can be written as:

$$\begin{aligned} \eta^+ &= \mu \\ \Psi_1^+(t) &= 0 \\ \Psi_1^+(t) &= 0 \end{aligned} \tag{34}$$

And it shows that the shear stress, τ_{xy} jumps instantaneously from zero to the steady value of viscosity at $t = 0$, the time at which the flow is imposed on the fluid.

2.5.4. Cessation of Steady Shear Flow

To perform this experiment, the shear rate $\dot{\gamma}$ of steady shear flow i suddenly stopped at a certain time, let's denote as $t = 0$.

While Newtonian fluids relax instantaneously when the flow stops (stress is proportional to the rate of deformation) and the all material functions becomes zero.
The condition for this experiment is:

$$\dot{\gamma} = \begin{cases} \dot{\gamma}, & t < 0, \\ 0, & t \geq 0. \end{cases} \tag{35}$$

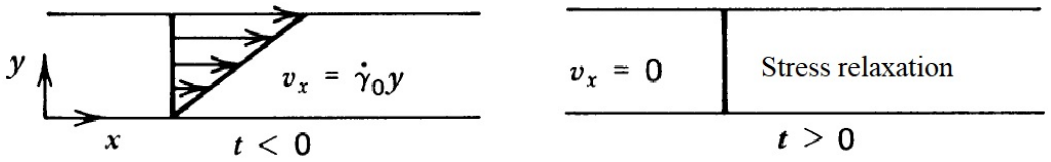

a. Fluid at rest b. Steady shear flow

Figure 17: Stress relaxation after cessation of steady shear flow [Bird et al., 1987a]

For polymeric fluids the stress doesn't goes to zero instantaneously, it decays over a time period. It has observed that the stresses relax monotonically to zero and that the relaxation happens more rapidly as the shear rate $\dot{\gamma}$ in the preceding state i.e., $t < 0$ is increased as shown in figure18. The material functions can be expressed as:

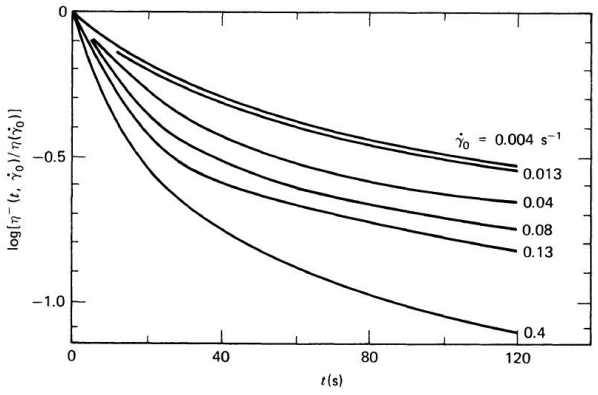

Figure 18: Shear Stress growth function $\eta^-(t, \dot{\gamma}_0)/\eta(\dot{\gamma}_0)$ for polyisobutylene melt [Bird et al., 1987a].

$$\tau_{xy} = -\eta^-(\dot{\gamma}_0, t)\dot{\gamma}_0 \tag{36}$$

$$\tau_{xx} - \tau_{yy} = -\Psi_1^-(\dot{\gamma}_0, t)\dot{\gamma}_0^2 \tag{37}$$

$$\tau_{yy} - \tau_{zz} = -\Psi_2^-(\dot{\gamma}_0, t)\dot{\gamma}_0^2 \tag{38}$$

The minus(-) sign indicates that the steady shear flow occurs before the observation. The material function will be observed in this experiment is the η^-. And it will be observed as a ratio of $\eta^-(t)/\eta(\dot{\gamma})$, where $\eta(\dot{\gamma})$ is the value when $t < 0$ i.e., when there was steady shear flow. And This property can be also measured in cone and plate instrument.

The material functions for Newtonian fluids:

$$\begin{aligned} \eta^- &= \mu \\ \Psi_1^-(t) &= 0 \\ \Psi_1^-(t) &= 0 \end{aligned} \tag{39}$$

2.6. Generalized Newtonian Fluid Model

Several models that comply with the Generalized Newtonian Fluid assumptions have been proposed in the literature. They vary in their form and in the number of parameters required to fit them to experimental results. These models have two general purposes: to obtain analytical solutions for different flow scenarios encountered in polymer processing, and to allow storage of the measured data with a minimum number of parameters [Osswald and Rudolph, 2014]. It is only assumed viscosity depends on the shear rate. The equation is similar to Newtonian constitutive equations, with an important note, that viscosity is a function dependent on components of stress tensor:

$$\boldsymbol{\tau} = -\eta(\dot{\gamma})\dot{\gamma} \tag{40}$$

All models are developed with aim to predict a linear region between two plateaus, i.e. power-law region on a plot viscosity vs shear rate.

2.6.1. The Power-Law Model

Ostwald and de Waele Proposed a simple model that accurately represents the shear thinning region in the viscosity versus shear rate curve, but neglects the Newtonian plateau observed at small strain rates, see Figure 19. The Power Law Model can be written as:

$$\eta = m(T)\dot{\gamma}^{n-1} \tag{41}$$

where m is often referred to as the consistency index and n as the Power Law or flow index. The Power Law index represents the shear thinning behavior of the polymer melt for $n < 1$ [Osswald and Rudolph, 2014].

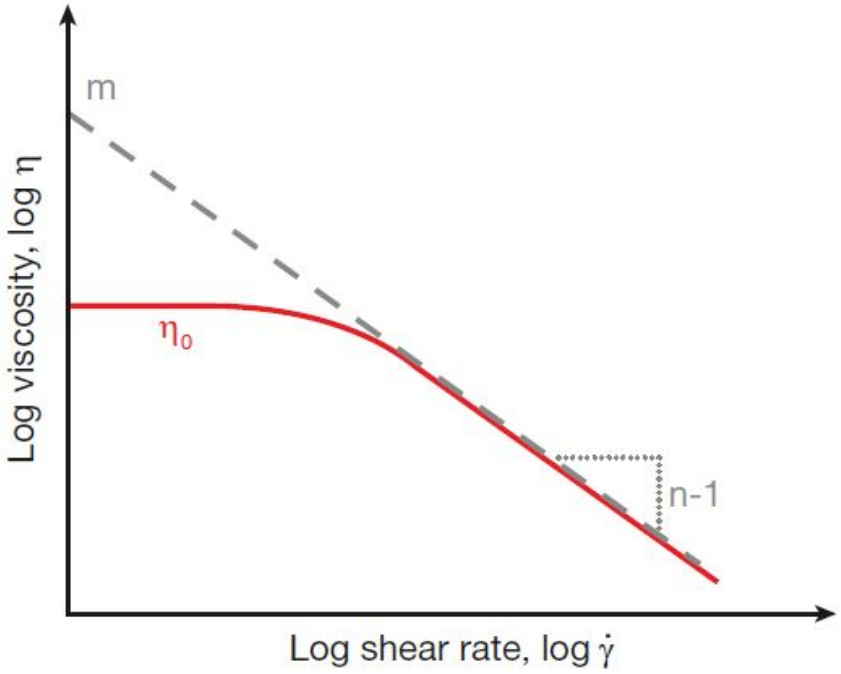

Figure 19: Viscosity curve (solid line) and approximation by the Power Law model (dashed line) in Eq. 41 [Osswald and Rudolph, 2014].

2.6.2. The Bird-Carreau-Yasuda Model

Bird, Carreau and Yasuda developed a model that accounts for the observed Newtonian plateaus and fits a wide range of strain rates [Osswald and Rudolph, 2014]:

$$\frac{\eta_{\dot{\gamma}} - \eta_\infty}{\eta_0 - \eta_\infty} = (1 + (\lambda\dot{\gamma})^2)^{\frac{n-2}{2}} \tag{42}$$

where η_0 is the zero shear rate viscosity, η_∞ is an infinite shear rate viscosity of the second Newtonian plateau, λ is a time constant, and n is the Power Law index, which accounts for the shear thinning behavior, see Fig. 20.

Some features of these *Generalized Newtonian Fluid Models* [Shogin, 2019]:

- Predict shear thinning
- Worked for steady shear flow
- Fail when flow is unsteady
- Don't predict the normal stress

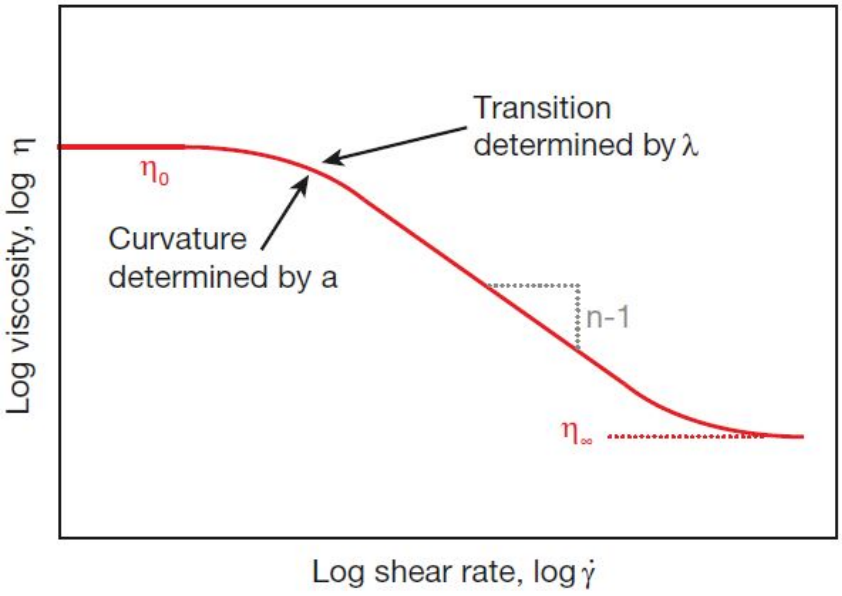

Figure 20: Viscosity approximation using the Bird-Carreau-Yasuda model in Eq. 42 [Osswald and Rudolph, 2014].

2.7. Physical non-Newtonian fluid models

Predicting flow behavior based only on mathematical derivatives are failed for all kind of models. Which implies that using only math is not enough to build a model with good prediction, the physical meaning should need to apply in mathematical equations.

Dumbbell Models

These models are used for diluted polymeric solutions, a solution where polymers interact more with the solvent than each other. In these models it is assumed that each polymer molecules are two spherical beads connected by spring or rod.

2.7.1. Hookean Dumbbells

In this model it is assumed that the two beads are connected by spring, Fig. 21. In Hookean model the force between beads assumed to be linear. It is assumed that the spring in this model obeys the Hook's law:

$$\boldsymbol{F} = H\boldsymbol{Q} \tag{43}$$

Where, $\boldsymbol{F}$ is the spring force and H is the spring stiffness and $\boldsymbol{Q}$ is the vector between beads. It turns out that this model is too simple; it does not describe shear thinning. This

Figure 21: Polymer molecule in Hookean Dumbbell model.

model does not take into account non-linearity and finite extensibility of real molecules.

2.7.2. Finitely Elongated Nonlinear Elastic (FENE) Dumbbell

Warner has proposed to consider non-linear elastic spring, which can expand only up to some maximum. In other words the connector force in this model is linear at very small extensions and is limited at high extensions.

$$\boldsymbol{F} = H\boldsymbol{Q}\frac{H\boldsymbol{Q}}{(1 - Q/Q_0)^2} \qquad Q \leq Q_0 \tag{44}$$

2.7.3. FENE-P Dumbbell

Here P stands for as an honor to Peterlin [Heel, 2000]. This model is succeeded to predict all the complex behavior that is required. Peterlin had proposed to replace the average of the elastic force by mean-squared value which is known as Peterlin's closure. The total stress tensor for FENE-P:

$$\boldsymbol{\tau} = \boldsymbol{\tau}_s + \boldsymbol{\tau}_p \tag{45}$$

Where, s represents the solvent contribution (which is assumed to be Newtonian) and p if the polymer contribution.

To find out the polymer contribution the following constitutive equation has been derived:

$$Z\boldsymbol{\tau}_p + \frac{C_3}{2}\boldsymbol{\tau}_p - (\frac{C_3}{2}\boldsymbol{\tau}_p - \boldsymbol{\delta})\frac{\mathrm{D}\ln Z}{Dt} = -\dot{\gamma} \tag{46}$$

$$Z = C_1\frac{2C_2}{C_3}\mathrm{tr}(\boldsymbol{\tau}_p) \tag{47}$$

Where C_1,C_2,C_3 are parameters of the model and constant and varies with polymer.

2.7.4. FENE-P Bead-Spring-Chain

This is an expanded version of FENE-P dumbbells, it considers polymer molecules as chains of beads connected by elastic FENE springs. It is assumed that the beads and springs are identical. N number of beads are connected with $N-1$ number of springs. And for that this model has additional N number parameters.It is expected that the molecular weight of the polymer increases with the increase in N [Bird et al., 1987b]. This model is similar to FENE-P dumbbells , but describes time-dependent flows much more realistically.

2.7.5. C-FENE-P Dumbbell Model

Proposed by Shogin and Amundsen [Shogin and Amundsen, 2019]. Where "C" stands for *charged*. Modified and extended version of FENE-P for diluted solutions of polyelectrolytes. In order to describe qualitatively the electric repulsion between the charged sections of the polymeric backbone, they have assumed the beads to carry identical effective charges q and the relative permittivity of the solvent to be ε [Shogin and Amundsen, 2019]. This modifies the connector force by an additional electrostatic Coulomb force, so that

$$\boldsymbol{F}_c = \frac{H\boldsymbol{Q}}{1-(Q/Q_0)^2} - \frac{q^2}{4\pi\varepsilon_0\varepsilon}\frac{\boldsymbol{Q}}{Q} \tag{48}$$

where, ε_0 is the permittivity of vacuum.

C-FENE-P dumbbell model contains four parameters. Of these, three are precisely those of the original FENE-P dumbbell model, and they have introduced a new dimensionless ratio E between the characteristic potential energy of the electric repulsion and the thermal energy scale of the dumbbells which is specific to C-FENE-P and describes the impact of solvent salinity on polymer rheology. The connection between E and the actual salt concentration is inverse: higher salinity means lower values of E, and vice versa. Where,

$$E = \frac{q^2/4\pi\varepsilon_0\varepsilon Q_0}{kT} \tag{49}$$

Larger values of E correspond to "stiffer" dumbbells, i. e. to increased dominance of electrostatic repulsion. In the limit E→0, the original(uncharged) FENE-P model is recovered, while the dumbbells become rigid as E→1 [Shogin and Amundsen, 2019].

2.7.6. Phan-Thien-Tanner model(PTT)

Describe the behavior of concentrated solution or melts. A solution can be called concentrated when the polymer molecules interacts mainly with each other rather than with the solvent.

The model was derived using network methodology (neuron networks)22. One of the main advantages of the model is that there are only two free parameters to be found from experiments [Thien and Tanner, 1977]. Even though the FENE-P model was build

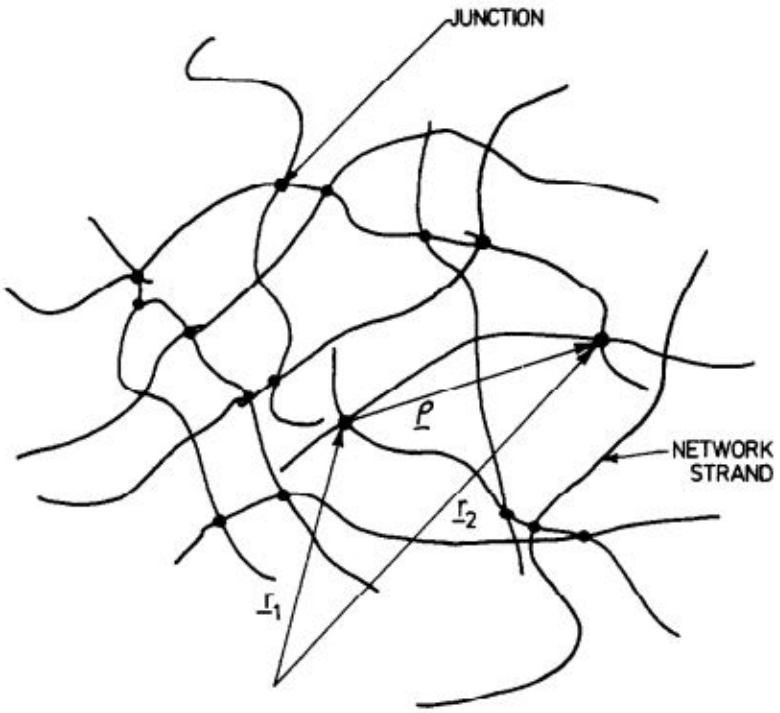

Figure 22: Typical network of polymer solutions [Thien and Tanner, 1977].

using kinetic theory and PPT was build using neuron network principles, in both cases for simple shear flow was obtained identical equations [Thien and Tanner, 1977].

3. Experimental

3.1. Work Flow

The laboratory work done in following iterative scheme:
First step was to prepare the desired concentrated solution from the pre-made "mother or stock solution" .
The next step was at rheometer laboratory to measure the material functions by the rheometer for further analysis.
Next steps were to identify zones of interest in Excel; data processing, and plot them for analysis.
The final step was to Plot these data against the respected models.

3.2. Polymers for the Experiment

In this work synthetic polymers were chosen to investigate. And tested synthetic polymers is a group of Flopaams.
Flopaam is a commercial name of group of polymers, in this work three polymers have been used: 5115VHM, 5115VLM, AN125VHM. For this group equipment parameters, measurements, diluted concentrations were taken in uniform style to have a good data set for further calculations.
Flopaams is a group of polyacrylamide polymers structural formula, figure 23 In their polymerization the key element is acrylamide. Polyacrylamide are water soluble polymers. The chemical formula $(C_3H_5NO)_n$. In polymer flooding, Polyacrylamides undergo partial hydrolysis, which causes anionic (negatively charged) carboxyl groups $(---COO^-)$ to be scattered along the backbone chain. These polymers are called Partially Hydrolyzed Polyacrylamides (HPAMs), the degree of hydrolysis is 25-35% of the Acrylamide monomers, the HPAM molecule is negatively charged [Prasad, 2018]. Three Flopaam samples were taken for this experiment.

3.3. Preparation of Polymer Solutions

A "mother/stick solution" has been made At the beginning of the experiment for every type of polymers. Then the required solutions were prepared from this mother solution by diluting some portion of it. The procedure of calculating the concentration of the solutions

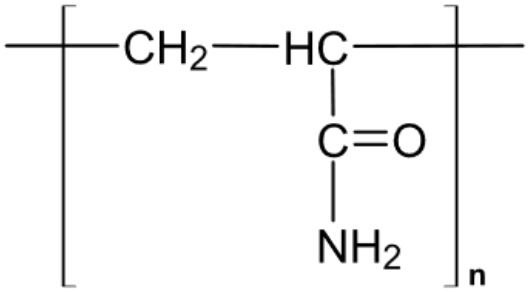

Figure 23: The structure of polyacrylamide (PAM).

Table 1: Main Parameters of Used Flopaam polymers

Flopaam	Group	Anionicity	Molecular weight
5115VHM	Acrylamide acid polymers	Medium	Very high
AN125VHM	co-polymers of ATBS	Medium	Very High
5115VLM	Acrylamide acid polymers	Medium	Very Low

has be described later. First the steps o making the solutions has been discussed.

Before making the ”mother solution”, the amount of required polymer powder and water has been calculated. To have an uniform concentration at least 500-700 gram concentrated solutions has been prepared.

This mother solution has been prepared in the ”mud-lab”. Equipment that had been used to prepare the mother solutions: laboratory scales, to weight the polymer powder and the solvent i.e., water; laboratory mixer; laboratory stirrer, mixing beakers; jars to store the ’mother solutions’.

The powder was poured into the water while the the water beaker was kept on the mixer and the mixing blade was running. Two blades mixer was chosen due to it provides proper mixing and minimum bubbles.

The mother solution had been mixed in the mixer for 24 hours to have an uniform and proper solution. Then the polymers were poured into a jar and stored in fridge to preserve and for further uses.

The experimented dilute solutions had been made from this mother solutions. The procedure was followed exactly as the mother solution except using the powder polymer, the

mother solution was is used as a source of polymer. After preparing the diluted solution, it had been mixed on the magnetic mixing stirrer before testing at the rheometer.
Equipment needed for the solution preparation:
-mixer
-magnetic stirrer
-beaker for preparing the mother solution
-scale to measure the weight
-measuring spoon
-plastic cup
-small container to store the dissolved polymer

3.3.1. Concentration Measurement

Following method was being used to calculate the concentration of the "mother solutions" and the diluted solutions:

Concentration of the Mother Solution

Supposed it was planned to prepare a mother solution with 700 g distilled water. But the water had taken after measurement was 705.59 g. And the required concentration of the polymer was 10000 ppm. Thus required amount of polymer:

$$M_p = \frac{cM_s \times 10^{-6}}{1 - c \times 10^{-6}} \tag{50}$$

where,
M_p is the required mass of polymer, g
M_s is the measured mass of solvent (in this case water) = 705.59 g
c is the desired concentration = 10000 ppm
Thus,

$$M_p = \frac{10000 \times 705.59 \times 10^{-6}}{1 - 10000 \times 10^{-6}} = 7.12718$$

Since it's not possible to take exact 7.12718 g polymer powder, the amount of powder had been taken was 7.14 g. Thus the actual concentration of the polymer became:

$$c = \frac{M_p}{(M_p + M_s) \times 10^{-}6} = 10017.8 \text{ ppm}$$

Concentration of the Dilute Solution

Supposed it was planned to prepare a diluted solution of 2000 ppm of 30 g. Thus required amount of polymer from the mother solution:

$$M_c = \frac{c}{c_0 \times m} \tag{51}$$

Where,

M_c is the theoretical mass of the concentrated polymer, g

c is the he desired concentration of the diluted solution = 2000 ppm

c_0 is the true concentration of the concentrated solution = 10017.8 ppm

m is the desired total mass of the diluted solution= 30 g

Thus the required amount of concentrated polymer:

$$M_c = \frac{2000}{10017.8 \times 30} = 5.98934 \tag{52}$$

If the amount of concentrated polymer isn't exactly 5.98934 g. The total mass of the dilute solution needed to be recalculated. The concentrated solution was taken for this case was 6.0 g. Thus the newly evaluated new total mass of the dilute solution is:

$$m = \frac{M_c c_0}{c} = \frac{6.0 \times 10017.8}{2000} = 30.0534$$

But after pouring the distill water in to the container with concentrated polymer the weight became 30.13 gram. Thus the final concentration of the diluted polymer became:

$$c = \frac{M_c c_0}{m} = \frac{6 \times 10017.8}{30.13} = 1994.92 \tag{53}$$

The calculation shown above was for preparing the "mother solution" the solution of 2000 ppm of Flopaam AN125VHM. Same calculation had been used for the other polymers.

3.4. Rheometer

Anton Paar's rheometer MCR302 was available for the experiment. Several different measuring system (MS) can be used to perform the experiments. As example:

- Concentric cylinder measuring system
- Parallel-plate measuring system

- Mooney/Ewart measuring system
- Cone-and-plate measuring system

and so on. In this experiment, cone-and-plate (CP) measuring system (MS) is been used. In this tool *constant shear rate* can be achievable due to its geometrical shape.

A cone-and-plate MS consists of a relatively flat circular cone and a plate. The term relatively has been used cause of the cone angle (α) which is recommended $\alpha = 1°$. According to DIN standards, the diameter of the cone plate should be between 2 to 20 cm. A schematic diagram of the CP MS has been shown on figure 24 [Mezger, 2006].

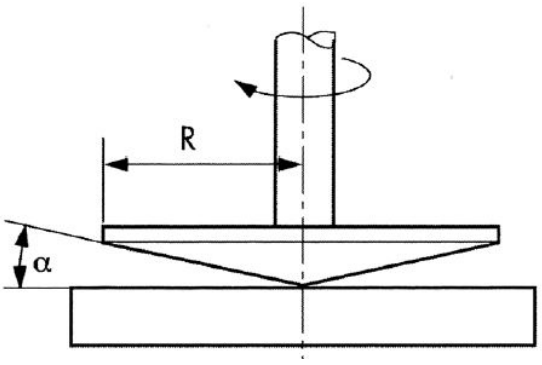

Figure 24: Cone-and-Plate measuring system [Mezger, 2006].

Main rheometer parameters

- Technical parameters

  cone angle for cone/plate tool, $\alpha = 1°$

  plate diameter, $d = 25$ mm

  gap between plates $a = 50$ μm

The preset parameters were defined during the experiment which varied experiment to experiment. The set temperature was 20°C and the normal force was $0N$.

The rheometer is connected to a PC, allowing software to process data. Different parameters and dependencies both in graphical and table can be displayed and form this allows to control the process of measurement and make changes on the early stage of experiment.

The detailed description of fluid dynamic under rheological measurement under cone/plate tool can be found in book [Bird et al., 1987a] and [Mezger, 2006].

3.5. Methods for determining the properties

3.5.1. Method for determination of apparent viscosity

Controlled shear rate (CSR) method had been used to investigate the viscosity of the polymers. With CSR, the profile of $\dot{\gamma}(t)$ is in the form of step-like function. **Calculations**

Table 2: Raw data and rheological parameter with CSR

Rotation CSR	Test present	Results
Raw data	Rotational speed, n[min^{-1}]	Torques, M[mNm]
Rheological parameter	Shear rate, $\dot{\gamma}$ [s^{-1}]	Shear stress, τ [Pa]

Following calculations has been used by the computer to calculate the properties:

Shear stress in the CP gap

$$\begin{aligned} \tau &= \frac{3M}{2\pi R^3} \\ &= C_{ss} M \end{aligned} \tag{54}$$

Where,

M is the torque

R is the cone Radius

The term C_{ss} is known as the conversion factor between M and τ and only depends on the cone radius R.

Shear rate in the CP gap

$$\begin{aligned} \dot{\gamma}(R) &= \frac{\omega}{\tan \alpha} \\ &\approx \frac{\omega}{\alpha} \\ &= C_{sr} n \end{aligned} \tag{55}$$

where,

n is the rotation per minute

α is the cone angle

ω is the angular velocity, $[rad/s] = 2\pi \frac{n}{60}$

The term C_{sr} is known as the conversion factor between n and $\dot{\gamma}$ and only depends on the cone angle α.

Thus the viscosity in the CP gap:

$$\eta = \frac{\tau}{\dot{\gamma}} \tag{56}$$

where, τ and $\dot{\gamma}$ can be found from the equations 54 and 55 respectively. The shear rate range had been used for this experiment was 0.1 to 200 s^{-1}. And the time frame was "no time limit".

3.5.2. Method for Determination of loss and storage Modulus

Frequency sweep test had been used to investigate the loss modulus G'' and storage modulus G'. Frequency sweep are oscillatory tests which is performed at variable frequencies, keeping the amplitude at a constant value. Before performing this frequency sweep test, Amplitude sweep test needed to be performed to find the Linear ViscoElastic (LVE) range [Mezger, 2006].
The storage $G'\prime$ and loss modulus G'' can be measured as:

$$G^{'} = \frac{\tau_A}{\gamma_A} \cos\delta \tag{57}$$

$$G^{"} = \frac{\tau_A}{\gamma_A} \sin\delta \tag{58}$$

Where, δ is the phase shift angle between the present and the resulting curve. γ_A is the shear strain (deformation) amplitude(%).

3.5.3. Method for Determination of Star up and Relaxation Time

The Rheological parameter can be found in this experiment is the change of shear stress over time due to sudden start or relax of the flow. The shear stress in the CP gap can is calculated by equation 54. Since $\dot{\gamma}$ is constant the ration of $\tau^{+}_{xy}/\tau_{xy}(\dot{\gamma}_0)_{xy}$ will be equal to $\eta^{+}/\eta(\dot{\gamma}_0)$.
And so for $\tau^{-}_{xy}/\tau_{xy}(\dot{\gamma}_0)_{xy}$ will be equal to $\eta^{-}/\eta(\dot{\gamma}_0)$.

4. Analysis of the Obtained Data

Graphical presentation of obtained data is the most convenient analysis of existing relations between measured parameters. During such analysis a number of points with anomaly behavior were chosen, and to confirm these points the measurements were carried out again. The repeated measurements showed random character of that anomaly points.

To perform this experiment, 5 different concentrations (one concentrated 2000 ppm, one semi diluted 1500 ppm,and three diluted 1000 ppm,500 ppm,200 ppm) has been chosen. As it is quite impossible to prepare the exact concentration, the actual concentrations of the polymers is given in table 3.

Table 3: Experimented concentrations of the polymers

flopaam	2000 ppm	1500 ppm	1000 ppm	500 ppm	200 ppm
5115VHM	1996.39	1500.12	999.513	498.457	203.234
AN125VHM	1994.92	1488.77	1000.44	500.89	198.32
5115VLM	1991.91	1501.67	994.8931	497.966	198.522

Before analyzing these plots, it is good to remember that less exactness is obtained at low shear rates for solutions with lower concentration, due to rheometer's measuring torque, and for very dilute solutions it has a very small values.

4.1. Shear Thinning Behavior

Here presented summary graphs of viscosity vs shear rate for a polymer at different concentrations. Also scaled experimental data are presented to compare with the models.

Figure 25, 26, 27 represent the viscosity and shear rates relationship for different concentration for tested polymers.

For very high molecular (VHM) weighted polymers i.e. Flopaam AN124VHM and 5115VHM, it can be noticed that the trends are pretty identical (fig. 25, 26). For higher concentration the viscosity curves are sharp linear from the beginning i.e. lower shear rate at 0.1 s^{-1}. Which is well pronounced.

For lower concentration it seems that at very low shear rate the Lower Newtonian Region is emerged. but it can be due to flow instability at low shear rate.

It is observable that both VHM polymers are showing identical trends at low and high concentration. At high concentration longer linear region have higher slope from the beginning than the lower concentration. But none of them have reached zero-shear rate viscosity region at experimented shear-rate interval. To find the zero-shear rate interval which is discussed in 2.5.1, it is needed to investigate at much lower shear rate.

On the other hand, Flowpaam 5115VLM exhibits plateau at lower shear rate, (figure 27) for lower concentration which is much clearly noticeable. The zero shear rate viscosity region is reached at this experimented region i.e. 0.1 s^{-1}. Though this region isn't longer and well pronounced as the linear region.
After this observation, it can be safely said that the viscosity trend at different shear rates doesn't only depend on the concentration of the polymer but also on the molecular weight.

These trends can be explained by Dumbbell models, specially by FENE-P chain model, section 2.7. The more beads are in the polymer molecule, the longer chain that represents this molecule, hence higher molecular weight.

Attempts has been taken by [Lutskina, 2018] to fit the experimental data with different models. Figure 4.1, 4.1, and 4.1 shows the experimental result of this work and the model fitting results from [Lutskina, 2018]. It is needed to remember that the model fitting

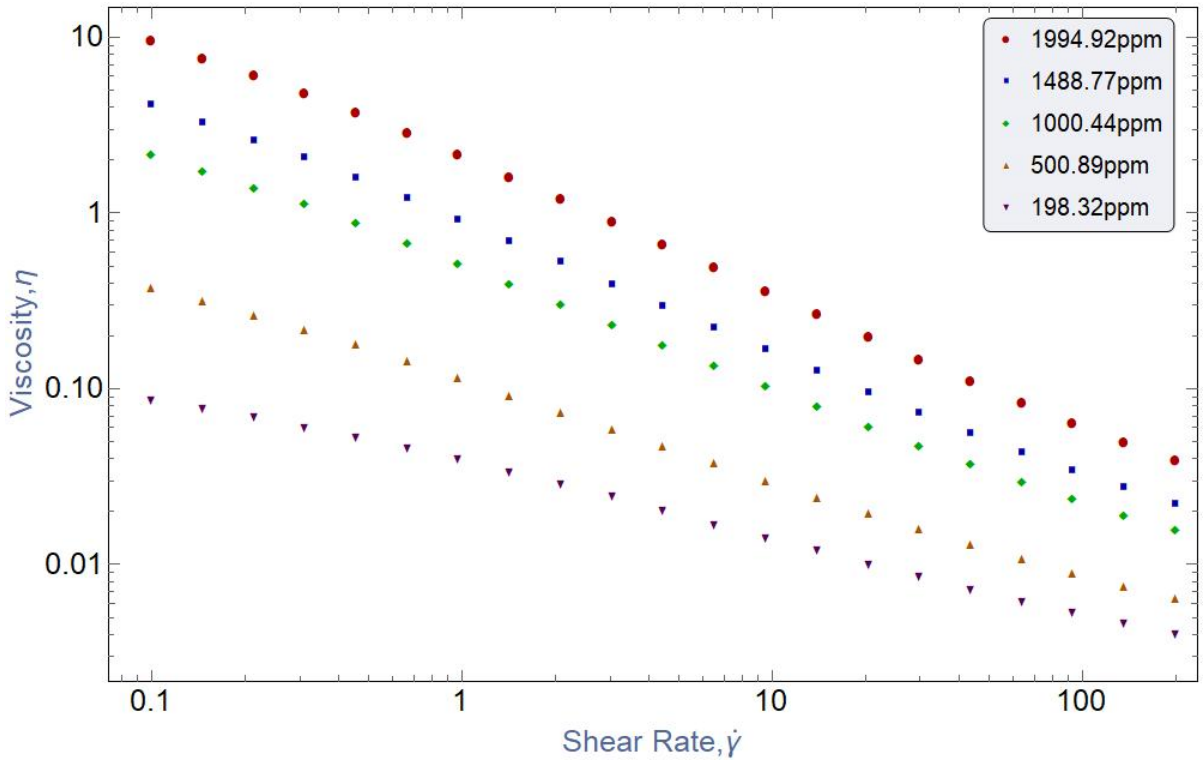

Figure 25: Viscosity vs shear rate at different concentrations, Flopaam AN125VHM.

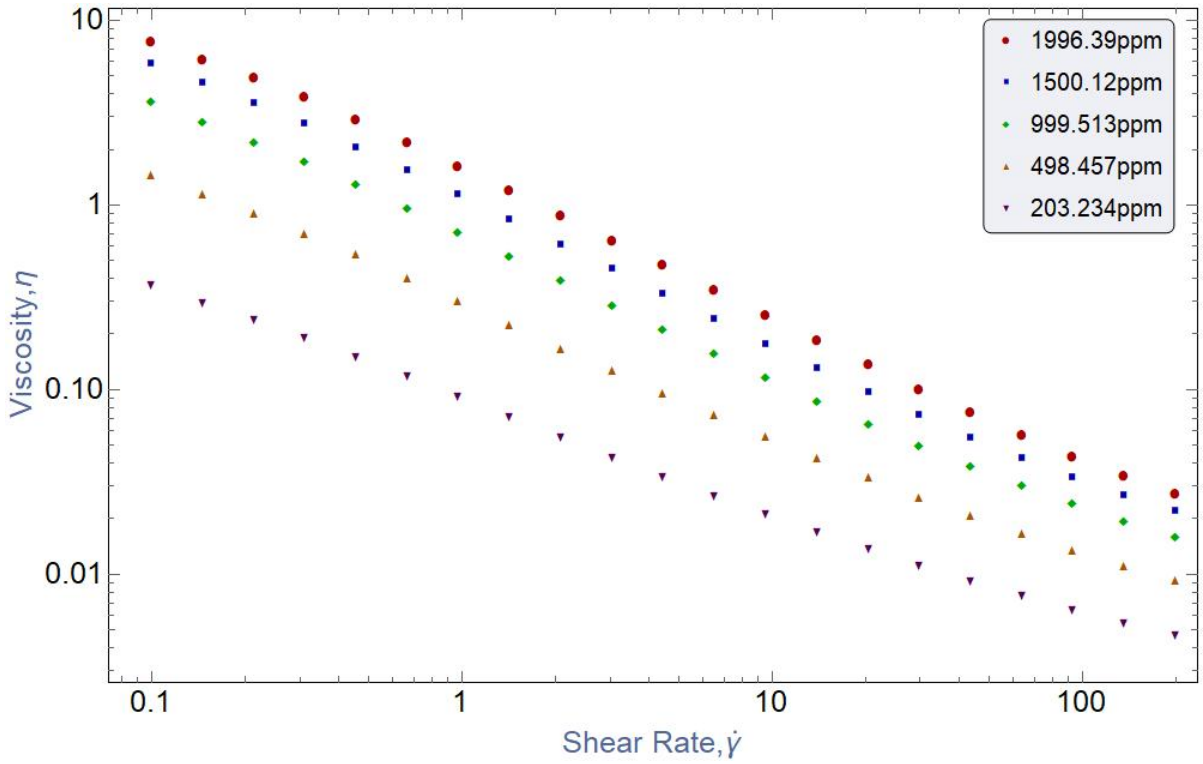

Figure 26: Viscosity vs shear rate at different concentrations, Flopaam 5115VHM.

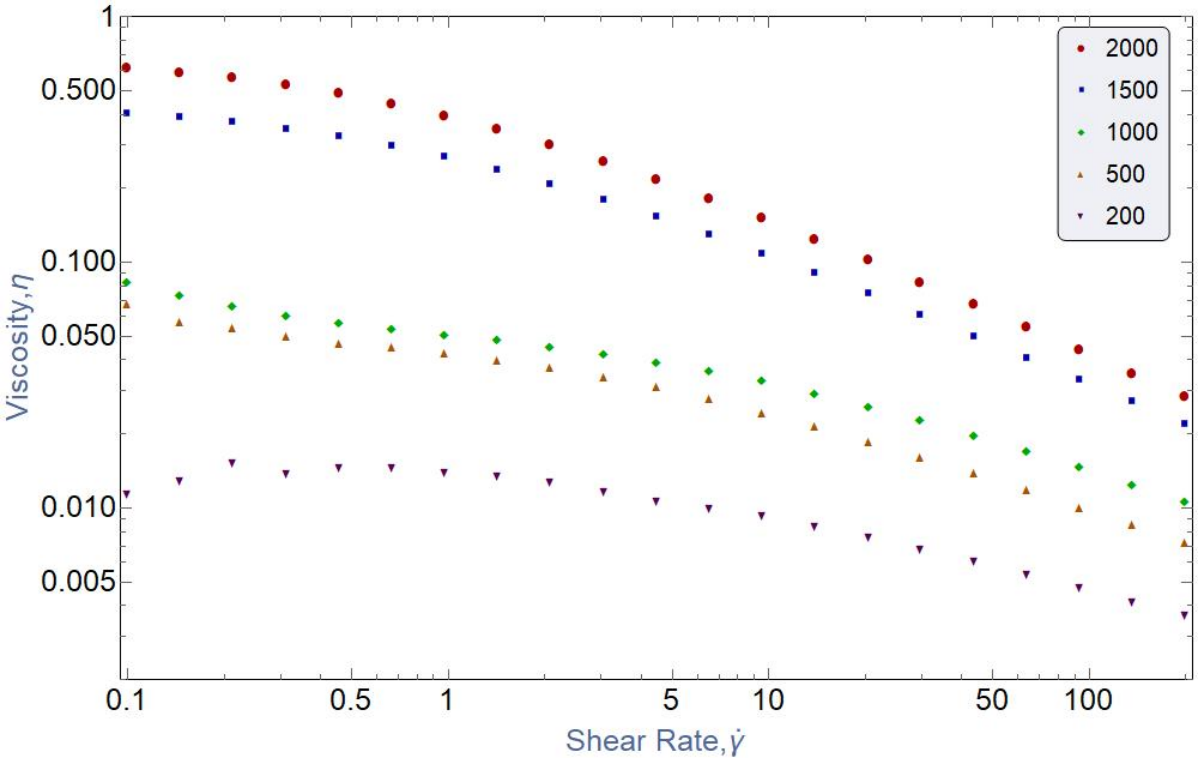

Figure 27: Viscosity vs shear rate at different concentrations, Flopaam 5115VLM.

results are scaled based on model while the experimental ones are not. Different trends are observed for different types of polymers.

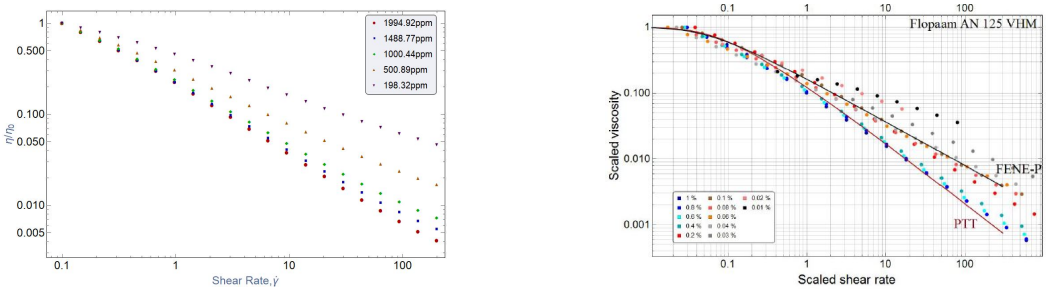

a. Experimented data b. Model fitting results [Lutskina, 2018]

Figure 28: Scaled curves viscosity vs shear rate at different concenttrations, Flopaam AN125VHM

It can be concluded that there is no one universal model that can be applied to all polymers. There are different models should be used, even for one polymer, to describe high, low and mid concentrations. This means that any flow prediction should start with laboratory test to identify which model can be applied [Lutskina, 2018].

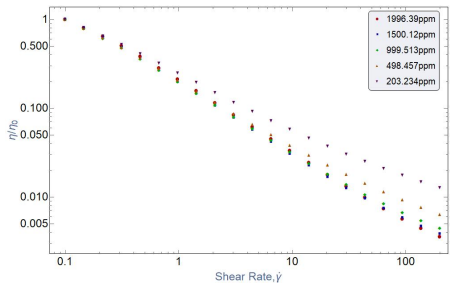

a. Experimental data

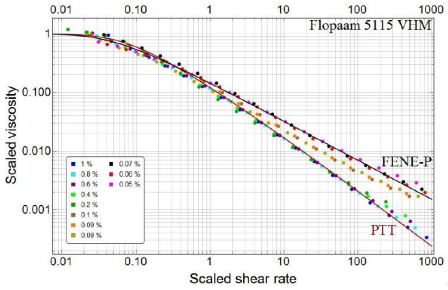

b. Model fitting results [Lutskina, 2018]

Figure 29: Scaled curves viscosity vs shear rate at different concenttrations, Flopaam 5115VHM

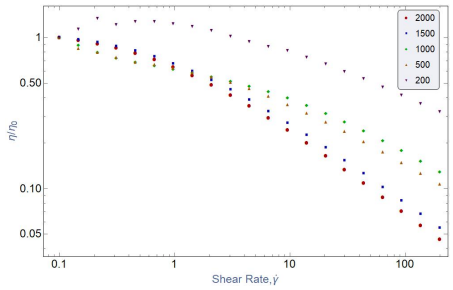

a. Experimental data

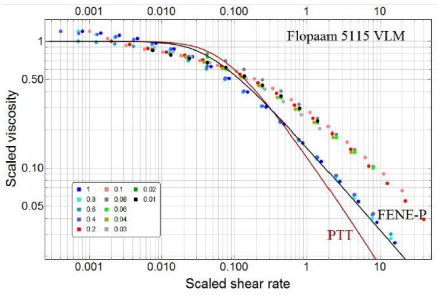

b. Model fitting results [Lutskina, 2018]

Figure 30: Scaled curves viscosity vs shear rate at different concenttrations, Flopaam 5115vlm

4.2. Storage and Loss Modulus

The storage modulus is a monotonically increasing function of frequency. At high frequency it tends to a constant value. In this experiment it is tested in a small range and thus the constant value cant be observed in the plots (figure 31) top two and bottom left. When the storage modulus is numerically plotted in normalized form, the G' is a square function of ω at lower frequency. And it tends to a constant value at higher frequency [Shogin and Amundsen, 2019] (figure 31 bottom right).

The loss modulus,G'' shows an increasing behavior at lower frequency and reaches to a maximum value called plateau. And then starts decreasing to a value of zero. In this experiment the maximum value is not observed, maybe it will appear in more higher frequency (figure 32) top two and bottom left.

When the loss modulus is numerically plotted in normalized form, the G'' shows a linear

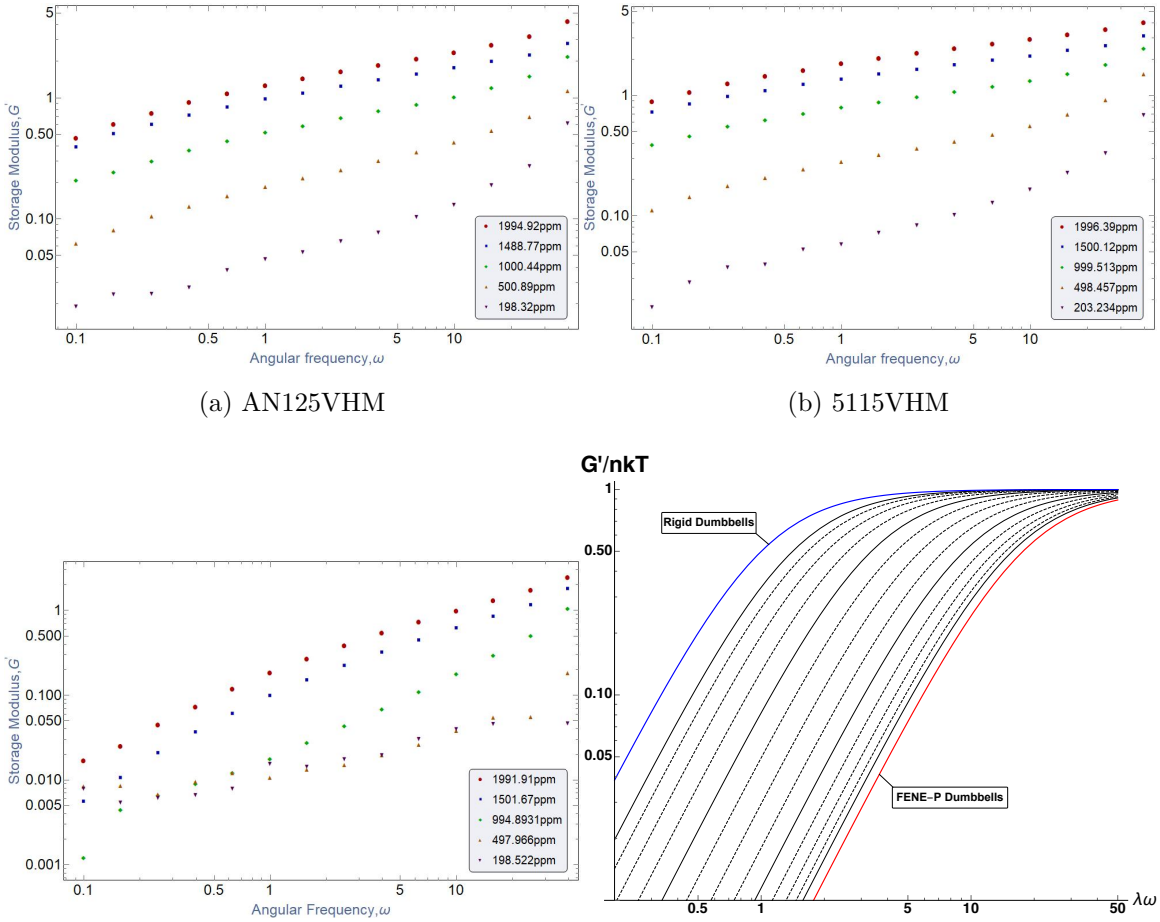

(a) AN125VHM

(b) 5115VHM

(c) 5115VLM

(d) C-FENE-P

Figure 31: Experimented storage modulus for different polymers and normalized of the C-FENE-P and FENE-P [Shogin and Amundsen, 2019] dumbbell as a function of the dimensionless frequency (bellow right).

function of ω at lower frequency and reaches a maximum value. And it tends to decrease slowly to zero with a function of ω^{-1} at higher frequency [Shogin and Amundsen, 2019] (figure 32 bottom right).

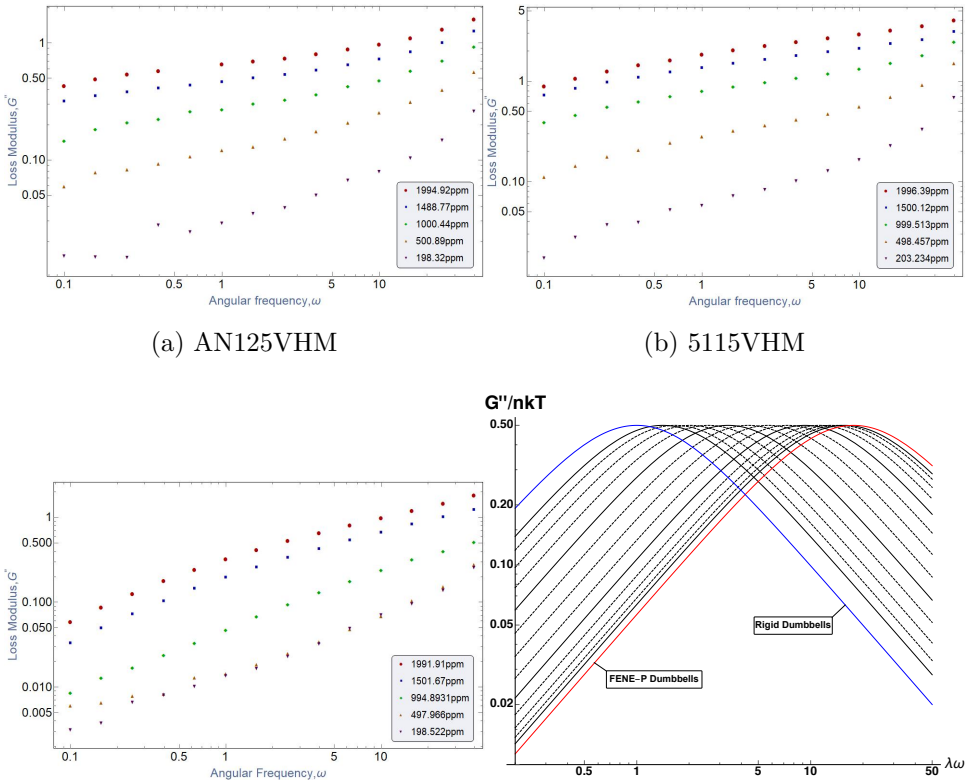

(a) AN125VHM (b) 5115VHM

(c) 5115VLM (d) C-FENE-P

Figure 32: Experimented loss modulus for different polymers and normalized of the C-FENE-P and FENE-P [Shogin and Amundsen, 2019] dumbbell as a function of the dimensionless frequency (bellow right).

Theoretically in Dumbbell models it is expected that the storage and loss modulus intersects each other at the maximum of G''. But in experiment that does not happen at the maximum of G''. A reasonable explanation can be, Dumbbell models are to simplistic, Bead-Spring-Chain models can provide more precise information [Shogin, 2019]. To observe this trend two (highest and lowest) concentration is plotted for each polymer. This intersection phenomenon is not observed in this experiment, (figure 33 top two and bottom left). And this experiment is performed on the left side of the trend plot of G' and G'' (fig 33 bottom left). To observe this total trend of G' and G'' it is needed to experiment at higher frequency.

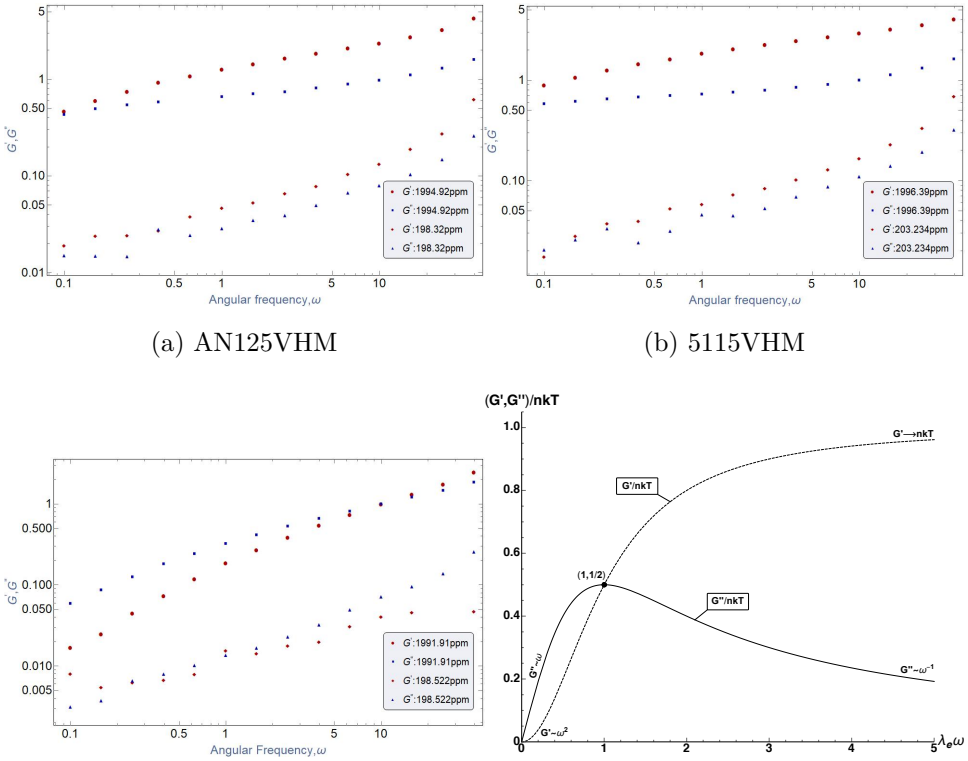

(a) AN125VHM (b) 5115VHM

(c) 5115VLM (d) C-FENE-P

Figure 33: Experimented storage and modulus for different polymers and scaled (linear) of the C-FENE-P and FENE-P dumbbell [Shogin and Amundsen, 2019] as a function of the dimensionless frequency (bellow right).

4.3. Start up and Relaxation of Steady Shear Flow

Both Start up and relaxation of steady shear flow experiment are performed with five different shear rates, $0.5s^{-1}$, $1s^{-1}$, $5s^{-1}$, $20s^{-1}$, $50s^{-1}$. The data could have been plotted in various ways. As examples, $\eta^{\pm}/\eta(\dot{\gamma}_0)$ vs t of same concentration with different shear rate for same polymer, $\eta^{\pm}/\eta(\dot{\gamma}_0)$ vs t in same shear rate for different polymers in same concentration, etc. Here, $\eta^{\pm}/\eta(\dot{\gamma}_0)$ vs t are plotted for similar shear rate (as example, $0.5s^{-1}$) for different concentration of a polymer.

4.3.1. Startup of Steady Shear Flow

Figures 34 to 38 show the stress growth distribution over time for flopaam AN125VHM.

Though it is known that at lower shear rate reaches the flow to its stable or steady state value monotonically. This phenomena is not observable in this range for this polymer. To observe this phenomena further experiment will be needed at the range which is much lower than $\dot{\gamma}_0 = 0.5s^{-1}$.

An interesting trend is found out when the relaxation time is observed for different concentration at same shear rate. The relative overshoot size first increases monotonically with increasing concentration but then start to decrease after 1000 ppm.

The overshoot can go that high that, the shear stress at the beginning of the flow can reach 2.7 times higher or even more than that for the steady state condition.

Another observation can be made from these plots is that though it is predicted that the higher the overshoot the quicker it reaches to its steady shear flow, the time needs to reach at the steady state value is looked to be almost independent at a fixed shear rate for different concentrations.

Both the overshoots and undershoots were higher for 1000 concentration ppm than the concentrations which are even higher. The reason can be as the polymer solution at 1000 ppm reaches to its semi-dilute or concentrated region from dilute region, the polymer-polymer interaction starts to take place. Besides, as there is not much data or papers are available on this kind of experiment, it was not possible to cross examine the data.

Though the overshoot for $\dot{\gamma}_0 = 1s^{-1}$, (figure 34) is observed lower than that for $\dot{\gamma}_0 = 1s^{-1}$, it's not a true representation. Rather it indicates to not having enough data points for

resolving the overshoot. This is because some data points are needed to be eliminated as there have been flow instability in the rheometer due to the recoil from the CP tool.

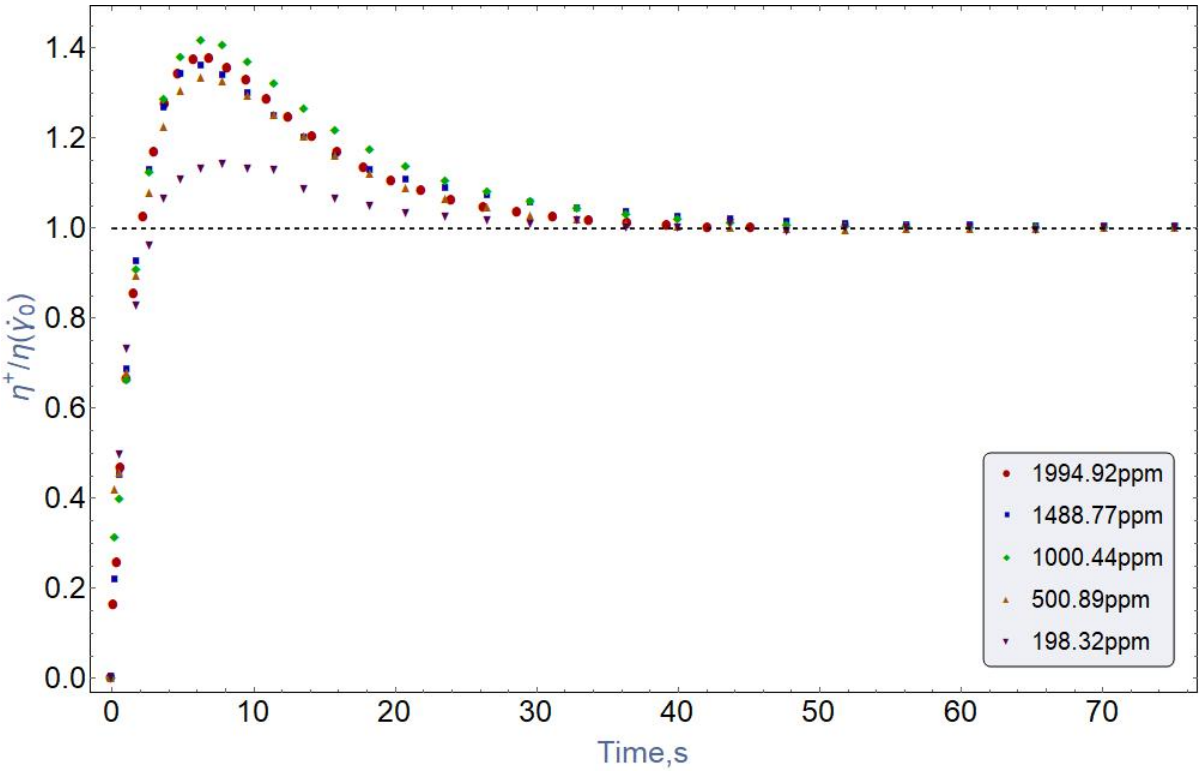

Figure 34: Shear stress growth function $\eta^+(t, \dot{\gamma}_0)/\eta(\dot{\gamma})$ for AN125VHM at $\dot{\gamma}_0 = 0.5$.

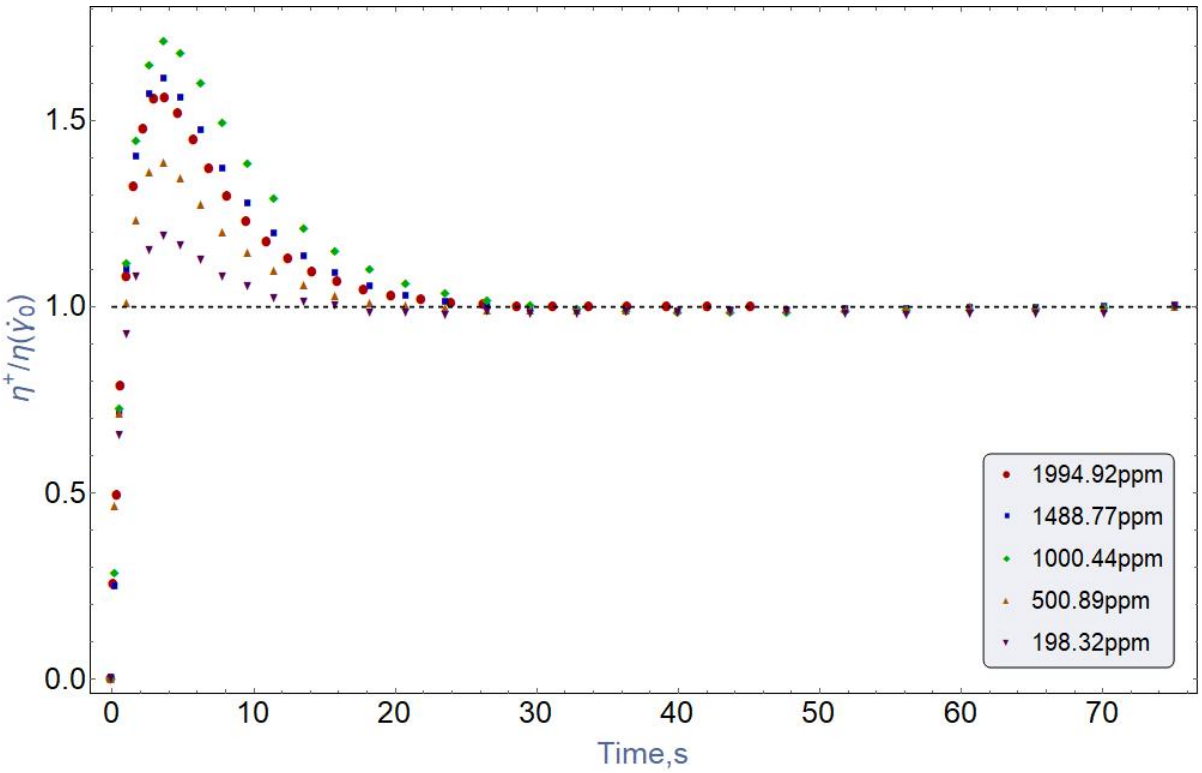

Figure 35: Shear stress growth function $\eta^+(t, \dot{\gamma}_0)/\eta(\dot{\gamma})$ for AN125VHM at $\dot{\gamma}_0 = 1$.

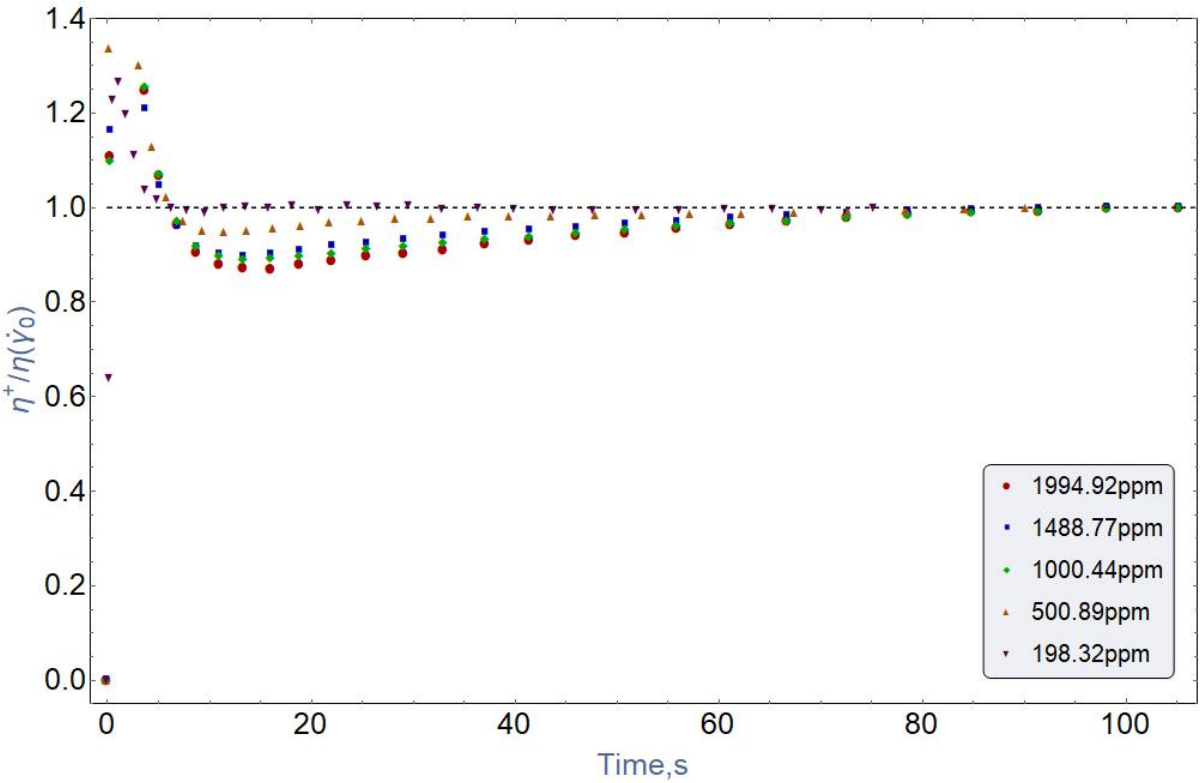

Figure 36: Shear stress growth function $\eta^+(t, \dot{\gamma}_0)/\eta(\dot{\gamma})$ for AN125VHM at $\dot{\gamma}_0 = 5$.

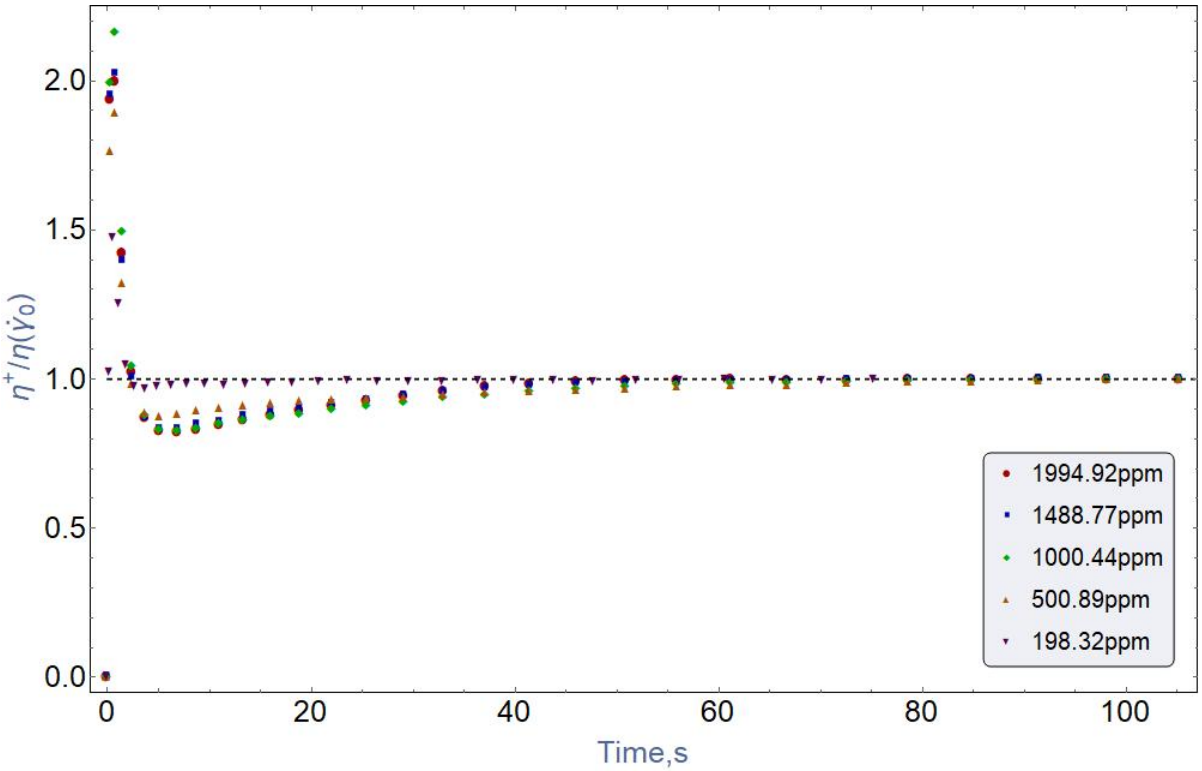

Figure 37: Shear stress growth function $\eta^+(t, \dot{\gamma}_0)/\eta(\dot{\gamma})$ for AN125VHM at $\dot{\gamma}_0 = 20$.

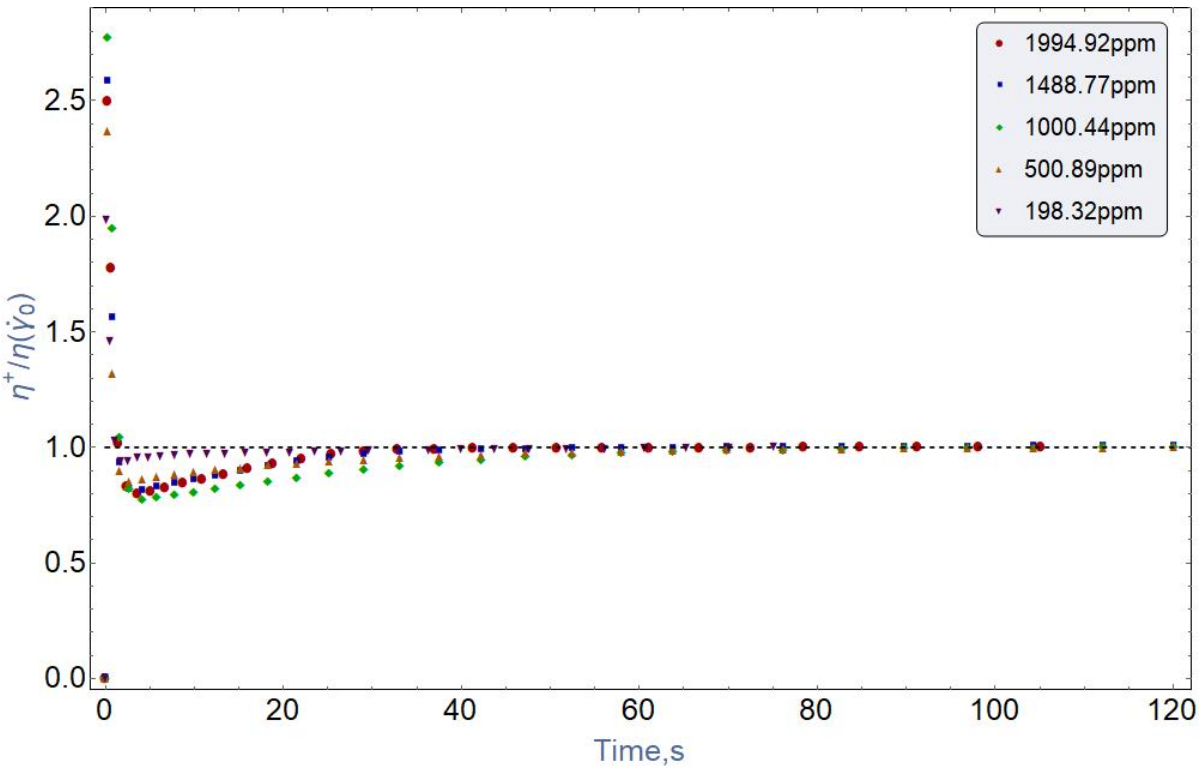

Figure 38: Shear stress growth function $\eta^+(t, \dot{\gamma}_0)/\eta(\dot{\gamma})$ for AN125VHM at $\dot{\gamma}_0 = 50$.

Another VHM polymer Flopaam 5115VHM figures 39 to 43 exhibit similar trends as the previous one.

The overshoot relative size starts to increase with increasing concentration and after reaching 1500 ppm, it starts to decay. Here it can be observed more evidently that the start-up time i.e. reaching the steady shear flow time does not depend on the concentrations. At a specific shear rate, the flow reaches to it steady zone after a sudden fix time.

Though It cannot be assumed that since the relative shear stress growth overshoot is

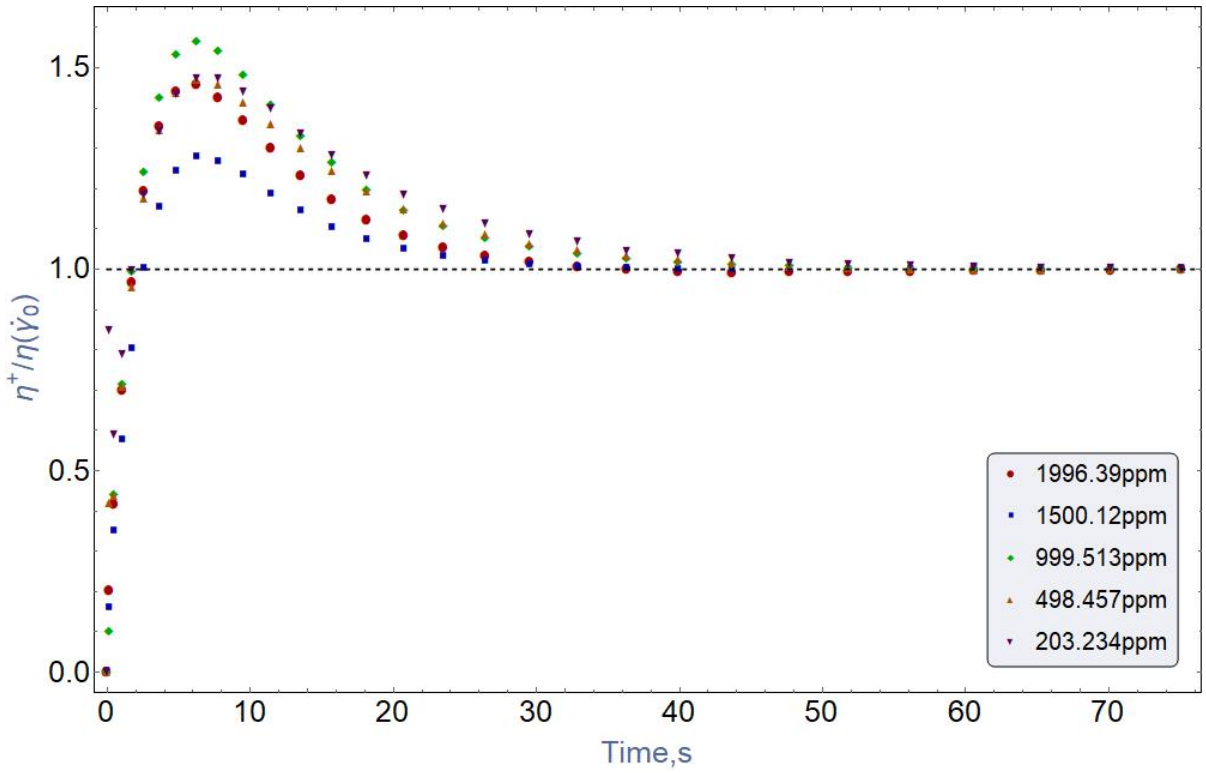

Figure 39: Shear stress growth function $\eta^+(t, \dot{\gamma}_0)/\eta(\dot{\gamma})$ for 5115VHM at $\dot{\gamma}_0 = 0.5$.

higher at 1000 and 1500 ppm for AN125VHM anf 5115VHM respectively, the shear stress also goes maximum for these two concentrations. It is important to note that that here only the relative stress growth is represented i.e, how much the shear stress departs at the beginning of a steady shear flow relative to its steady state shear stress. For 2000 ppm concentrated solution the steady state shear stress is higher than both for 1500 and 1000 ppm ones.

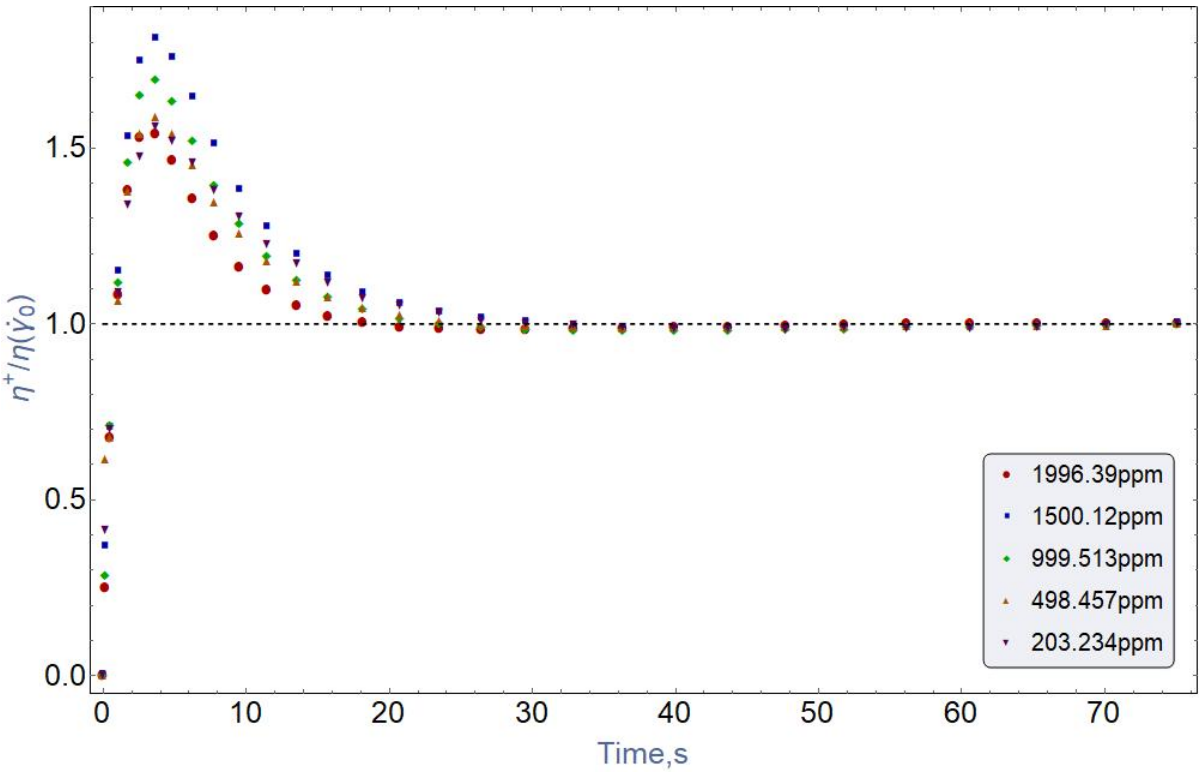

Figure 40: Shear stress growth function $\eta^+(t, \dot{\gamma}_0)/\eta(\dot{\gamma})$ for 5115VHM at $\dot{\gamma}_0 = 1$.

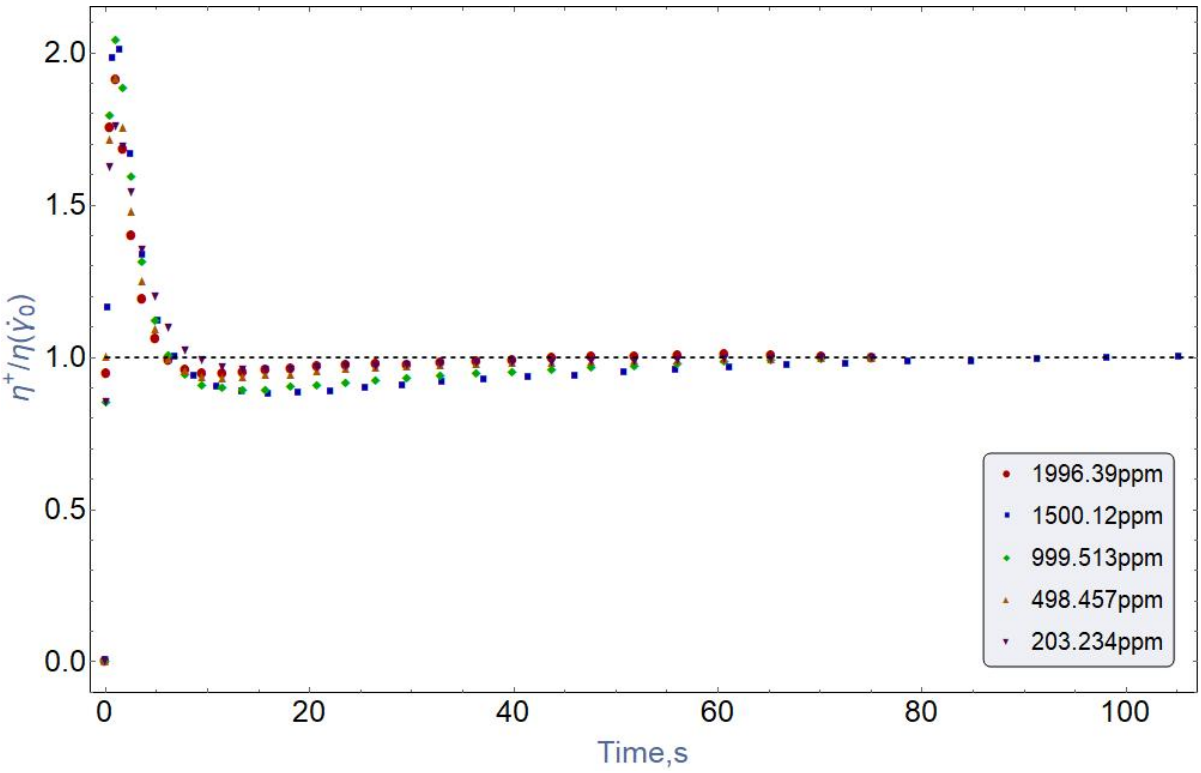

Figure 41: Shear stress growth function $\eta^+(t, \dot{\gamma}_0)/\eta(\dot{\gamma})$ for 5115VHM at $\dot{\gamma}_0 = 5$.

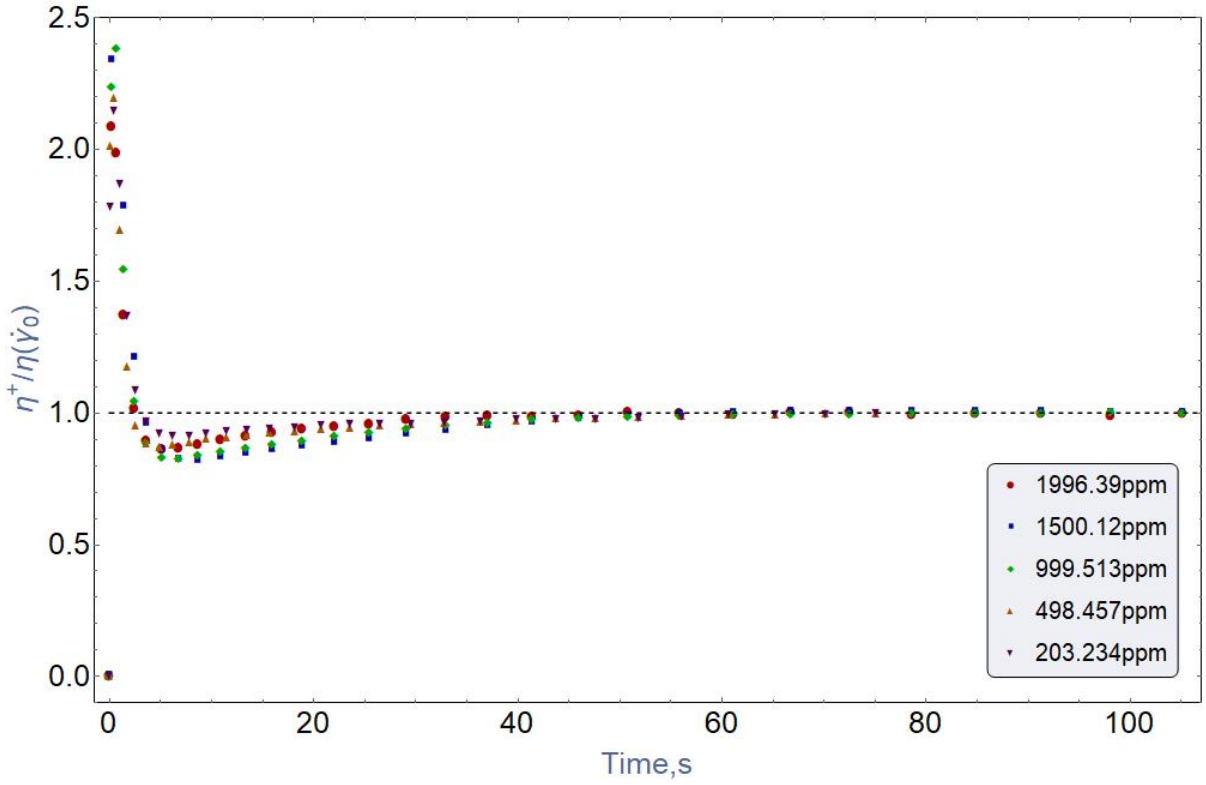

Figure 42: Shear stress growth function $\eta^+(t, \dot{\gamma}_0)/\eta(\dot{\gamma})$ for 5115VHM at $\dot{\gamma}_0 = 20$.

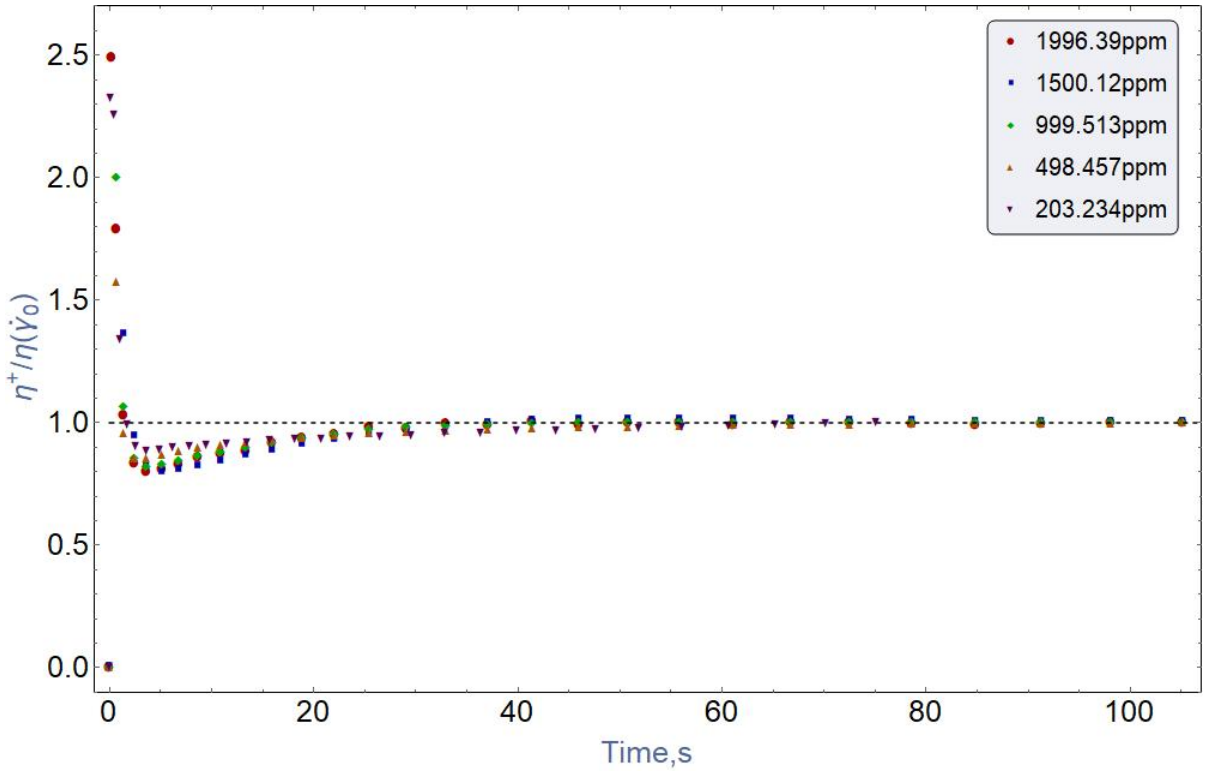

Figure 43: Shear stress growth function $\eta^+(t, \dot{\gamma}_0)/\eta(\dot{\gamma})$ for 5115VHM at $\dot{\gamma}_0 = 50$.

As a VLM group polymer, Flopaam 5115VlM (figurs 44 to 48) doesn't have as high obershoots as VHM polymers. Even for lower concentrated solutions, overshoot originally absent and it appears for higher solutions. At very lower concentrations (200 and 500 ppm) it seems that they have not reach to their steady state flow. It can happen due to two reasons. One of them is, since this polymer has very low molecular weight, at low concentration it is very diluted and the shear stress at that low concentration is very low, and this small difference between the stresses gives higher value than 1. Another reason can be at very diluted solutions noise in the data become more significant and does not give appropriate data. Further investigation is needed to identify the reason.

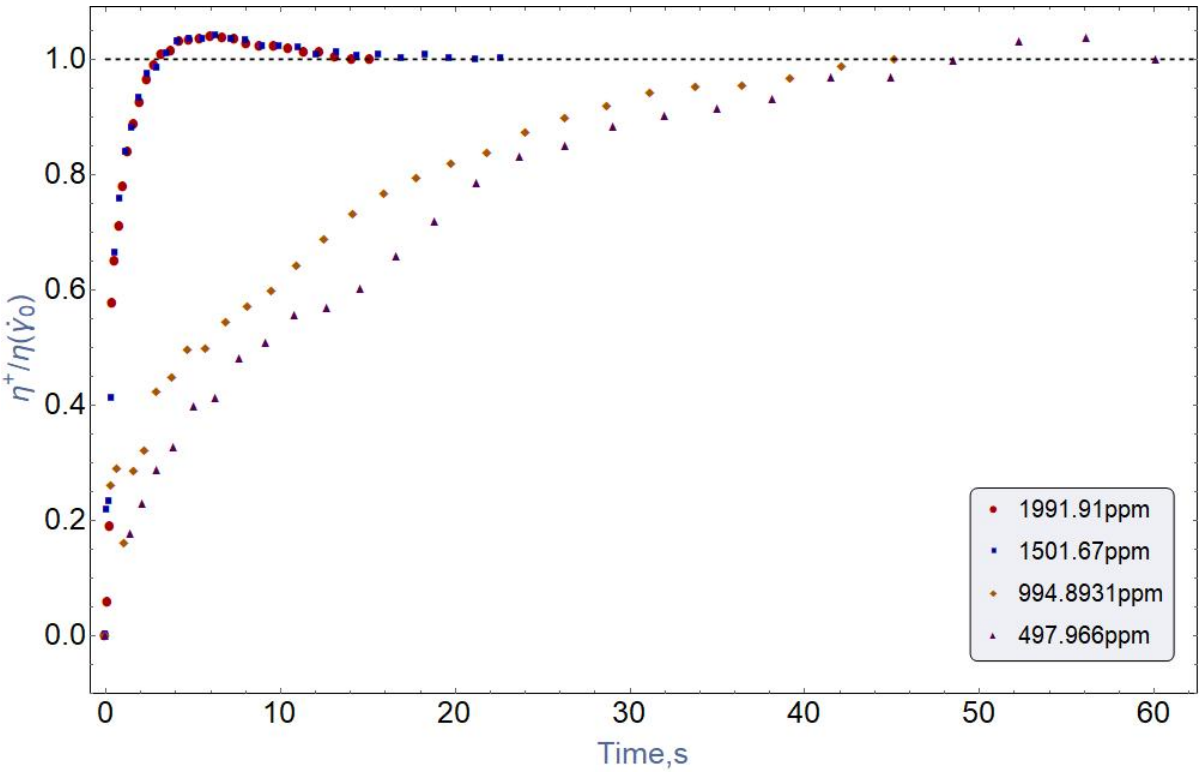

Figure 44: Shear stress growth function $\eta^+(t, \dot{\gamma}_0)/\eta(\dot{\gamma})$ for 51155VLM at $\dot{\gamma}_0 = 0.5$.

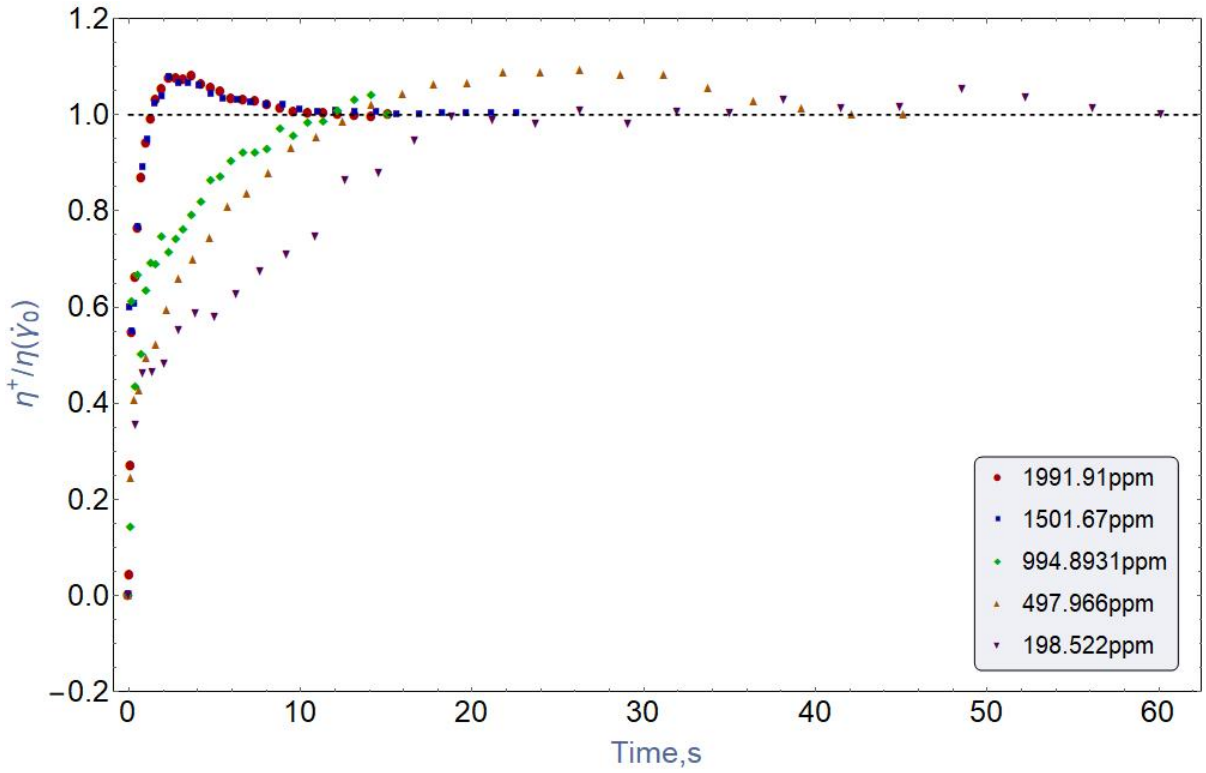

Figure 45: Shear stress growth function $\eta^+(t, \dot{\gamma}_0)/\eta(\dot{\gamma})$ for 5115VLM at $\dot{\gamma}_0 = 1$.

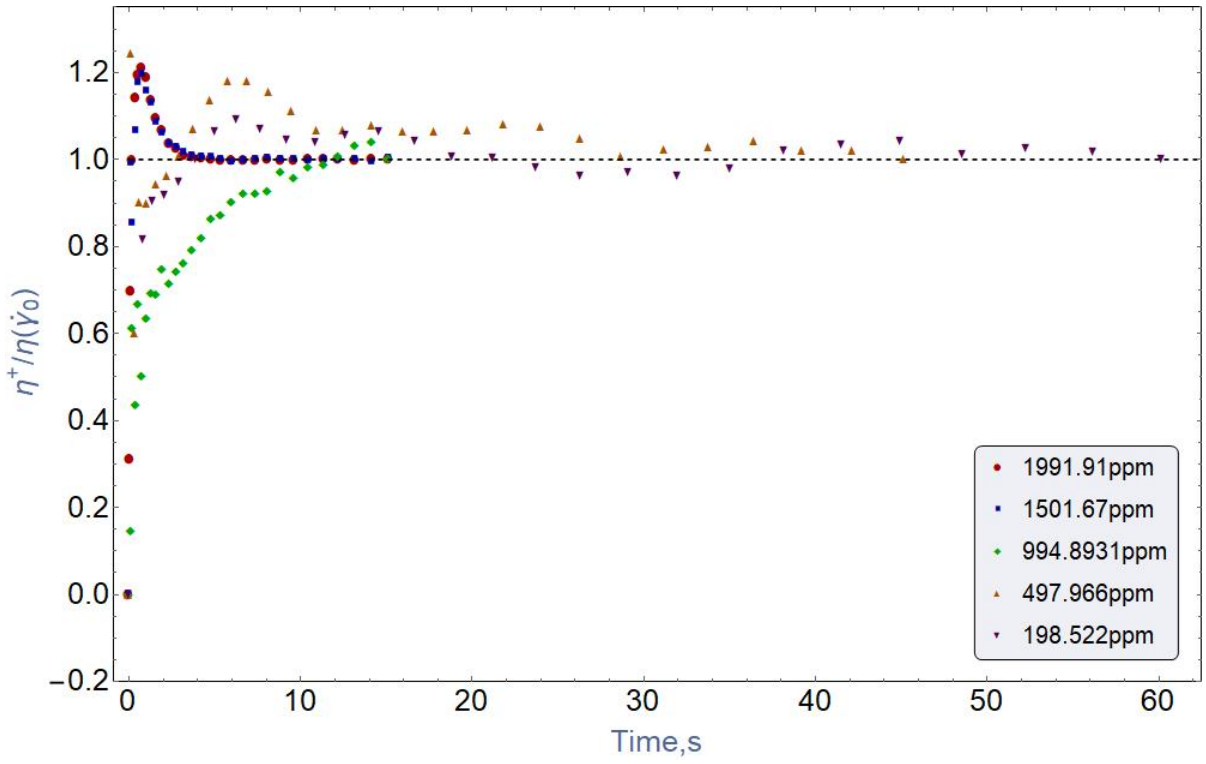

Figure 46: Shear stress growth function $\eta^+(t, \dot{\gamma}_0)/\eta(\dot{\gamma})$ for 5115VLM at $\dot{\gamma}_0 = 5$.

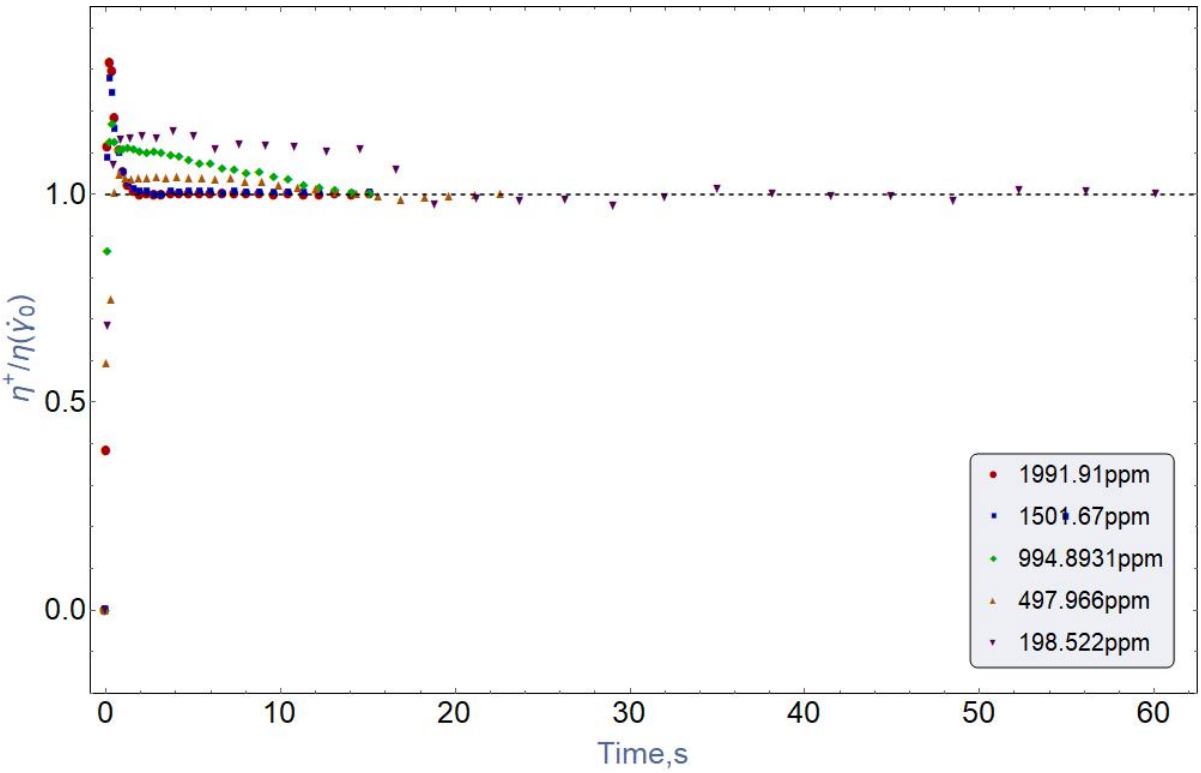

Figure 47: Shear stress growth function $\eta^+(t, \dot{\gamma}_0)/\eta(\dot{\gamma})$ for 5115VLM at $\dot{\gamma}_0 = 20$.

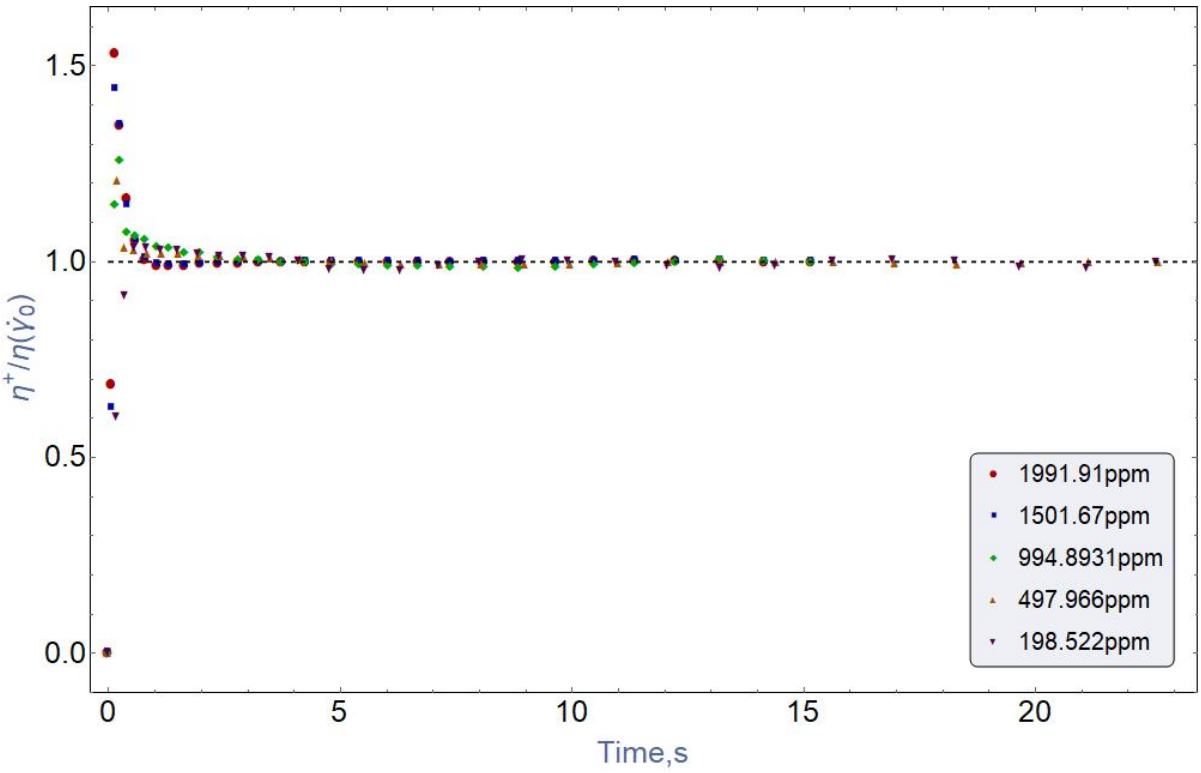

Figure 48: Shear stress growth function $\eta^+(t, \dot{\gamma}_0)/\eta(\dot{\gamma})$ for 5115VLM at $\dot{\gamma}_0 = 50$.

In conclusion, analysis of graphs for all tested polymers shows that overshoot position with respect to time is independent of concentration. The time needed to establish the steady shear flow also seems to be independent of concentration.

Figure, 49 represents the shear stress growth of AN125VHM at 1994.92 ppm concentration for different shear rates.

As mentioned earlier, the overshoot with shear rate reaches to the stable stage at earlier time at higher $\dot{\gamma}_0$. At which $\dot{\gamma}_0$ the first undershoot happens to reach the stable stage it takes more time than the previous lower $\dot{\gamma}_0$. All Kinetic models suggest that establishing

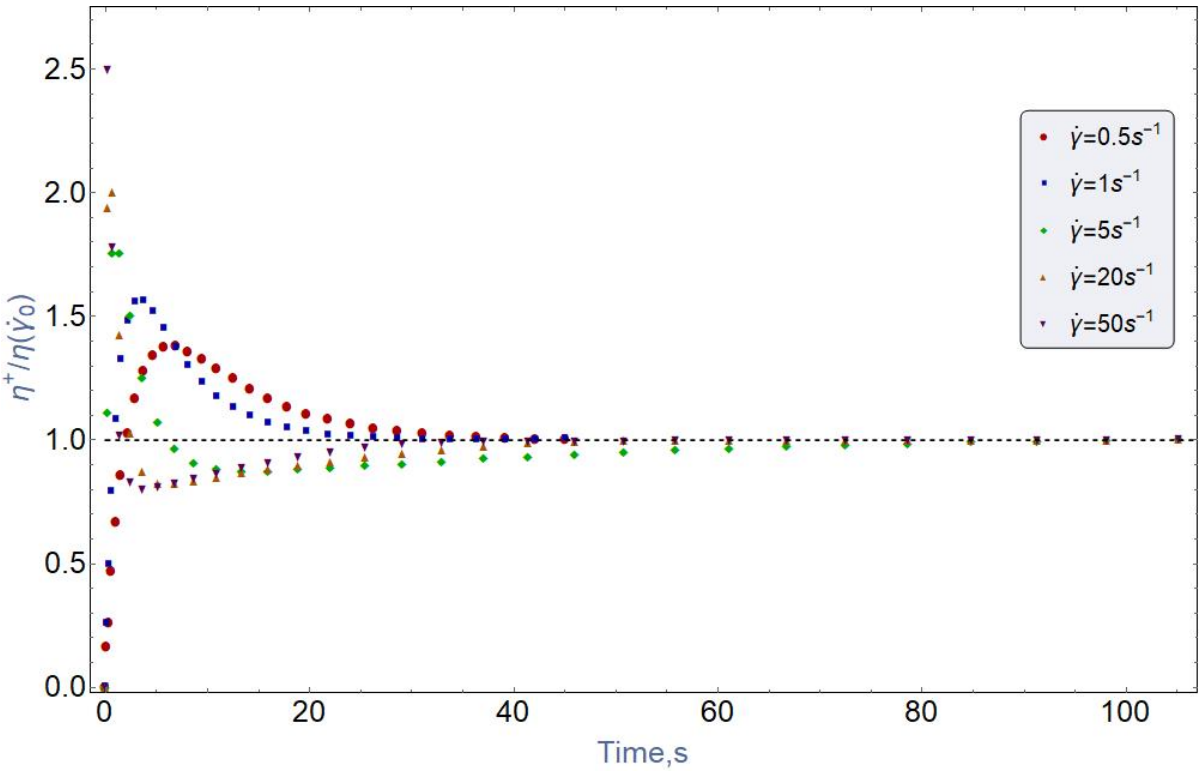

Figure 49: Shear stress growth function $\eta^+(t, \dot{\gamma}_0)/\eta(\dot{\gamma})$ for AN125VHM at 1994.92 ppm.

steady shear flow does not depend on the concentration which is observed in all the polymers. Both FENE-P and C-FENE-P model predicts the monotonic increasing of the overshoot with shear rate and arriving at the steady shear flow at earlier time.

Figure 50 shows the numerical results for the start-up case. The overshoot highly depends on the flexibility of the molecules as it can be seen by comparing the overshoot of VHM and VLM type polymers.

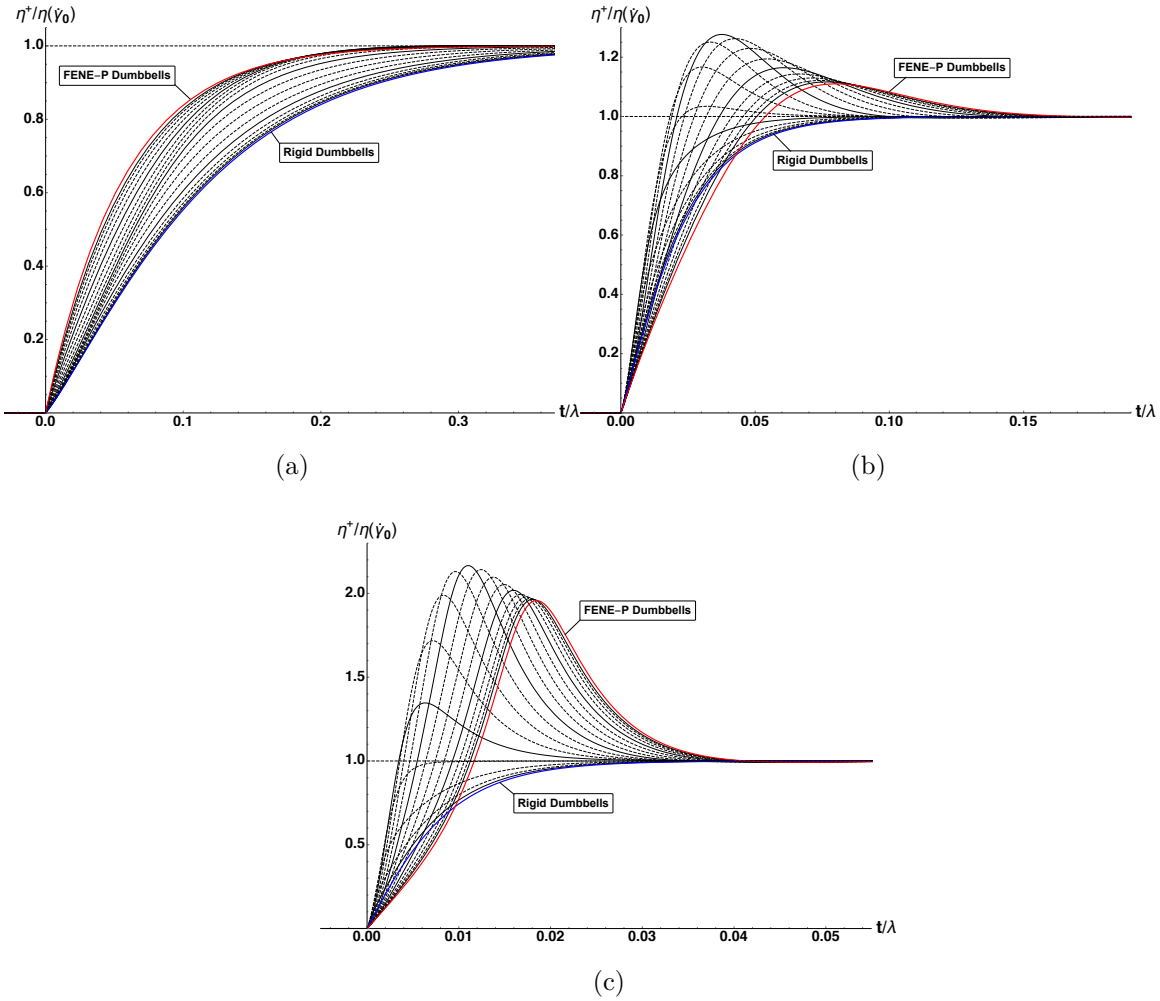

Figure 50: The normalised shear stress growth functions of the C-FENE-P dumbbells, plotted against the dimensionless time t/λ at $\lambda\dot{\gamma}_0 = 10$ (top); $\lambda\dot{\gamma}_0 = 100$ (middle); and $\lambda\dot{\gamma}_0 = 500$ (bottom). The colored lines show the limiting cases $E = 0$ (red) and $E\infty 1$ (blue). The black lines are drawn at $\log_{10} E$ varying from -1 to 3 with a step of 0.25, bottom up at late times; solid black lines correspond to integer values of $\log_{10} E$. All curves are plotted at $b = 50$ [Shogin and Amundsen, 2019].

4.3.2. Relaxation of Steady Shear Flow

It is not been possible to reach at zero shear stress as it can take infinite (unknown) time to reach it.

For Newtonian Fluid after sudden stop of the steady shear flow, the shear stress goes to zero immediately. But for these experimented polymers the shear stress decays monotonically and at early stage it decays faster than exponential and later times it reduces exponentially.

This can be explained by polyelectrolyte nature of these polymers.

Figure 51to 55 show the stress relaxation distribution over time for Flopaam AN125VHM. For lower concentrated polymer, the stress decays more rapidly at the beginning than high concentrated solutions which follows until 1000 ppm and then the rate starts to increase again. It can be explained by realizing that lower concentration has fewer molecules that's why less polymer-polymer interactions which helps to release the shear stress faster.

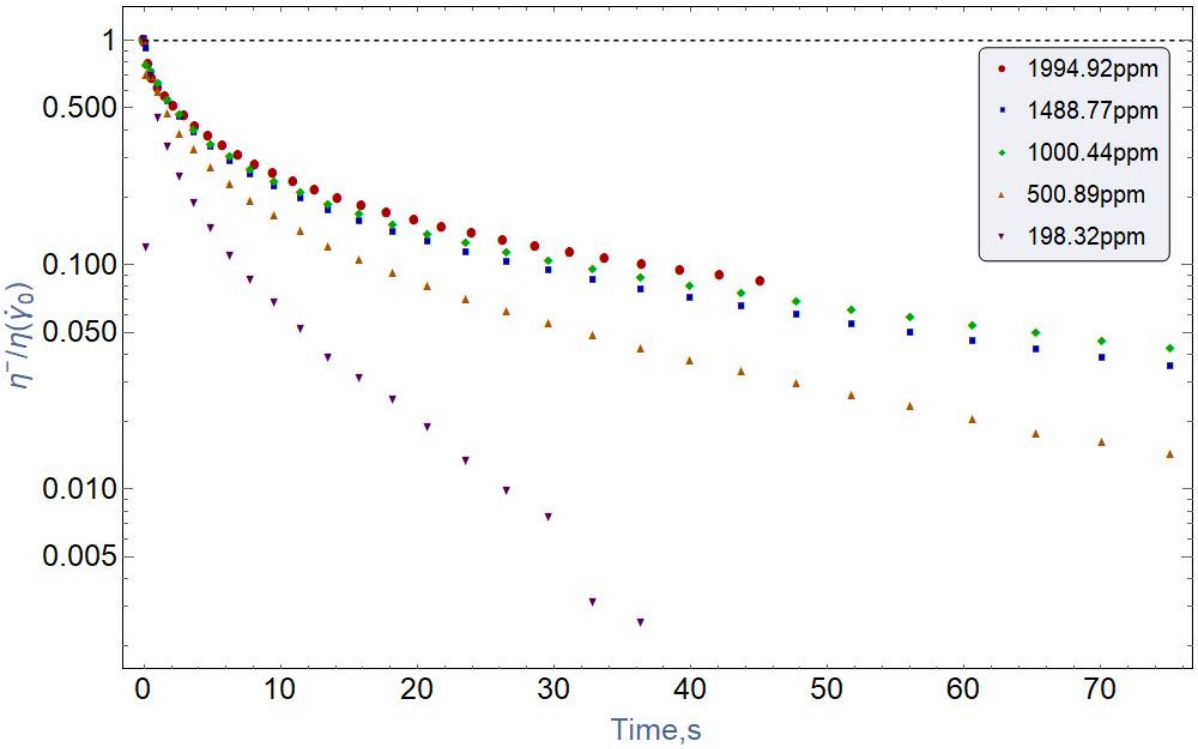

Figure 51: Shear stress relaxation function $\eta^-(t, \dot{\gamma}_0)/\eta(\dot{\gamma})$ for AN125VHM at $\dot{\gamma}_0 = 0.5$.

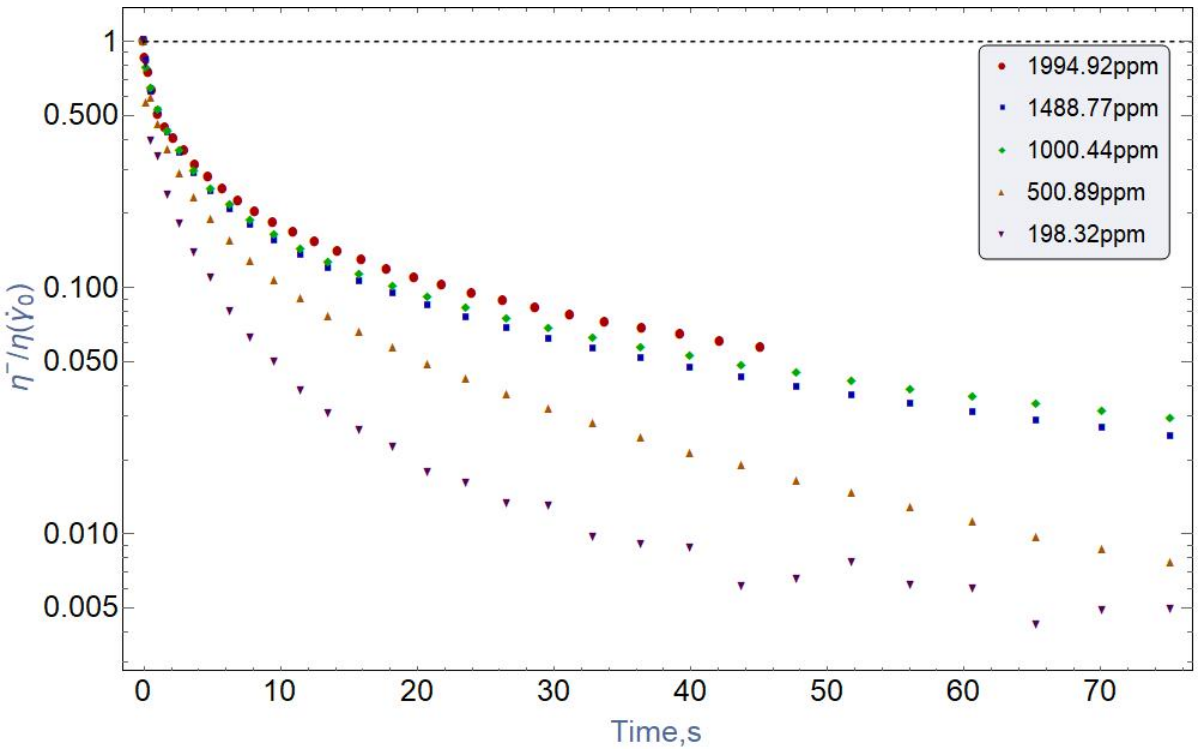

Figure 52: Shear stress relaxation function $\eta^-(t, \dot{\gamma}_0)/\eta(\dot{\gamma})$ for AN125VHM at $\dot{\gamma}_0 = 1$.

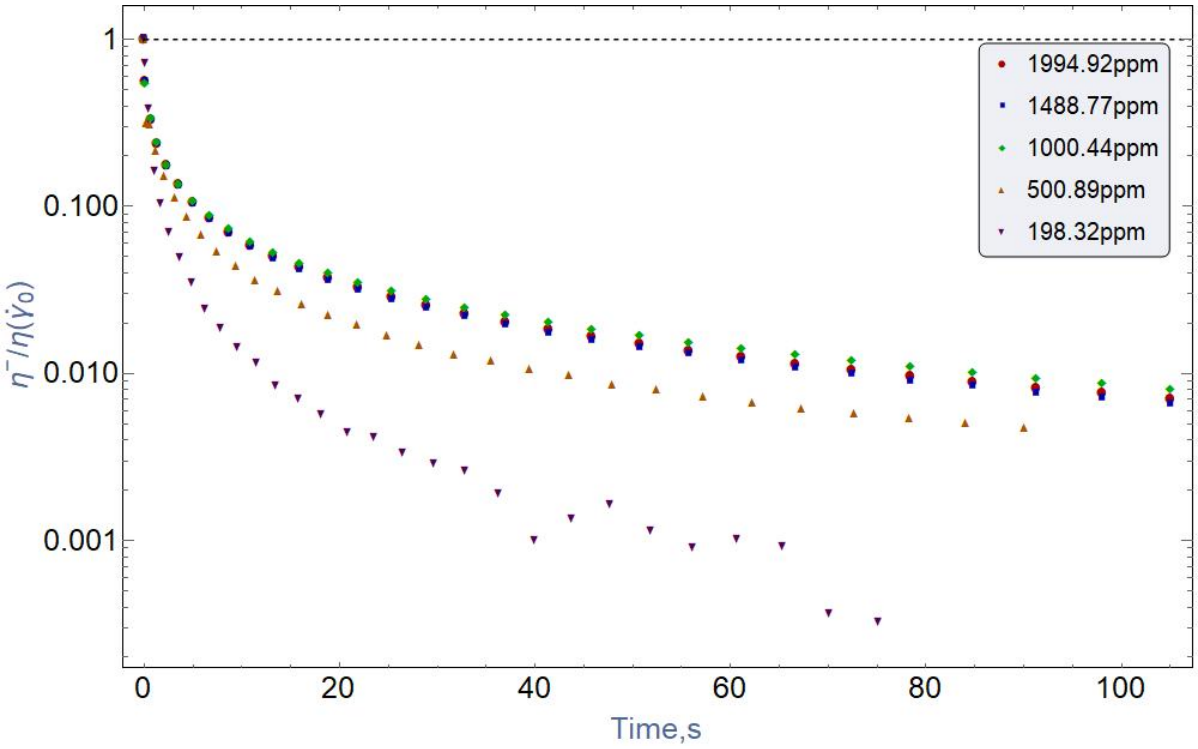

Figure 53: Shear stress relaxation function $\eta^-(t, \dot{\gamma}_0)/\eta(\dot{\gamma})$ for AN125VHM at $\dot{\gamma}_0 = 5$.

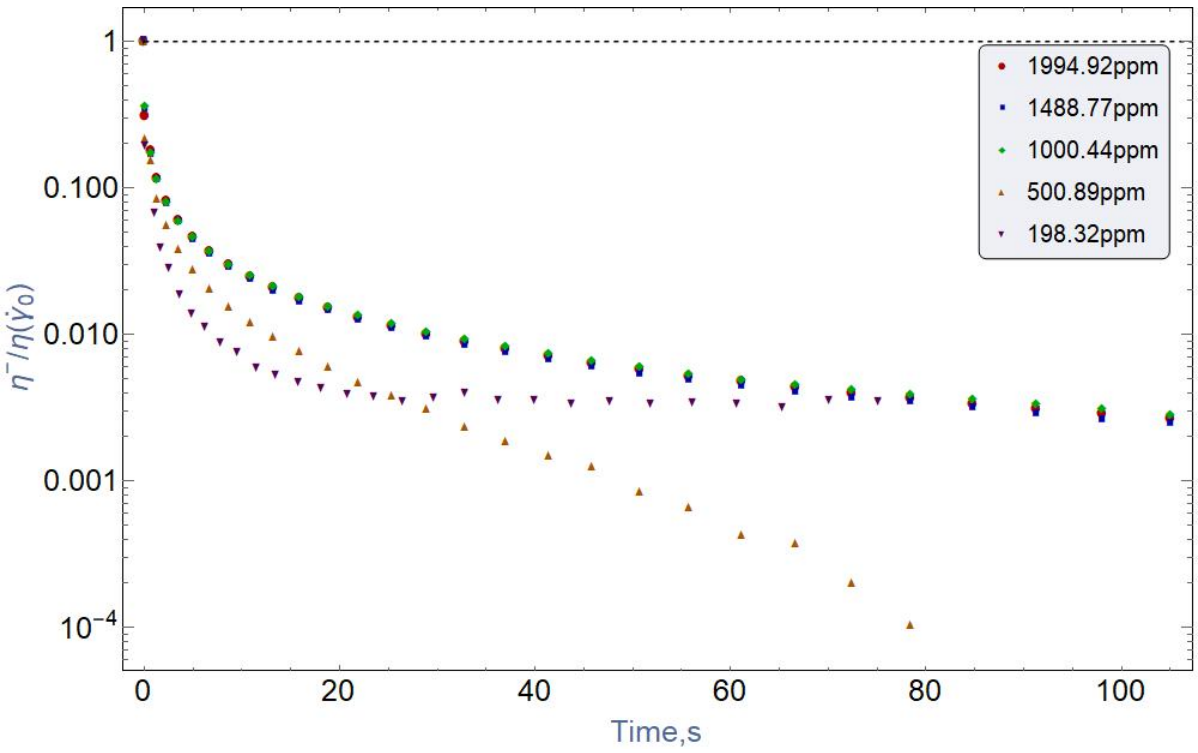

Figure 54: Shear stress relaxation function $\eta^-(t, \dot{\gamma}_0)/\eta(\dot{\gamma})$ for AN125VHM at $\dot{\gamma}_0 = 20$.

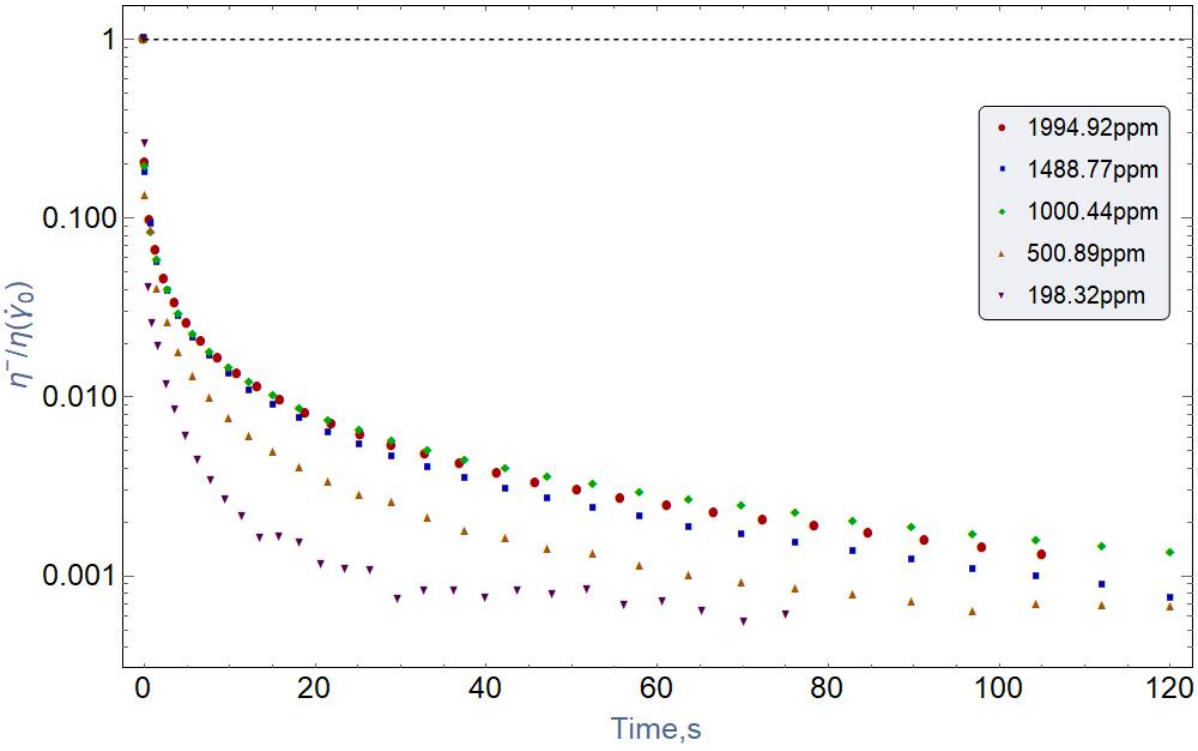

Figure 55: Shear stress relaxation function $\eta^-(t, \dot{\gamma}_0)/\eta(\dot{\gamma})$ for AN125VHM at $\dot{\gamma}_0 = 50$.

Another VHM polymer Flopaam 5115VHM, (figure 56 to 60) shows similar trends as previous one. The decline rate is higher at the beginning and then goes exponentially. In the exponential region the decay rate does not depend on the concentration anymore. The decreasing rate at a fix shear rate starts to decay with increasing concentration until it reaches to 1500 ppm and then it starts to increase again.

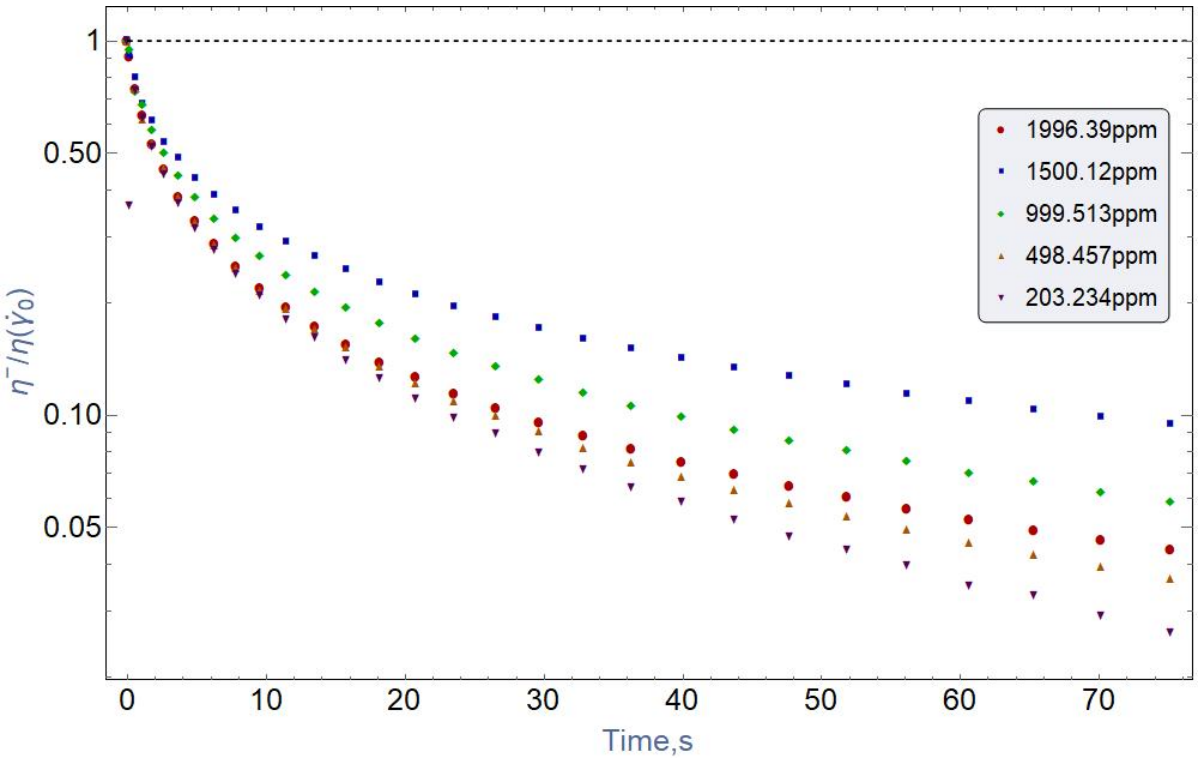

Figure 56: Shear stress relaxation function $\eta^-(t, \dot{\gamma}_0)/\eta(\dot{\gamma})$ for 5115VHM at $\dot{\gamma}_0 = 0.5$.

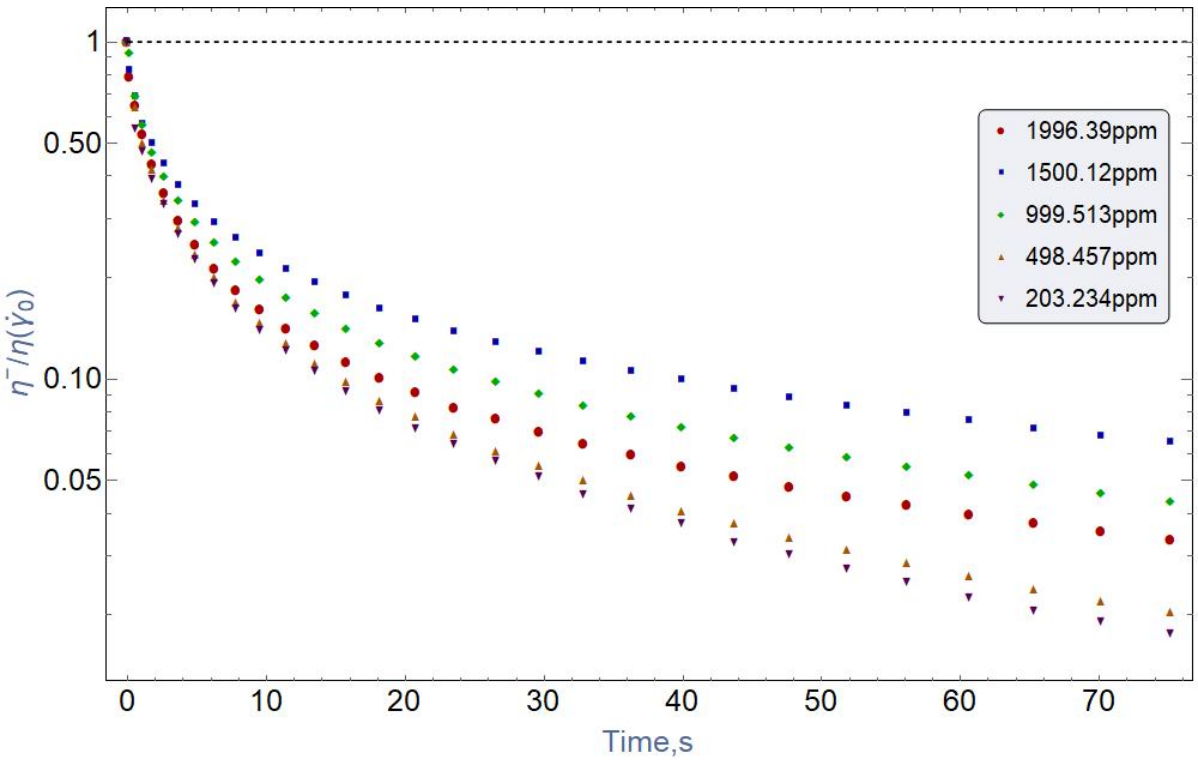

Figure 57: Shear stress relaxation function $\eta^-(t, \dot{\gamma}_0)/\eta(\dot{\gamma})$ for 5115VHM at $\dot{\gamma}_0 = 1$.

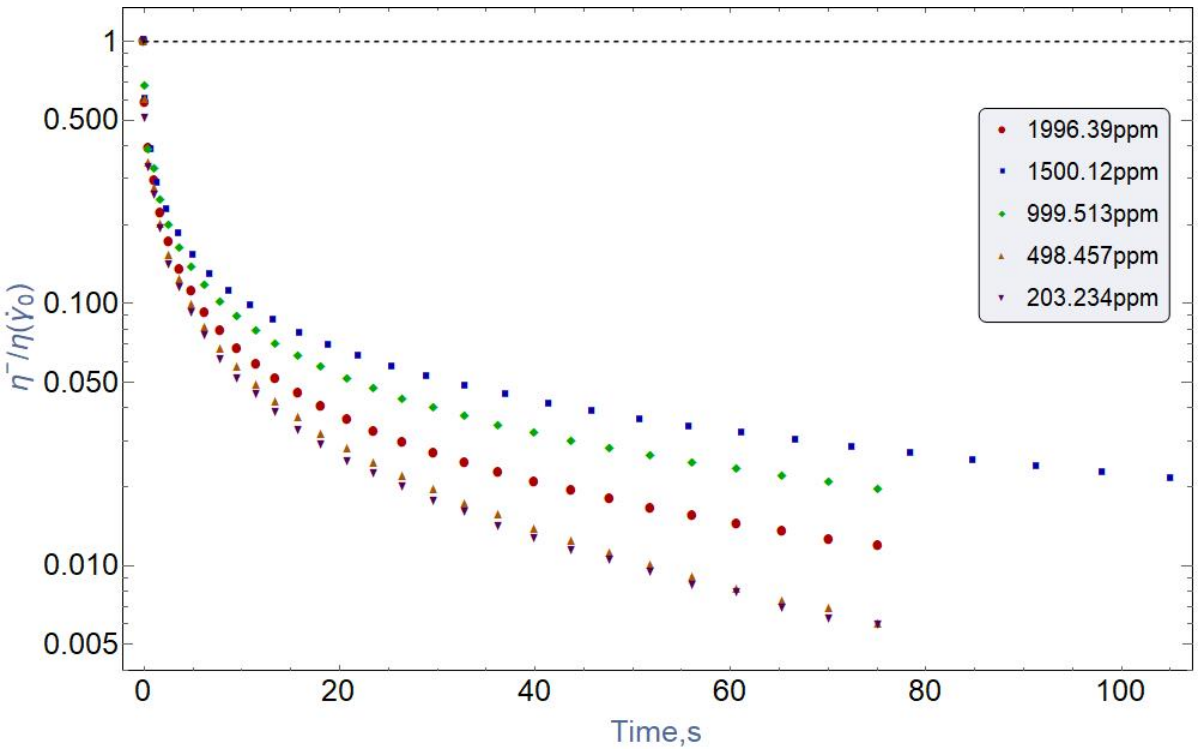

Figure 58: Shear stress relaxation function $\eta^-(t, \dot{\gamma}_0)/\eta(\dot{\gamma})$ for 5115VHM at $\dot{\gamma}_0 = 5$.

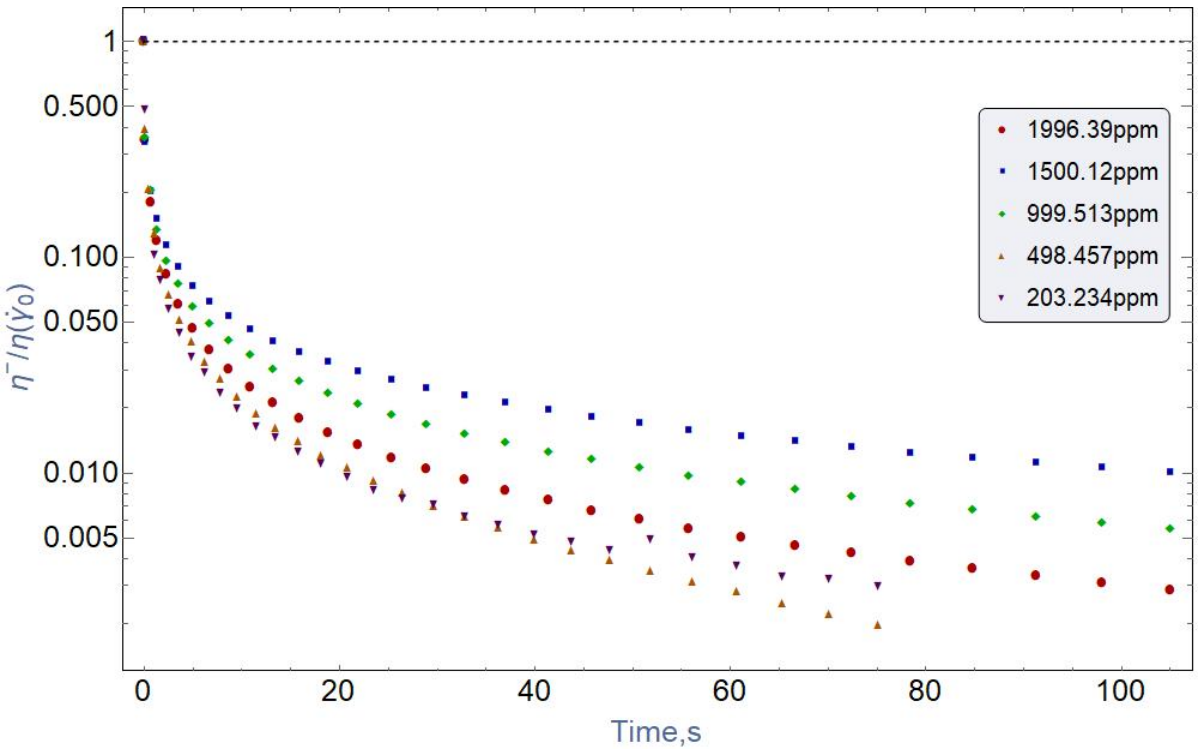

Figure 59: Shear stress relaxation function $\eta^-(t, \dot{\gamma}_0)/\eta(\dot{\gamma})$ for 5115VHM at $\dot{\gamma}_0 = 20$.

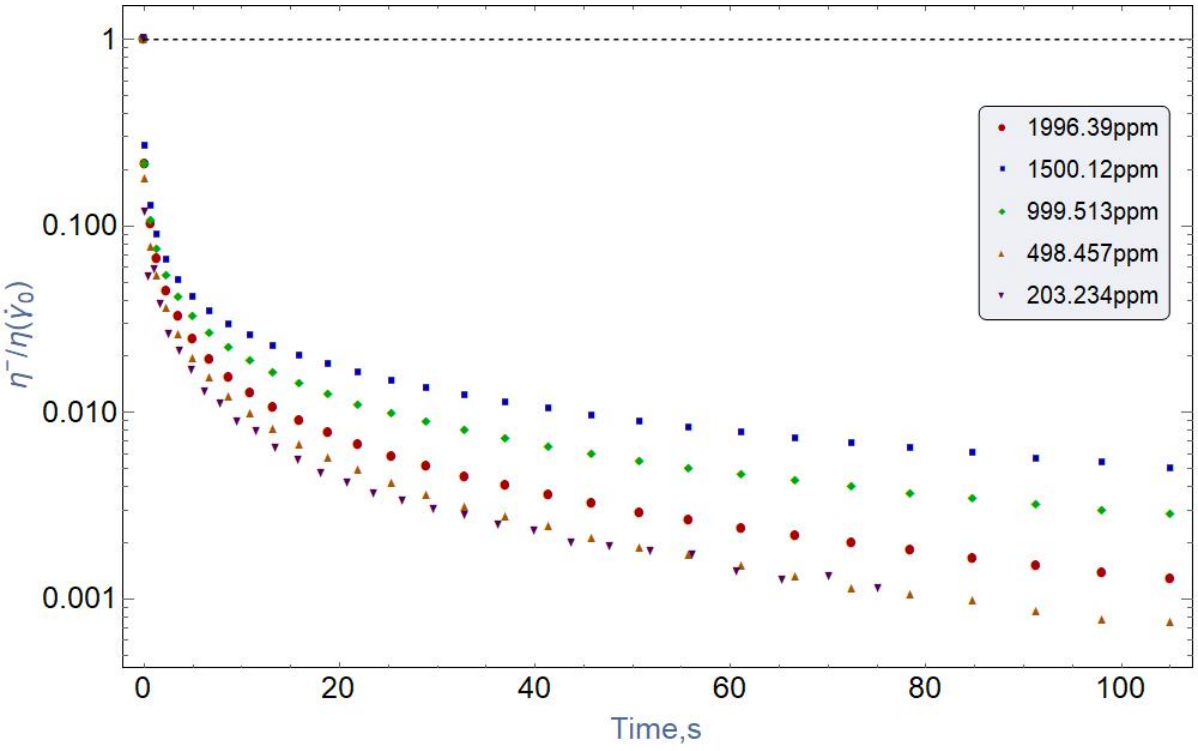

Figure 60: Shear stress relaxation function $\eta^-(t, \dot{\gamma}_0)/\eta(\dot{\gamma})$ for 5115VHM at $\dot{\gamma}_0 = 50$.

As a VLM group polymer, Flopaam 5115VlM (figure 61 to 64) doesn't follow the trend of VHM polymers.

It shows that for higher concentration the shear stress decay is quicker than lower ones. It is because at higher concentration the polymer-polymer interaction happens and which leads to higher stress, thus larger forces act to bring the fluid to the equilibrium when it is stopped suddenly . Again, here stress decay ratio is presented with respect to initial shear stress. Which means for higher concentration as example 2000 ppm the shear stress at $t = 0$ was high and after sudden stop of the flow the shear stress goes too low and thus the ratio is lower.

On the other hand, for lower concentrations as example for 200 ppm the shear stress was much lower during steady shear flow and thus after sudden drop it can't go much lower anymore and the ratio is thus higher.

Another trend can be derived from these figures, at higher concentration the relative decay rate does not depend on concentration anymore. And no exponential region has been established in the experimented region. May be it can be reached after.

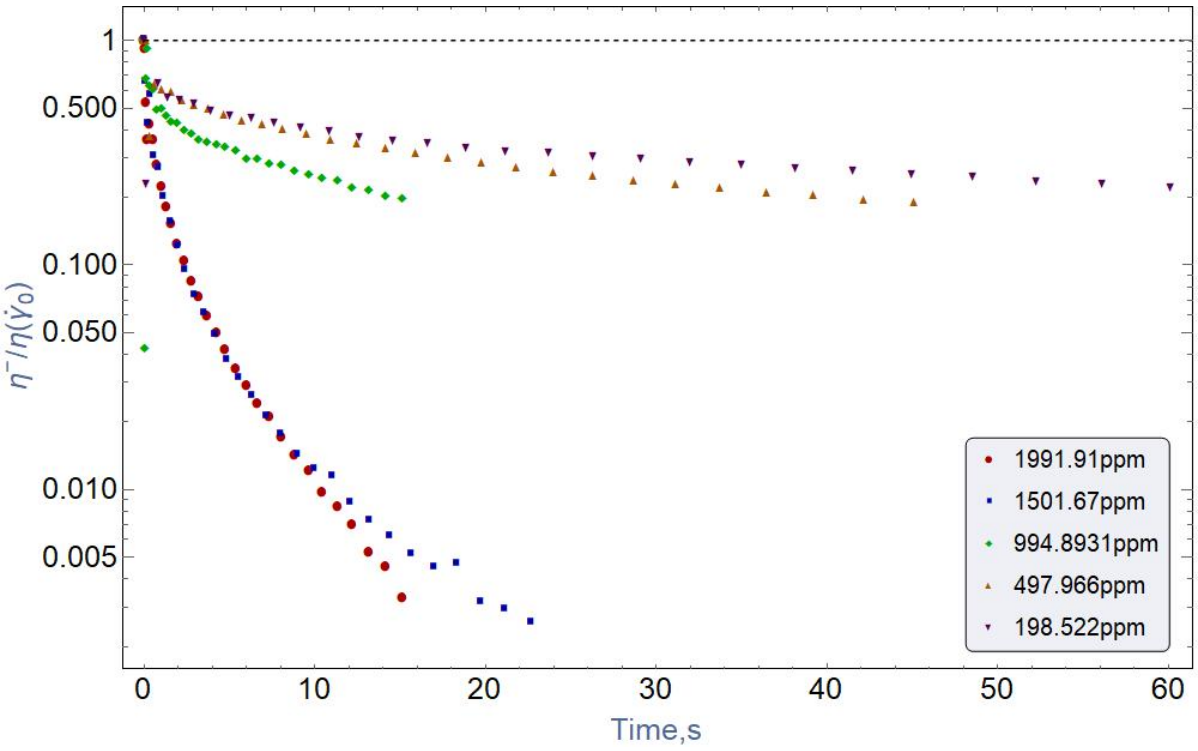

Figure 61: Shear stress relaxation function $\eta^-(t, \dot{\gamma}_0)/\eta(\dot{\gamma})$ for 5115VLM at $\dot{\gamma}_0 = 1$.

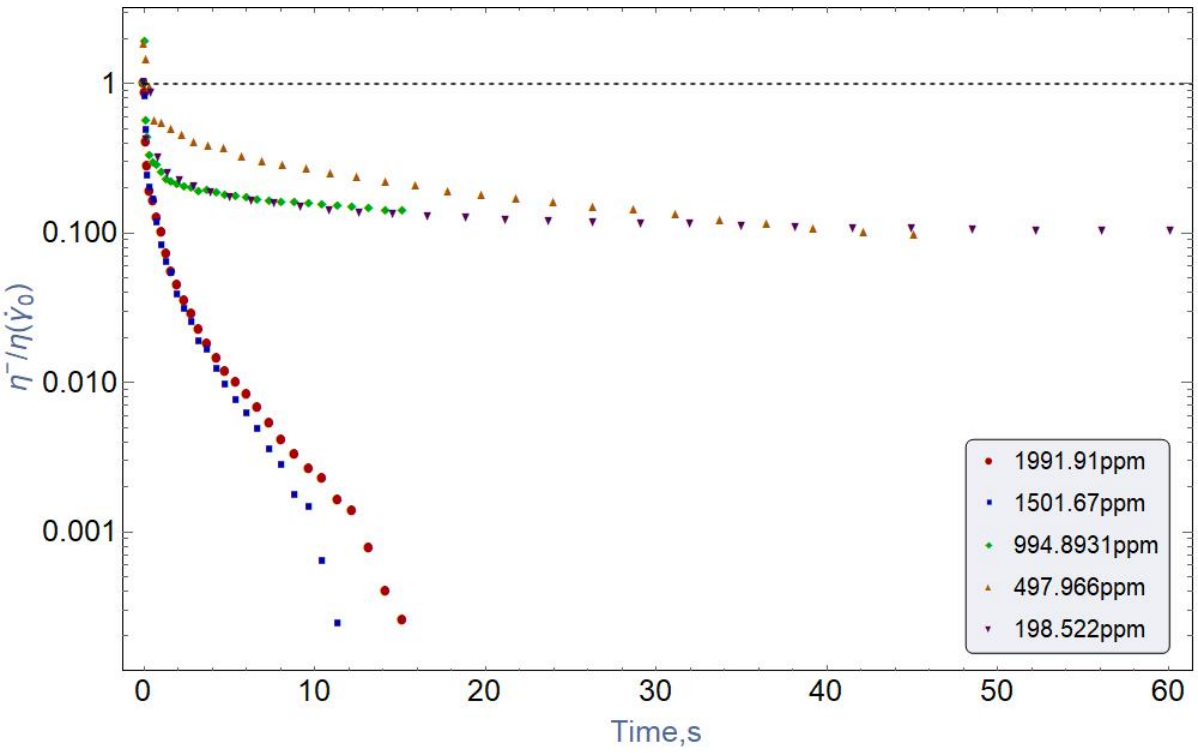

Figure 62: Shear stress relaxation function $\eta^-(t, \dot{\gamma}_0)/\eta(\dot{\gamma})$ for 5115VLM at $\dot{\gamma}_0 = 5$.

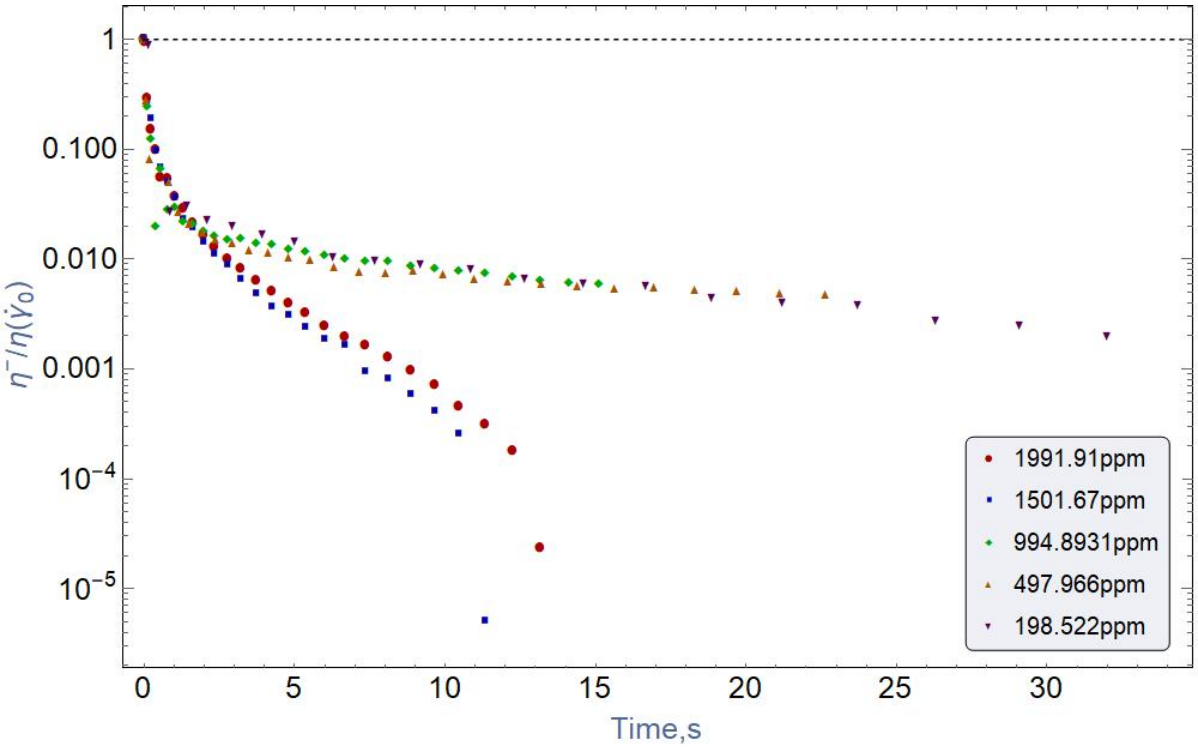

Figure 63: Shear stress relaxation function $\eta^-(t, \dot{\gamma}_0)/\eta(\dot{\gamma})$ for 5115VLM at $\dot{\gamma}_0 = 20$.

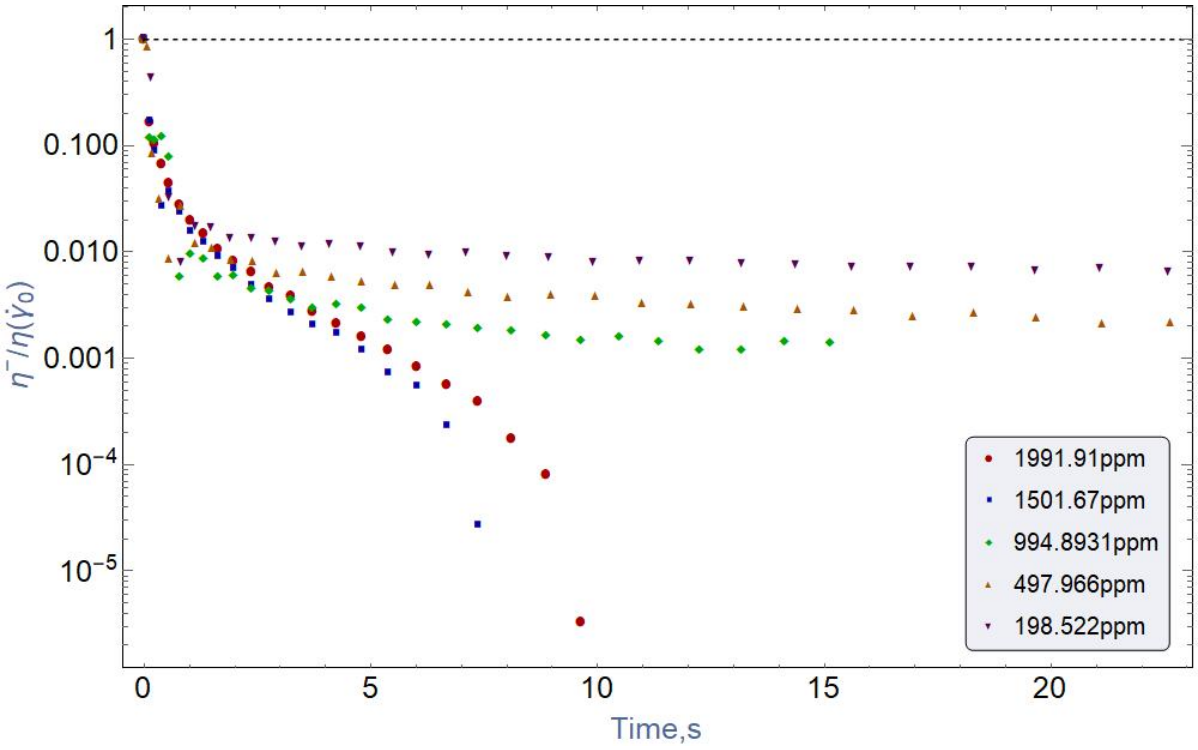

Figure 64: Shear stress relaxation function $\eta^-(t, \dot{\gamma}_0)/\eta(\dot{\gamma})$ for 5115VLM at $\dot{\gamma}_0 = 50$.

In conclusion it can be said that the relative degradation of shear stress at the beginning of the relaxation is faster than exponential decrease. Which explains the polyelectrolyte behavior of polymers. This region is predicted by C-FENE-P Dumbbell model but not by FENE-P Dumbbell.

The relaxation of polymer solution depends on concentration non-monotonically. With a general trend that the decay is a bit slower at high concentration (AN125VHM, 5115VHM untill a certain concentration) and vice versa at very high concentration (which is observed for all polymers and can be clearly seen for 5115VLM).The reason behind of this can be polymer-polymer interaction. And for that larger stress produce which brings the polymer solution into equilibrium faster

Figure, 65 represents the stress relaxation of AN125VHM at 1994.92 ppm concentration for different shear rates. As mentioned earlier, the shear stress decay is faster for higher shear rate and reaches to the zero shear stress quicker at higher $\dot{\gamma}_0$. The reason behind that is, at higher shear rate, higher shear stress forms and brings the liquid equilibrium quickly. The stress relaxation for 50 s^{-1} is somewhat almost 15 times faster that for 0.5 s^{-1} after 5 seconds when the flow has stopped.

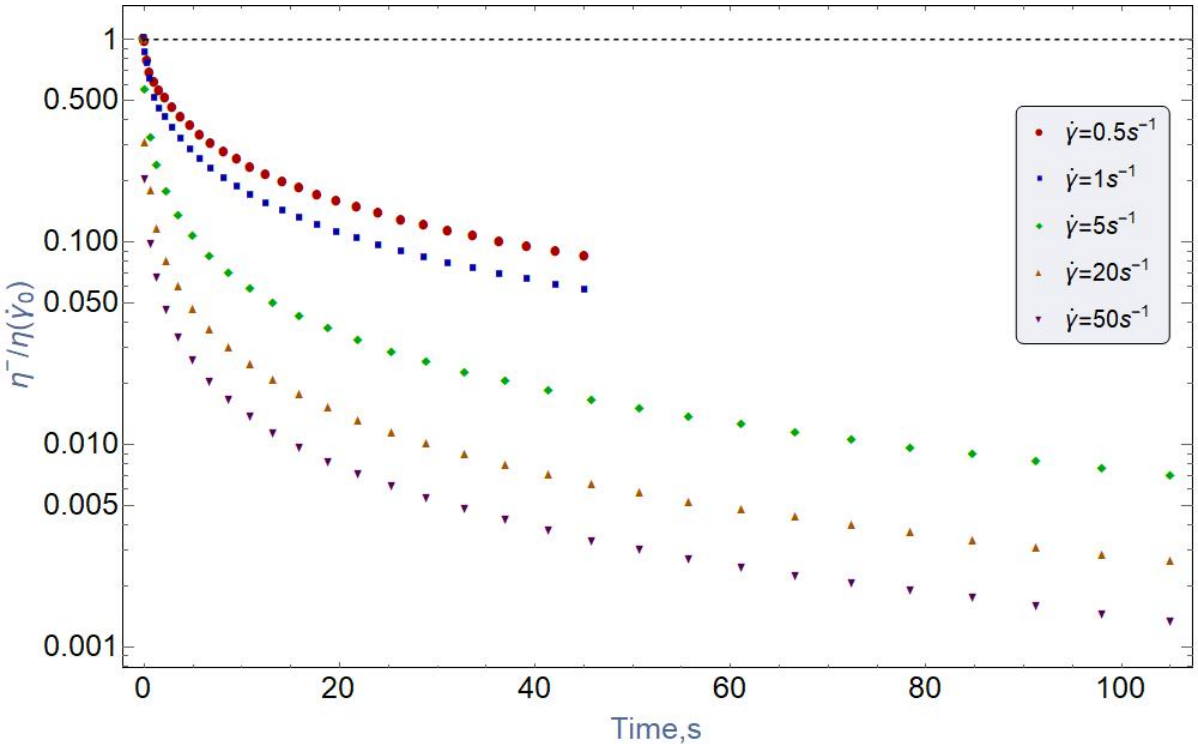

Figure 65: Shear stress relaxation function $\eta^-(t, \dot{\gamma}_0)/\eta(\dot{\gamma})$ for AN125VHM at 1994.92 ppm.

Figure 66 show the numerical results for the relaxation case. Though in this numerical plot dimensionless time is plotted, it can be said that neither RDB model nor FENE-P Dumbbell model can predict the initial shear stress relaxation behavior exactly while C-FENE-P can predict the behaviour.

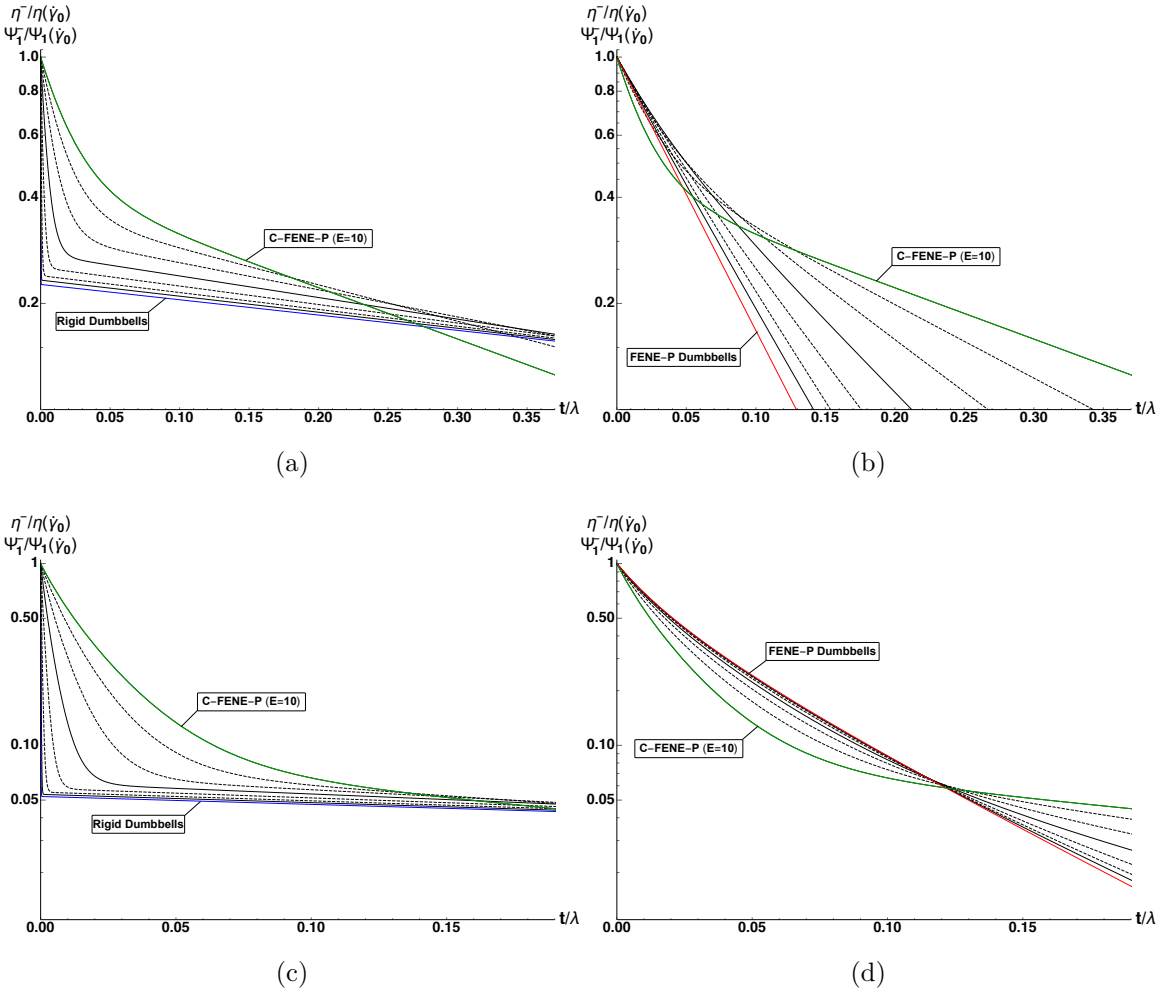

Figure 66: The normalised shear stress relaxation functions of the C-FENE-P dumbbells, plotted against the dimensionless time t/λ at $\lambda\dot{\gamma}_0 = 10$ (top); $\lambda\dot{\gamma}_0 = 100$ (bottom).The coloured lines show the FENE-P limit $E = 0$ (red), the RDB limit $E\infty1$ (blue), and the case when $E = 10$ (green). The black lines are drawn at $\log_{10} E$ varying from -1 to 2=3 (left, from red towards green) and from 4/3 to 3 (right, from green towards blue), with a step of 1/3; solid black lines correspond to integer values of $\log_{10} E$. The value of b is set to 50. The vertical axes are scaled logarithmically [Shogin and Amundsen, 2019].

5. Conclusion

Initial intention of this work was to investigate the material functions of EOR polymers experimentally at different shear flow; particularity start-up and relaxation behaviour of steady shear flow. Since a lot of experiments have been performed for investigating the shear thinning behavior and the SAOS flow material functions, the main focus of this work is devoted to investigate the start-up and relaxation behaviour of steady shear flow.

It is discovered that both shear stress growth and decay is a non-monotonic function of concentration while both are highly dependent on shear rate of the flow. The higher the shear rate the quicker the flow reaches to its stable stage, but the deformation of the stress is also higher which can lead to degradation of the molecules of polymer and finally to the degradation of viscosity.

Another discovery by this experiment is that the exponent in the exponential region at relaxation of fluid is independent for both of concentration and of $\dot{\gamma}_0$.

The results are being qualitatively analyzed and compared with different Dumbbell models. It is concluded that neither FENE-P Dumbbell model nor Rigid Dumbbell model can predict the relative shear stress growth and decay well. While these phenomena can be well explained by C-FENE-P Dumbbell model. Tough more experiments is needed to perform at higher concentration and shear rate for vast number of polymers.

The shear viscosity and storage and loss moduli were qualitatively compared with models and previous works.

The outcomes from the start-up and relaxation experiment can be implemented in both industrial and experimental world. The overshoot at the beginning of the flow can be used to predict the degradation of the viscosity of the polymers. And which will help to reduce that degradation of the viscosity and thus less polymer loss and more mobility ratio.

The needed time to establish the steady shear flow can also be used to design experiments and experimental tools. As now the time to start the steady shear flow is found out, it can be used in the equations and the tools can also be design in such a way that the start of the calculation will start after this sudden time which will lead to utilize time and resources.

The relaxation time behavior and results can also be implemented at experimental field.

As by knowledge this is the first attempt to experiment the shear stress growth and decay, further investigation is needed before implementing the results. Due to the limitations of the CP tool, it was difficult to investigate at very low and very high shear rate. Different methods can be performed to cross examine the results.

References

[Aho, 2011] Aho, J. (2011). Rheological characterization of polymer melts in shear and extension: measurement reliability and data for practical processing. *Tampere University of Technology*.

[Bird et al., 1987a] Bird, R. B., Armstrong, R. C., and Hassager, O. (1987a). *Dynamics of polymeric liquids*, volume 1: Fluid mechanics. Wiley-Interscience Publication, second edition.

[Bird et al., 1987b] Bird, R. H., Curtiss, C. F., Armstrong, R. C., and Hassager, O. (1987b). *Dynamics of polymeric liquids*, volume 2: kinetic theory. Wiley.

[Heel, 2000] Heel, V. (2000). *Simulation of viscometric fluids*. PhD thesis, Technical University Delf.

[Hyun et al., 2011] Hyun, K., Wilhelm, M., Klein, C. O., Cho, K. S., Nam, J. G., Ahn, K. H., Lee, S. J., Ewoldt, R. H., and McKinley, G. H. (2011). A review of nonlinear oscillatory shear tests: analysis and application of large amplitude oscillatory shear (laos). *Progress in Polymer Science*, 36(12):1697–1753.

[Irgens, 2007] Irgens, F. (2007). *Rheology and non-newtonian fluids*. Springer.

[Jahn et al., 2008] Jahn, F., Cook, M., and Graham, M. (2008). *Hydrocarbon exploration and production*, volume 55. Elsevier.

[Kádár et al., 2016] Kádár, R., Naue, I. F. C., and Wilhelm, M. (2016). First normal stress difference and in-situ spectral dynamics in a high sensitivity extrusion die for capillary rheometry via the "hole effect". *Polymer*, 104:193–203.

[Kaufman and Joseph J. Falcetta, 1978] Kaufman, H. S. and Joseph J. Falcetta, E. (1978). *Introduction to polymer science and technology : an SPE textbook*. New York : Wiley.

[Krishnan et al., 2010] Krishnan, J. M., Deshpande, A. P., and Kumar, P. B. S. (2010). *Rheology of complex fluids*. Springer.

[Lutskina, 2018] Lutskina, M. (2018). Describing viscosity of ior polymer solutions with differential non-newtonian fluid models. Master's thesis, University of Stavanger.

[Mezger, 2006] Mezger, T. G. (2006). *The rheology handbook: for users of rotational and oscillatory rheometers*. Vincentz Network GmbH & Co KG, second edition.

[Morrison, 2001] Morrison, F. A. (2001). *Understanding rheology*. Oxford University Press, Inc.

[NPD, 2017] NPD (2017). https://www.npd.no/globalassets/1-npd/publikasjoner/norsk-sokkel-en/arcive/norsk-sokkel-eng-nett.pdf.

[NPD, 2018] NPD (2018). https://www.npd.no/en/facts/publications/norwegian-continental-shelf/norwegian-continental-shelf-no.-1—2018/a-global-focal-point-for-boosting-recovery/.

[Osswald and Rudolph, 2014] Osswald, T. A. and Rudolph, N. (2014). *Polymer rheology fundamentals and applications*. Carl Hanser Verlag GmbH & Co. KG.

[Prasad, 2018] Prasad, D. R. G. (2018). Enhanced oil recovery by using polymer flooding in oil and gas industry in tertiary recovery process. *International Journal for Research in Applied Science & Engineering Technology (IJRASET)*, 6.

[Rellegadla et al., 2017] Rellegadla, S., Prajapat, G., and Agrawal, A. (2017). Polymers for enhanced oil recovery: fundamentals and selection criteria. *Applied microbiology and biotechnology*, 101(11):4387–4402.

[Shogin, 2019] Shogin, D. (2019). Lecture notes on non-newtonian fluid.

[Shogin and Amundsen, 2019] Shogin, D. and Amundsen, P. A. (2019). The charged fene-p dumbbelled model for dilute solutions of polyelectrolytes (working tytle). *To be published*.

[Thien and Tanner, 1977] Thien, N. P. and Tanner, R. I. (1977). A new constitutive equation derived from network theory. *Journal of Non-Newtonian Fluid Mechanics*, 2(4):353–365.

[Thomas, 2016] Thomas, A. (2016). Polymer flooding. In Romero-Zerón, L., editor, *Chemical enhanced oil recovery (cEOR)*, chapter 2. IntechOpen.

[Thompson et al., 2015] Thompson, R. L., Alicke, A. A., and de Souza Mendes, P. R. (2015). Model-based material functions for saos and laos analyses. *Journal of Non-Newtonian Fluid Mechanics*, 215:19–30.

[typhonix.com, 2019] typhonix.com (2019). https://www.typhonix.com/home/low-shear-oil-production/improved-oil-recovery-by-low-shear-handling-of-injection-polymers.

[Weissenberg, 1947] Weissenberg, K. (1947). A continuum theory of rhelogical phenomena. *Nature*.

[Wnek, 2008] Wnek, G. E. (2008). Polymers. In Wnek, G. E. and Bowlin, G. L., editors, *Encyclopedia of biomaterials and biomedical engineering*. Informa Healthcare, second edition.